SURVIVABILITY SCHEMES FOR DYNAMIC TRAFFIC IN OPTICAL NETWORKS

HE RONG

(B.Eng. Shanghai Jiao Tong University)

A THESIS SUBMITTED

FOR THE DEGREE OF DOCTOR OF PHILOSOPHY

DEPARTMENT OF ELECTRICAL AND COMPUTER ENGINEERING

NATIONAL UNIVERSITY OF SINGAPORE

2010

To my parents...

who gave me their wonderful support...

Acknowledgements

I am truly indebted to my supervisors, Professor Chua Kee Chaing and Associate Professor Mohan Gurusamy for their continuous guidance and support during this work. Without their guidance, this work would not be possible.

I am deeply indebted to the National University of Singapore for the award of a research scholarship. I would also like to give thanks to all the researchers in the Optical Network Engineering (ONE) lab, who greatly enriched both my knowledge and life with their intelligence and optimism. Lastly, I would like to thank my parents and my friends for their endless love and support.

He Rong

February 2010

Contents

Acknowledgements **ii**

Summary **ix**

List of Abbreviations **xi**

List of Tables **xv**

List of Figures **xvii**

1 Introduction **1**

1.1 Communication Network Architecture 3

1.2 Network Failures 5

1.3 Network Survivability 7

1.4 Research Objectives and Scope 8

1.4.1 Thesis Outline 13

1.5 Thesis Contribution 15

2 Background and Related Work **16**

2.1 Fundamentals of Transport Networks 16

2.1.1 Layering 16

2.1.2 Switching Technology 18

2.1.3 Wavelength Division Multiplexing 21

2.2 Network Survivability Techniques 23

2.2.1 Physical Layer Survivability Techniques 24

2.2.2 System Layer Survivability Techniques 24

2.2.3 Logical Layer Survivability Techniques 30

2.2.4 Service Layer Survivability Techniques 42

2.2.5 Summary 43

3 Protected Working Lightpath Envelope **44**

3.1 Introduction 44

3.2 Concept of Protected Working Lightpath Envelope 45

3.3 Design of PWLE 50

3.3.1 Compatible Grouping 50

3.3.2 MILP Formulation 56

3.4 Routing and Operation of PWLE 61
3.4.1 Compatible Group Routing (CGR) 61
3.4.2 Operation Upon Failure 67
3.5 Numerical Results and Discussions 68
3.5.1 Optimization Result 68
3.5.2 Blocking Performance 72
3.5.3 Control Overheads 74
3.6 Summary 79
3.7 Formulation of PWCE_WP/WC Model 79

4 Lightpath-protecting *p*-Cycle Selection for Protected Working Lightpath Envelope 83

4.1 Introduction 83
4.2 Design of Lightpath-protecting p-Cycle Selection for PWLE 85
4.2.1 AttachNode-Based Cycle Generation (ANCG) 85
4.2.2 Heuristic Algorithms of Lightpath-protecting p-Cycle Selection (HALCS) 89
4.3 Numerical Results and Discussions 98
4.3.1 Pre-computation of Candidate Cycles 98
4.3.2 Performance Comparison with the Optimal 99
4.3.3 Performance Comparison among HALCSs 102

4.4 Summary 104

5 Connectivity Aware Protected Working Lightpath Envelope 105

5.1 Introduction 105

5.2 Motivation and Concept of CAPWLE 106

5.3 Design of CAPWLE 110

5.3.1 Effective Envelope 110

5.3.2 Optimization of CAPWLE 120

5.4 Numerical Results and Discussions 123

5.4.1 Optimization Result 123

5.4.2 Blocking Performance: Dynamic Stationary Traffic 124

5.4.3 Blocking Performance: Dynamic Evolving Traffic 125

5.5 Summary 128

6 Efficient Configuration of *p*-Cycles Under Time-variant Traffic 129

6.1 Introduction 129

6.2 Joint Static Configuration Approach 131

6.2.1 Concept of JSCA 131

6.2.2 Value of JSCA 135

6.3 Optimization Model 137

6.3.1 Terminology and Notation 137

6.3.2 MILP Formulation 139

6.3.3 Extension to JSCA-based PWCE 141
6.4 Sub-optimal Solution 142
6.4.1 Sub-optimal Solution to JSCA 142
6.4.2 Sub-optimal Solution to JSCA-based PWCE 144
6.5 Extension to Path-protected Networks 144
6.5.1 Optimization of JSCAP 146
6.5.2 Extension to JSCAP-based PWLE 149
6.6 Numerical Results and Discussions 150
6.6.1 Traffic Pattern Generation 151
6.6.2 Optimization of JSCA 153
6.6.3 Impact of Limiting Inflation Of Working Capacity 155
6.6.4 Sub-optimal Solution to JSCA 156
6.6.5 Optimization of JSCA-based PWCE 158
6.6.6 Extension to Path-oriented Protection 163
6.7 Summary 167

7 Conclusions and Further Research 168

7.1 Conclusions 168
7.2 Contributions of this Thesis 170
7.3 Further Research 172
7.4 Publications 174

Bibliography 175

Summary

As networks carry more high bandwidth services, survivability becomes crucial since the failure of a fiber link may affect thousands of connections and cause huge data losses. p-Cycle is an innovative mechanism in optical network protection. p-Cycle uses pre-connected cycles of spare capacity to restore disrupted working traffic and combines the speed of a ring topology and the efficiency of a mesh topology. In this thesis, we present four advanced studies of transport network survivability mechanisms for dynamic traffic based on p-Cycles and its extensions.

We propose and develop Protected Working Lightpath Envelope (PWLE) which is based on lightpath-protecting p-Cycles and optimized using Mixed Integer Linear Programming (MILP). Then, we develop a distributed routing algorithm for PWLE which is Compatible Group Routing (CGR). We evaluate the performance

improvement of PWLE in capacity efficiency, blocking performance and control overheads through numerical results obtained from CPLEX and simulations.

Further, to deal with the high computational complexity of the optimization model of PWLE, we develop a cycle pre-computation algorithm and heuristic algorithms for cycle selection. Besides, to take into account the network connectivity, we integrate the factor of network connectivity into the design of PWLE and thus propose Connectivity Aware Protected Working Lightpath Envelope (CAPWLE) which is based on *Effective Envelope*. Numerical studies are carried out to show the effectiveness of the heuristic algorithms as well as the performance enhancement of CAPWLE relative to PWLE.

Finally, the configuration of p-Cycle-based survivability schemes under time-variant traffic is studied. We start with span-protected networks and propose an efficient off-line static configuration of span-protecting p-Cycles, Joint Static Configuration Approach (JSCA). We also discuss the application of JSCA in Protected Working Capacity Envelope (PWCE) and thus produce JSCA-based PWCE. To deal with the high computational complexity of optimization models, we also develop the sub-optimal solutions to JSCA and JSCA-based PWCE. Furthermore, we extend the studies on span-protected networks to path-protected networks. The effectiveness of JSCA and JSCA-based PWCE as well as their extensions to path-protected networks is verified by numerical results.

List of Abbreviations

p-Cycle	Pre-configured Protection Cycle
ADM	Add Drop Multiplexer
AER	Actual Efficiency Ratio
ANCG	AttachNode-Based Cycle Generation
APS	Automatic Protection Switching
APWCE	Adaptive PWCE
AT	Active Table
BLSR	Bidirectional Line Switched Ring
CAPWLE	Connectivity Aware Protected Working Lightpath Envelope

CG	Compatible Group
CGR	Compatible Group Routing
CIDA	Capacitated Iterative Design Algorithm
CWDM	Coarse WDM
DCS	Digital Cross-Connect Switch
DFS	Depth First Search
DSL	Digital Subscriber Line
DWDM	Dense WDM
ER	Efficiency Ratio
FIPP	Failure Independent Path-Protecting
HALCS	Heuristic Algorithms of Lightpath-protecting p-Cycle Selection
ILP	Integer Linear Programming
IRA	Independent Reconfiguration Approach
IRAP	Independent Reconfiguration Approach for Path Protection
IT	Inactive Table
JCG	Joint Compatible Group

JSCA	Joint Static Configuration Approach
JSCAP	Joint Static Configuration Approach for Path Protection
LAN	Local Area Network
LSA	Link State Advertisement
MAN	Metropolitan Area Network
MCFP	Maximum Concurrent Flow Problem
MILP	Mixed Integer Linear Programming
MSCA	Maximal Static Configuration Approach
MSCAP	Maximal Static Configuration Approach for Path Protection
NEPC	Node-Encircling p-Cycle
OCDC	Oriented Cycle Double Cover
OXC	Optical Cross-connect
PCD	Protection Cardinality of Demand
PWLE	Protected Working Lightpath Envelope
PWLE	Protected Working Lightpath Envelope
QoP	Quality of Protection

QoS	Quality of Service
SBPP	Shared Backup Path Protection
SP	Stochastic Programming
TAER	Traffic Pattern Related AER
TPRC	Traffic Pattern Relevance for Cycle
TPRG	Traffic Pattern Relevance for CG
UPSR	Unidirectional Path Switched Ring
VWP	Virtual Wavelength Path
WAN	Wide Area Network
WC	Wavelength Converter
WDCS	Weighted DFS-based Cycle Search
WDM	Wavelength-Division Multiplexing
WP	Wavelength Path

List of Tables

3.1 Comparison of Volume of Working Envelope for Network NSFNET (Average Node Degree: 3) 69

3.2 Comparison of Volume of Working Envelope for Network Bellcore (Average Node Degree: 3.7) 70

3.3 Comparison of Volume of Working Envelope for Network COST239 (Average Node Degree: 4.7) 70

4.1 Precomputed Candidate Cycles by ANCG 99

4.2 Comparison of Volume of Working Envelope between HALCS Algorithms and MILP for Network NSFNET 100

4.3 Comparison of Volume of Working Envelope between HALCS Algorithms and MILP for Network BellCore 101

4.4 Comparison of Volume of Working Envelope between HALCS Algorithms and MILP for Network COST239 102

5.1 Working Envelope of PWLE and CAPWLE 124

List of Figures

1.1 Illustration of Access, Metropolitan and Long-haul Networks 5

1.2 Survivability Schemes at Various Layers (Adapted from [1]) 9

2.1 Transport Network Layering (Adapted from [1]) 17

2.2 Functional Block Diagram of an ADM 19

2.3 Functional Block Diagram of a Digital/Optical Cross Connect Switch 20

2.4 1+1 APS system 25

2.5 UPSR protection operation 26

2.6 BLSR protection operation 28

2.7 Illustration of OCDC 29

2.8 Illustration of Span Restoration (a) Network Topology (b) Restoration Routes 31

2.9 Illustration of Path Restoration (a) Working Path (b) Possible Backup Paths 33

2.10 Illustration of Shared Backup Path Protection (SBPP) 34

2.11 p-Cycle Protection Operation 37

2.12 An Example of FIPP 37

2.13 An Example of Protected Working Capacity Envelope (PWCE) . . 40

3.1 (a) An Example of Lightpath-protecting p-Cycle (b) An Example of Span-protecting p-Cycle 48

3.2 (a) Illustration of Compatible Grouping (b) Illustration of MILP Model 51

3.3 (a) Illustrative Network Protected by Two Lightpath-protecting p-Cycles: I 0-2-3-10-6-8-0 and II 0-1-2-7-6-9-0 (b) The CG Table (CGT) of I at Node 0 (c) The JCG Table ($JCGT$) of I at Node 0 (d) The CG Table (CGT) of II at Node 0 (Note: entries in grey are actually excluded) (e) The JCG Table ($JCGT$) of II at Node 0 (f) The Active Table (AT) at Node 2 (g) An Example of the Message Used in the Group Signaling in CGR 63

3.4 Test Networks for Optimization(a) NSFNET (b) Bellcore (c) COST239 68

3.5 Comparison of Blocking Performance between PWLE and PWCE_WP/WC 74

3.6 Control Overhead Comparison between PWLE (left) and PWCE (right), COST239, 19 source-destination node pairs, traffic load between each node pair: 0.8 Erlangs 75

3.7 Average Control Overhead Comparison between PWLE (left) and PWCE (right), COST239, 19 and 25 source-destination node pairs, traffic load between each node pair: 0.8 Erlangs 77

3.8 Comparison of Control Overhead between PWLE and PWCE . . . 78

4.1 Illustration of Weight Assignment of ANCG Algorithm 88

4.2 Illustration of the Calculation of Metrics. 93

4.3 Performance Comparison among HALCSs 103

5.1 (a) Illustration of Lightpath-protecting p-Cycle (b) & (c) Illustration of the Imperfection of *ER* 107

5.2 Concurrent Flow and Concurrent Connectivity [15]. 112

5.3 Divide Off-cycle Protected Capacity into *CG*s (or *JCG*s) 115

5.4 Basic Topology (a)Topology I (b)Topology II 117

5.5 (a) Basic Topology III (b) Decomposition Component A (c) Decomposition Component B 119

5.6 Improvement in Blocking Performance 125

5.7 Blocking Performance Under Evolving Traffic 126

6.1 Sharing of Resources Between Traffic Matrices at Different Characteristic Instants (a) Traffic Matrix D^1 (b) Traffic Matrix D^2 (c) Traffic Matrix D^{max} 134

6.2 Comparison of Resource Usage under Different Approaches (IRA, JSCA, MSCA) 154

6.3 The Impact of Limiting Inflation of Working Capacity 156

6.4 The Effectiveness of Sub-optimal Solutions in Resource Utilization . 157

6.5 Relation Between the Level of the Spare Capacity Budget and the Feasibility of Schemes (JSCA-based PWCE, Sub-optimal Solution to JSCA-based PWCE, MSCA-based PWCE) 160

6.6 Comparison of the Volume of Working Capacity Envelope under Different Approaches (JSCA-based PWCE, the Sub-optimal Solution to JSCA-based PWCE) given the spare capacity budget (Level II) . 160

6.7 Comparison of the Volume of Working Capacity Envelope under Different Approaches (JSCA-based PWCE, the Sub-optimal Solution to JSCA-based PWCE, MSCA-based PWCE) given the spare capacity budget (Level III) 162

6.8 Comparison of Resource Usage under Different Approaches (IRAP, JSCAP, MSCAP) 164

6.9 Comparison of the Volume of Working Capacity Envelope under Different Approaches (JSCAP-based PWLE, MSCAP-based PWLE) given the spare capacity budget (Level III) 166

Chapter 1

Introduction

Internet technology is becoming more and more complex with the continuously increasing demand for high bandwidth services. Supporting over a billion users, it runs over a backbone transport network system serving not only the Internet but also other services including mobile communication, bank machines, leased lines, etc. Various services are accommodated in corresponding virtual networks built on top of the common infrastructure of the transport network. Therefore, the number of users supported by transport network is much greater than that by Internet.

The transport network has been supported by the photonic communication technology, notably wavelength-division multiplexing (WDM) and photonic ultra-high-capacity switching devices such as optical cross-connects (OXCs). With the WDM technology, hundreds of independent lightpaths are allowed to be multiplexed along a single fiber carrying huge amount of data traffic steered by the

OXCs. Due to the potentially huge amount of bandwidth carried in a single fiber, the occurrence of a failure may affect millions of end users. Hence, network survivability, which is concerned with how to minimize the impact of failures when they happen, is of paramount importance to today's transport network and is the central topic of this thesis.

In some transport networks that are based on microwave towers and satellite transmission systems, the network is as reliable as the individual components (i.e., the reliability of satellite ground stations and microwave towers). It is fairly difficult to "cut"electromagnetic waves except in the extreme case of weather disturbances and magnetic storms. Redundant microwave transmission equipment that is securely protected inside an operator's premises rarely break down. Optical fiber technologies have largely overtaken microwave transport networks because of their incredible capacities of carrying data. However, optical fibers are housed in cables that are routed across thousands of miles of land, over poles, underground, under-water and cable cuts are fairly common and frequent occurrence. Optical network transmission and receiving equipment is also far more complex than microwave or satellite equipment and is therefore relatively less reliable. Fiber cuts cause outages in many higher layer services simultaneously and therefore affect a lager number of users at once.

To minimize the impact of failures, survivability mechanisms have been developed in optical networks to provide service replacement solutions in the event of

network failures so that service may fully or partially continue for some or all of the clients that would otherwise lose service. A recent development in transport network survivability is p-Cycle (Pre-configured Protection Cycle) [2][3][4]. It offers fast protection switching by pre-configuring spare capacity for protection along the cycle. It also achieves high spare capacity efficiency by supporting independent routing of traffic without constraints arising from the placement of protection structures. p-Cycle offers an intriguing and promising alternative to conventional optical network technologies and thus there is considerable motivation to further explore this technology. This thesis is comprised of four advanced studies of transport network survivability mechanisms for dynamic traffic based on p-Cycles and the extensions. The ultimate aim is to design economically viable communication backbones that survive network failures elegantly, simply and quickly. In the subsequent sections of Chapter 1, we will introduce some of the fundamental concepts of this field including the basics of communication network architecture and network failures, followed by the objectives and scope of this thesis.

1.1 Communication Network Architecture

Communication networks can be categorized into three-level hierarchy based on function and size: Local Area Networks (LAN) that are contained within a building or a small area, Metropolitan Area Networks (MAN) that cover a metropolitan area

or a campus, and Wide Area Networks (WAN) that can extend to wide areas up to thousands of kilometers [5]. LAN is typically characterized by a wide range of access mechanisms and protocols and usually represent the outer edge of the communication network infrastructure. In LANs (access networks), all kinds of traffic from resident users, which can be dial-up, Digital Subscriber Line (DSL) or on cable modems, are aggregated at a local switching office and are routed onto a larger MAN.

MANs are positioned at the second level of the hierarchy. MANs typically use fiber optical cables as underlying physical transport technology providing date rates ranging from DS1 at 1.5Mbit/s to OC-192 at 10Gbit/s. An average sized city is typically covered by many MANs which exchange data through points of presence (POPs). Traffic that is not destined for the neighboring MANs is then aggregated onto a WAN which is positioned at the top of the hierarchy. Almost completely boosted by fiber optic systems, WANs normally span thousands of kilometers and carry intercontinental traffic. Because of the huge capacity and operational expenses that WANs are involved due to their size and function, the infrastructure has been nationalized in many countries. Figure 1.1 shows a network which is geographically partitioned into three separate sub-networks. The LAN connects the corporate or residential users to nearby central offices, which are connected together by the MAN. The MAN usually contains one or more big hubs which transit all the traffic that is going out of the MAN into the WAN.

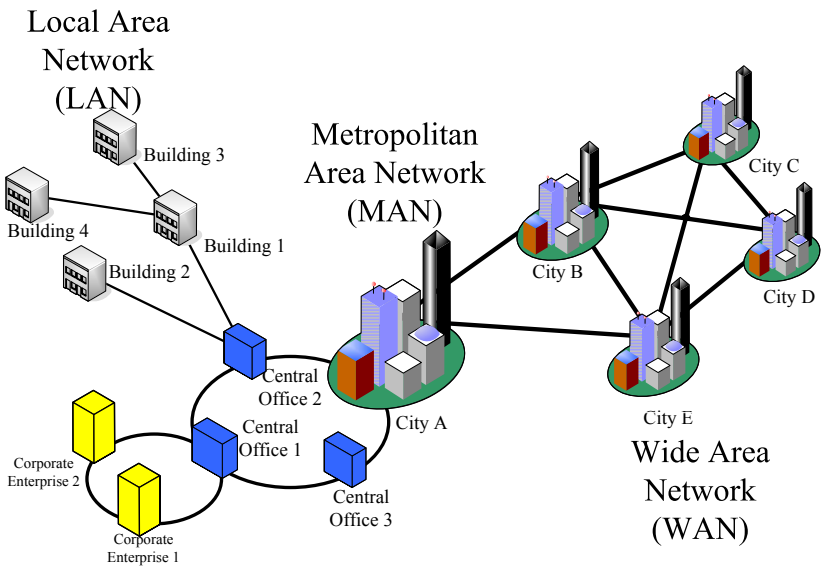

Figure 1.1: Illustration of Access, Metropolitan and Long-haul Networks

MANs and WANs are referred to as Transport Networks. In MANs and WANs, the main goal is to reliably transport huge amounts of data bits from one point to another without actually considering details about the services that generated them. In this thesis, we primarily deal with problems that address issues in MANs and WANs.

1.2 Network Failures

Any modern network can fail at some unspecified time. In some transport network such as microwave or satellite networks, it is fairly difficult to “cut”electromagnetic

waves. Redundant microwave equipment is normally securely protected inside operators' premises. Hence, the network is usually as reliable as the individual components. In optical network, optical fibers on the other hand are housed in cables which are routed across thousands of miles of land, underground, underwater, etc. Therefore, cable cuts are the most frequent causes of failures of fiber-based backbone networks.

A study in [6] estimated that any given mile of cable will operate about 228 years before it is damaged (4.39 cuts/year/1000 sheath miles). This means more than one cut per day on average on 100,000 installed route miles, which implies one failure occurs every day for a typical Long-haul Network and one failure every four days for a typical MAN. In 2002, the Federal Communications Commission (FCC) published findings that metro networks experience 13 cuts for every 1000 miles of fiber per year, and long-haul networks experience 3 cuts for 1000 miles of fiber [7]. The frequency of cable cut events is hundreds to thousands of times higher than reports of transport layer node failures. Moreover, cable cuts cause outages in many higher layer services simultaneously and therefore affect a large number of users at once, which could lead to huge financial losses and significant societal impacts. Therefore, network survivability designs in this thesis focus on recovery from span failures arising from cable cuts.

1.3 Network Survivability

The ability of a network to protect against unexpected failures has become an increasingly important issue in today's environment where network operators, service providers and customers are constantly emphasizing the need for reliable communication. The Alliance for Telecommunications Industry Solutions (ATIS), a standards development organization, defines network survivability [8] as (1) the ability of a network to maintain or restore an acceptable level of performance during network failures by applying various [post-failure] restoration techniques, and (2) prevention or mitigation of service outages from network failures by applying preventive techniques.

To prevent network from cable cuts, the network designer/planner has two possible options. The first option is to protect fiber cable by adding metallic sheathing, using deep concrete ducts, burial in the earth, mooring to the seafloor, etc. However experience has shown that there is really no way to protect each and every mile of cable against essentially random events [9]. Instead of concentrating only on physical cable protection, the second option is to develop repair protocols and mechanisms such that when a cable gets cut, the failed data connections can be re-established automatically through alternate routes over redundant capacity pre-planned into the network. Physical cable repair can then be carried out while

the network is in the alternate working state. Once the repair is complete, the re-routed services can revert back to their normal routes. The time taken to physically re-splice or reconnect the cable will generally not affect the end users.

As shown in Fig. 1.2, various survivability schemes can be employed at four levels, namely physical layer, system layer, logical layer and service layer [1]. Each layer has a generic type of demand unit that it provides to the next higher layer. In this thesis, network survivability designs focus on logical layer techniques. Various basic survivability techniques at different layers will be reviewed in Chapter 2 where the advantages and limitations of different techniques will be compared and discussed.

1.4 Research Objectives and Scope

While various survivability schemes can be employed at different levels, this thesis focuses on designing survivability schemes in the logical layer for dynamic traffic. A recent development in transport network survivability is the p-Cycle-based Protected Working Capacity Envelope (PWCE) [1] [10] [11]. The concept of PWCE was first explored in a span-restorable network. It basically partitions the total network capacity into a working capacity and a protection capacity. The protection capacity is designed to guarantee restorability from any span failure. p-Cycle-based PWCE is an application of PWCE to p-Cycle protected networks by having a set of

Layer	Element	Service and Function	Demand Units Generated	Capacity Units Provided	Generic Survivability Techniques
Service	IP routers, LSRs telephone switches, ATM switches, smart channel banks	Circuit-switched telephone and data, Internet, B-ISDN private networks, multi-media	OC-3, OC-12, STS-1s, DS-1s, DS-3s GbE, etc.	N/A	Adaptive routing, demand splitting, application reattempt
Logical	OXC, DCS, ATM VP X-connects	Service grooming, logical transport configuration, bandwidth allocation and management	OC-48, OC-192, wavelength channels, wavebands	OC-3, OC-12, STS-1s, DS-1s, DS-3s GbE, etc.	Mesh protection or restoration, DCS-based ring p-cycle
System	SONET OC-n TM, LTE, ADMs, OADMs, WDM transmission systems	Point-to-point bit transmission at 10 to 40 Gbs/s, Point-to-point fiber or wavelengths	Fibers, cables	OC-48, OC-192, wavelength channels, wavebands	1:N APS, 1+1 DP APS, rings
Physical	Rights-of-way, conduits, pole-lines, huts, cables, ducts	Physical medium of transmission connectivity	N/A	Fibers, cables	Physical encasement, physical diversity

Figure 1.2: Survivability Schemes at Various Layers (Adapted from [1])

p-Cycles structured within the protection capacity to protect the working capacity. p-Cycle is a pre-configured span-protection scheme combining the speed of a ring topology and the efficiency of a mesh topology [2] [3]. Therefore, p-Cycle-based PWCE inherits p-Cycle's advantages in fast response time and high efficiency.

Nonetheless, among the literature on p-Cycle-based PWCE, the work in [11] assumes that each network node is equipped with full wavelength conversion capability which is expensive and currently not practical. To address this, p-Cycle-based PWCE with wavelength continuity constraint has been developed in [12]. However, although constructed for dynamic traffic, the optimal set of p-Cycles in [12] has been designed without considering matching demand patterns. Also, the service time of every connection request has been assumed to be infinite so that connections are not released once established. Meanwhile, there has been significant interests in extending the conventional span-protecting p-Cycle concept to a path-oriented framework for higher capacity efficiency. In the literature, the conventional span-protecting p-Cycle concept has been extended to path-segment protection in [13] and end-to-end path protection in [14]. In [14], Failure Independent Path-Protecting (FIPP) p-Cycle is proposed to achieve end-to-end failure independent path protection for span or node failure while maintaining the property of pre-configuration. Compared with span-protecting p-Cycles, FIPP p-Cycles exhibit very high capacity efficiency because of their path-oriented protection mechanism. Nevertheless, FIPP p-Cycles are more suitable for static traffic than for dynamic

traffic as they are designed based on pre-defined end-to-end working paths. While most of the research works focus on simple p-Cycles, non-simple structures have also been explored in [15] to enhance capacity efficiency by combining non-simple p-Cycles and pre-configured links. However, this is out of the scope of this thesis as we focus on simple p-Cycles throughout this thesis.

In this thesis, we design a scheme, called Protected Working Lightpath Envelope (PWLE), with the features of pre-configuration, path-orientation and the flexibility in dynamic routing to achieve high capacity efficiency and good blocking performance with much less wavelength conversions under dynamic traffic. Dynamic traffic is defined as traffic requests that arrive and depart dynamically following the Poisson Process throughout this thesis. The thesis explores the new scheme from the following four aspects:

1. The concept, the design, the issues of routing and operation of PWLE
2. Cycle generation and selection algorithms tailored for PWLE
3. Incorporating the network connectivity constraint in the design of PWLE to enhance the actual utilization of the protected capacity
4. Efficient configuration of p-Cycles in the presence of time-variant traffic

The first three aspects focus on the different issues of the design of PWLE and its variation, Connectivity Aware Protected Working Lightpath Envelope (CAP-WLE)(to be introduced). We first propose PWLE as a promising path-oriented

survivability scheme for dynamic traffic, which possesses the advantages of high capacity efficiency, good blocking performance, guaranteed optical transmission quality and much less wavelength conversions in comparison with p-Cycle-based PWCE. While PWLE can be designed for any particular traffic pattern, PWLE can also be employed when traffic forecasts are not available. Numerical studies based on Linear Programming and simulations have been carried out to show that PWLE could become a good alternative to existing survivability schemes for dynamic traffic. We next study effective cycle generation and selection algorithms which reduce the complexity of the cycle selection process of PWLE and yet produce solutions that are close to the optimal. These algorithms greatly enhance the potential of PWLE for practical applications. Finally we propose Connectivity Aware Protected Working Lightpath Envelope (CAPWLE) which further improves the design of PWLE by taking into consideration the impact of network connectivity on the actual utilization of protected capacity. We provide numerical results which show that, compared with PWLE, CAPWLE would improve the actual utilization of the protected capacity and thus improve the blocking performance under dynamic traffic characterized by various traffic patterns.

While most of the above works focus on the dynamic traffic which can be characterized by, if available, a single traffic matrix, we are also interested to carry out studies on time-variant traffic as traffic entering a network is intrinsically variable in time. Our final work provides an effective approach of configuring

p-Cycles to greatly improve the capacity efficiency of the survivability scheme under time-variant traffic characterized by a set of traffic matrices. We start with the conventional span-protecting p-Cycles and extend to several p-Cycle-based survivability schemes including PWLE.

Although there exist other promising path-oriented survivability schemes for dynamic traffic, such as SBPP (to be reviewed), this thesis focuses on pre-configuration strategy based particularly on p-Cycles because of their uniqueness of combining the capacity efficiency of a mesh topology and the speed of a ring topology. Besides, incorporating pre-configuration brings the benefits such as having a static protection layer and simplifying operations.

1.4.1 Thesis Outline

The remainder of the thesis is organized as follows:

Chapter 2 reviews several background topics in transport networks and research work related to this thesis.

Chapter 3 introduces the concept of Protected Working Lightpath Envelope (PWLE) and explores its design issues, including a technique organizing the protected capacity and the optimization model based on the Mixed Integer Linear Programming (MILP) formulation. The issues of the routing and operation of PWLE are addressed. Numerical studies are carried out on PWLE optimization, blocking performance as well as the control overheads of the routing algorithm

designed for PWLE.

Chapter 4 explores the issues of cycle selection for PWLE in two steps. Firstly, an algorithm, called AttachNode-Based Cycle Generation (ANCG), is developed for the pre-computation of candidate cycles in order to generate high quality cycles. Secondly, heuristic algorithms are developed to address the issue of cycle selection from the high quality cycles generated by ANCG.

Chapter 5 introduces the motivation and design of Connectivity Aware Protected Working Lightpath Envelope (CAPWLE), where a new concept called *Effective Envelope* is defined followed by the elaboration on its calculation method. Based on *Effective Envelope*, CAPWLE is then optimized using MILP.

Chapter 6 discusses the issues of configuring span-protecting p-Cycles in a capacity-efficient way under time-variant traffic, where the key idea of Joint Static Configuration Approach (JSCA) is introduced. The optimization model of JSCA and its sub-optimal solution are provided. Then the approach is extended to other p-Cycle-based survivability schemes including PWLE.

Chapter 7 concludes and summarizes the contributions of the work presented in this thesis and suggests some future research directions.

1.5 Thesis Contribution

This thesis proposes a survivability scheme for dynamic traffic, called PWLE, which has the advantage of higher capacity efficiency, better blocking performance and much less wavelength conversions compared with p-Cycle-based PWCE. To enhance the practicability of PWLE, algorithms for generating high quality cycles and cycle selections are also developed to achieve near-optimal solutions with much less complexity. Based on PWLE, a more advanced scheme, called Connectivity Aware Protected Lightpath Envelope (CAPWLE), is also proposed to incorporate the impact of network connectivity into the design of PWLE. The goal of CAPWLE is to improve the actual utilization of the protected capacity so that the blocking performance is improved under dynamic traffic. Finally, this thesis also investigates the configuration of p-Cycles under time-variant traffic to achieve a static network configuration with minimal spare capacity usage.

Chapter 2

Background and Related Work

As discussed in **Chapter 1**, in transport networks, the main goal is to reliably transport huge amounts of data to support a variety of upper layer services and applications. In this chapter, we first review several background topics in transport networks. Then we review different survivability schemes in various layers: physical layer, system layer, logical layer and service layer.

2.1 Fundamentals of Transport Networks

2.1.1 Layering

Today's backbone communication networks are structured in a multilayered fashion. The networks are usually composed of several resource layers, corresponding to different technologies that are stacked one upon another in order to achieve the

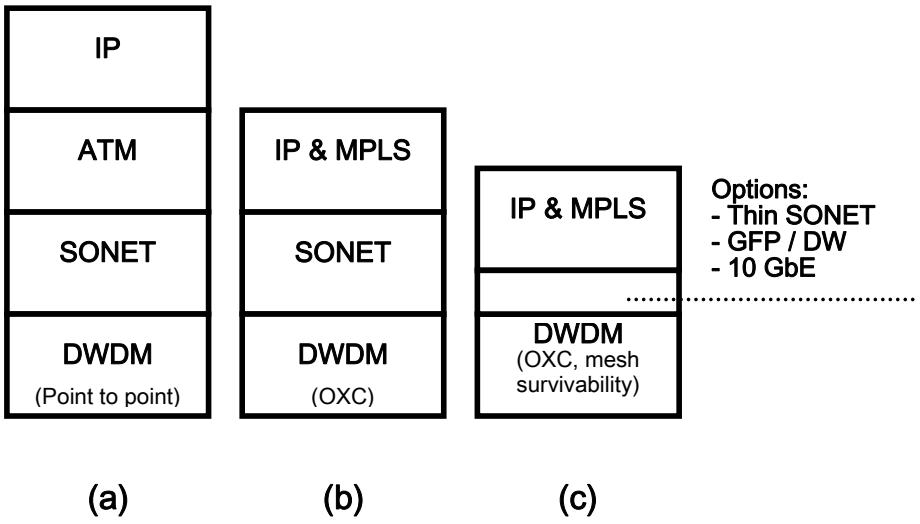

Figure 2.1: Transport Network Layering (Adapted from [1])

desired overall network functionality. Each layer has a set of important functions, and the interface between the different layers is well defined and standardized. In general, layering decreases overall system complexity when designing transport networks by precisely defining the inter-layer communication interface.

Figure 2.1 (a) shows a commonly used architecture which is IP over ATM over SONET over DWDM. Nowadays, IP traffic constitutes the majority of traffic carried in the networks. However, IP does not have any traffic engineering capabilities, QoS, or reliability-assuring mechanisms. Therefore, ATM is deployed to provide quality of service (QoS), reliability and flow control. Running IP over ATM complements IP with the features it lacks. Further, SONET is used as a transport

layer to carry traffic over fiber, because of its low delay, low error rate, inbuilt protection switching, and functionalities for management and monitoring. Finally, DWDM is used to effectively increase and share the capacity of fibers [1].

Unfortunately, multi-layered networks often result in inefficient resource utilization. Large traffic volumes make this inefficiency not acceptable. Hence, new and more efficient architectures are called for, which are shown in Fig. 2.1 (b) and (c). IP/MPLS over DWDM shown in Fig.2.1 (c) is the layer model for future networks evolving through the intermediate step shown in Fig. 2.1 (b). In IP/MPLS over DWDM model, functions of ATM are replaced by generalized MPLS (GMPLS) while many functions of SONET are delegated to DWDM. Still, a thin layer between IP/MPLS and DWDM will remain to convert the upper layer traffic into bit strings for the physical transmission, flow control, framing, error monitoring, etc. Transport network topology will also change with SONET rings being replaced by mesh interconnected Optical Cross Connects (OXCs) for the implementation of more effective recovery mechanisms.

2.1.2 Switching Technology

In transport networks, network nodes include Central Office buildings, electrical systems, and all the switching and line termination equipment located at the central offices. Among various types of switching elements, there are two basic types:

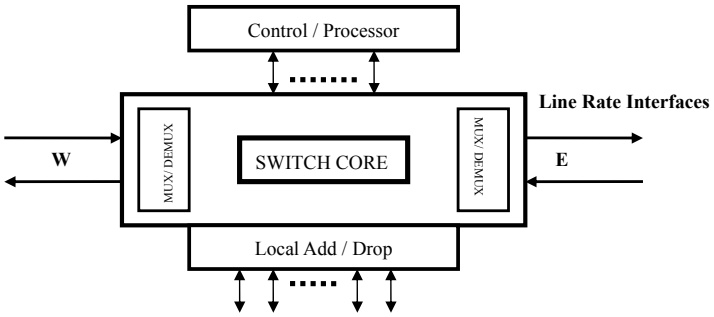

Figure 2.2: Functional Block Diagram of an ADM

- the Add Drop Multiplexer (ADM)
- the Digital and Optical Cross Connect Switch

We herein briefly introduce some of the key features of both these technologies.

Add Drop Multiplexer (ADM)

An ADM is a terminating device with only two main line rate interfaces which are typically referred to as East and West lines. An ADM may also have local ports that permit it to drop lower tributary rate traffic with destinations local to the ADM or to add locally soured tributaries into the outgoing interface. Figure 2.2 shows the functional block diagram of a typical ADM. More often ADMs are used in survivable ring architectures where the SONET K1/K2 byte-protocol supports rapid line-level protection switching.

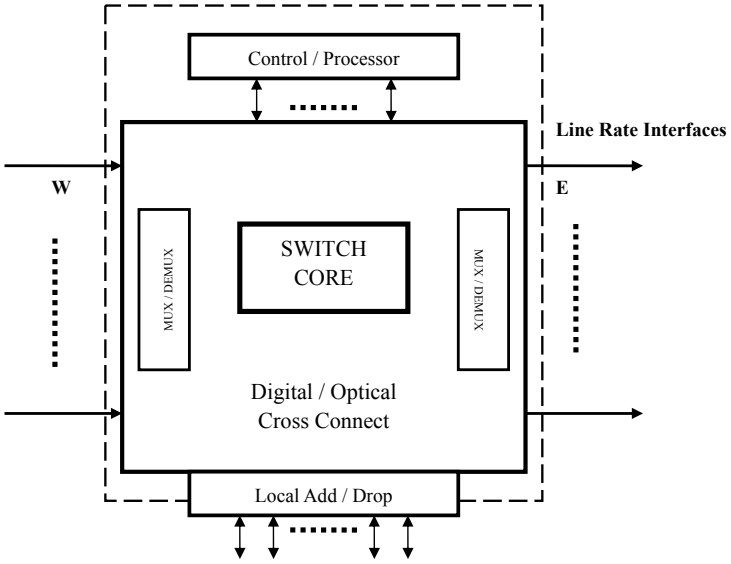

Figure 2.3: Functional Block Diagram of a Digital/Optical Cross Connect Switch

Digital/Optical Cross Connect Switch

A digital Cross-Connect Switch (DCS) is defined as a device which has the ability to switch data from a given input port to a specified output port. Figure 2.3 shows a functional block diagram of a typical DCS. An Optical Cross Connect (OXC)is a type of DCS that interfaces with optical fiber and switches data between wavelengths or fibers. In most cases, DCS and OXC are logically the same when discussing network design. Similar with ADMs, all cross connects have the same add-drop functionality allowing local traffic to be added or dropped. The major difference between an ADM and an OXC is the total capacity handled. An OXC may have hundreds of fibers, each may support different line-rates, terminated on

its interfaces. Hence, an OXC has a large switch core which can be either electronic or optical. For these OXCs with electronic switch cores, they are often referred to as Optical-Electrical-Optical (O-E-O) switches and need to convert the optical signals to the electrical domain before making any routing/switching/drop decisions. As electrical processing is currently limited to about 40 Gbps while a fiber can carry around 30 Tbps, it is thus attractive to adopt optical switch cores to switch the optical signal in the optical domain. Though being researched extensively, the commercial availability of Optical-Optical-Optical (O-O-O) switches is still a few years away.

2.1.3 Wavelength Division Multiplexing

Wavelength division multiplexing (WDM) refers to the scheme in which multiple optical carriers at different wavelengths are modulated by using independent electrical bit streams and are then transmitted over the same fiber. The optical signal at the receiver is demultiplexed into separate bandwidth offered by optical fibers. Extensive research works have been done to address the concepts, issues and network elements in WDM [16] [17] [18]. WDM has the potential to drastically increase the total available span capacity between existing nodes. For example, hundreds of 10-Gbps channels can be transmitted over the same fiber when channel spacing is reduced to below 100 GHz. A WDM system capable of carrying up to six wavelengths per fiber is called a Coarse WDM (CWDM) system while Dense

WDM (DWDM) systems may support many hundreds or thousands of wavelengths simultaneously. In DWDM the lasers are operated at very close frequencies. In CWDM, in contrast, up to four or six lasers operate at widely separated frequencies.

In DWDM networking, "all-optical" networking refers to transport networking in which each DWDM wavelength path must be routed from its source to destination without any electronic processing at intermediate nodes. The resulting path is said to be "transparent" because there is no dependency on the payload being in a specific format in terms of framing, bit-rate, line-coding, power level, jitter and so on, which is usually the case when electrical circuits are involved en route to handle the signal. Such an all-optical path that does not change wavelength is also called a pure Wavelength Path (WP). A pure WP network would also employ only O-O-O switches which generally take less power and space than the corresponding O-E-O switches.

The opposite of a WP network is called a Virtual Wavelength Path (VWP) network that is completely opaque. In a VWP network, each path may use various wavelengths along its route as at each node, the path is switched and managed in the electrical domain. At each node in this network, a device called a wavelength converter (WC) converts the data from one wavelength to another. Currently WC requires electrical processing. A fully opaque network implies O/E and E/O transponders at each node and large electronic switching cores, which are expensive

and power-consuming operating at 10 to 40 Gbps. Therefore, using large electronic core optical switches to form an entirely opaque network may not be feasible. To strike a balance between a WP network (transparent) and a VWP network (opaque), the concept of translucent optical networks was introduced. The key idea is to either have a relatively small set of O-E-O switches that can perform wavelength conversion and/or regeneration, or have small regions in the network called islands of transparency that are interconnected by O-E-O gateways.

2.2 Network Survivability Techniques

Survivability issue concerns how to minimize the impact of failure when it happens. The underlying principle of all survivability schemes is to provide redundant capacity to support re-routing of working capacity when failure happens. The main research problem in survivability scheme design is to develop a suitable compromise between two opposite targets: providing enough redundant resources for all demands to survive failure but with minimum cost. To minimize resource needs, the sharing of backup capacity is explored to protect against uncorrected network failures. However, if the primary working paths, which share backup resources, fail simultaneously, only one of the primary working path can survive by getting the backup services. Hence, the reduction in backup resource can degrade the level of survivability. According to [19], various survivability techniques can be employed

at four levels, namely physical layer, system layer, logical layer and service layer.

2.2.1 Physical Layer Survivability Techniques

The physical layer is the infrastructure of physical resources that provides geographical and media assets. In this layer, survivability schemes are primarily aimed at physical protection of signal-bearing assets and ensuring that the physical layer topology has a basic spatial diversity so as to enable higher layer survivability techniques to function. Physical layer survivability techniques fall into three categories.

- **Geographical diversity** : pairs of buildings are connected via multiple paths that do not share the same locations.
- **Security to human-caused intrusion** : increase and maintain a high level of physical security so as to ensure protection from damage caused by persons intent on disrupting telecommunication services.
- **Tolerance** : enhance building and telecommunication systems' ability to tolerate external and environmental effects.

2.2.2 System Layer Survivability Techniques

Next layer is the system layer. It represents the network transmission systems. Survivability techniques at the system layer are usually pre-armed and categorized as protection. The main characteristics of a protection scheme is that the protection

route and standby capacity are predefined. It usually involves redirecting the composite optical line signals as a whole without processing or identifying any of its constituent tributaries. We herein discuss several most commonly used solutions, namely Automatic Protection Switching (APS) and rings.

Automatic Protection Switching (APS)

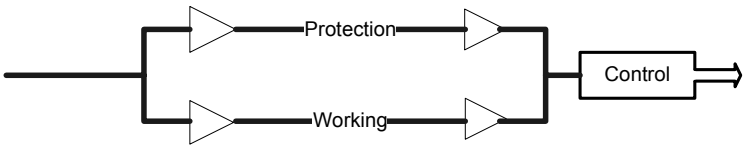

Figure 2.4: 1+1 APS system

APS is the simplest optical network survivability technique. In 1+1 APS, the same data is sent over two fibers simultaneously. The tail-end node monitors the two fibers and simply chooses the one with better optical signal quality [20]. Fig. 2.4 shows a simple 1+1 APS system. 1+1 denotes a dedicated standby arrangement: one working system and a completely reserved backup system in which the transmit line signal is copied and drives both signal paths. The fastest possible switching speed is obtained with 1+1 because the receivers need only monitor both received signal copies and switch from one to the other if either fails. In 1:1 APS, a variation of 1+1 APS, the backup fiber is allowed to route low-priority traffic when not in use for protection. Furthermore, the 1+1/1:1 Diverse Path (DP) APS variation adds the requirement of geographic diversity between the working and protection

fibers, thereby ensuring survivability to a cable cut. Other variations can be 1:N and M:N APS where one (or 'M') protection fiber is allowed to be shared among 'N' working fibers so as to improve capacity utilization of the system. A more in-depth review of APS can be found in [1].

A drawback of APS is that it is impossible to add or drop individual channels at intermediate locations. APS carries the entire traffic from the origin to the destination and is therefore justified only if large point-to-point demand exists. Hence, we have two main ring-based type systems evolving from APS systems, namely Unidirectional Path Switched Rings (UPSRs) and Bidirectional Line Switched Rings (BLSRs).

Unidirectional Path Switched Ring (UPSR)

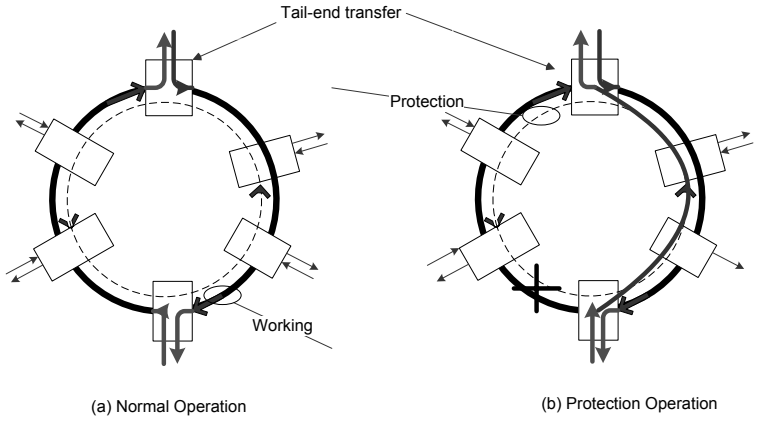

Figure 2.5: UPSR protection operation

UPSR can be viewed as a number of 1+1 APS systems on a set of nodes

aggregated onto a common closed-loop path as shown in Fig. 2.5(a). Nodes are connected by two fiber rings where one clockwise ring is called "working" ring and one anticlockwise "protection" ring. Under normal conditions, the demand between pairs of nodes in the ring is transmitted on the working fiber in one direction around the ring. A copy of each demand is also transmitted on the protection fiber in the opposite direction. At the receiving node, a path selector continuously monitors the working and protection signals and switches from the working to the protection fiber when the working signal is lost or degraded. Protection switching decisions are made individually for each path rather than for the entire line. Therefore, no signaling is needed in UPSR. For instance, as shown in Fig. 2.5(b), in the case of a cable cut, the tail-end node switches from the working fiber to the protection fiber. Notice that the working signal is transmitted all the way around a UPSR, which implies that the total demand on any span equals the sum of all the demands between all nodes on the ring. This implies that the UPSR line transmission rate must be greater than the sum of all demands served by the ring. Besides, there is no sharing of backup capacity in UPSR, which means UPSR is at least 100% redundant. For more information about UPSR, please refer to [21].

Bidirectional Line Switched Ring (BLSR)

Unlike UPSR which uses receive path selection, BLSR protects affected demands by looping the entire working line signal back onto the protection fiber at both

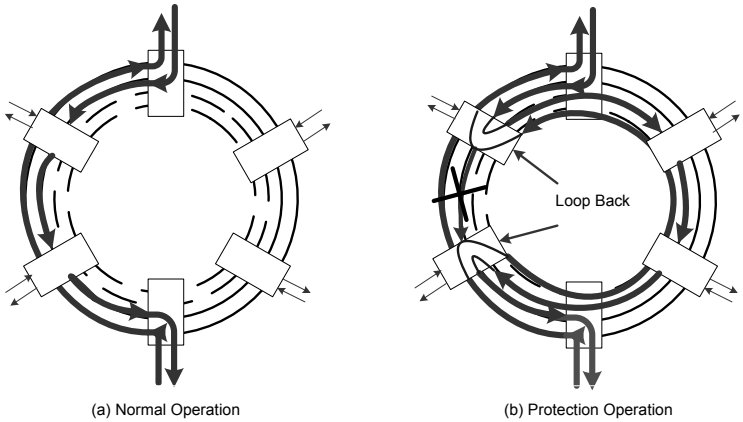

Figure 2.6: BLSR protection operation

nodes adjacent to the failed segment as shown in Fig. 2.6. Therefore, the access to the protection facility must be coordinated at both end nodes of the failure and signaling is needed. An advantage of BLSRs over UPSRs is that the channels can be reused around the ring and the protection bandwidth is shared among all working span sections. The demands travel directly between the source and destination nodes and are usually routed on the shortest paths between nodes on the ring instead of being all the way around the ring as in a UPSR. This implies that the same channel can be reused for other demands on unused spans and the load on any span equals the sum of demands that are routed over that span in contrast to the sum of all demands served by the ring as in a UPSR. As to the protection capacity of BLSR, although it is shared among multiple different working sections, the protection fiber system has to have equal capacity to the working system so as to guarantee 100% restorable. For more details of BLSR, please refer to [22].

Ring Covers

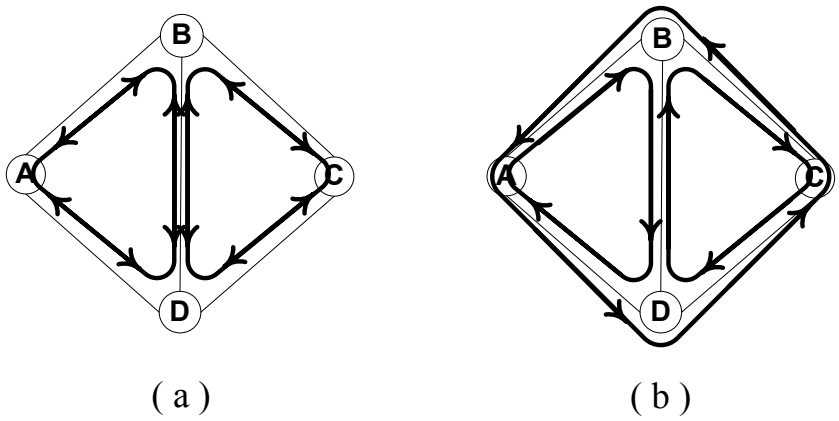

Figure 2.7: Illustration of OCDC

A single BLSR is usually said to be 100% redundant because each pair of bidirectional working fibers is provided with a pair of protection fibers. However, when transport networks are designed with multiple interconnected rings, the total installed capacity is usually much more than two times the capacity needed only to route all demands via shortest paths. One reason is that as the routing of demands has to follow ring-constrained paths rather than shortest paths over the graph, it takes longer routes than they otherwise would. Another reason is that ring covers usually involve some span overlaps where a span whose working capacity could be handled by one ring alone is yet covered by two rings for topological layout reasons. For example, in the network shown in Fig. 2.7, suppose each span needs to be covered by at least one BLSR ring. Then it is easy to see in general that

anywhere an odd-degree node is involved, an ordinary bidirectional cycle cover is not possible without at least one span overlap such as the two cycles overlapping on span B-D as shown in Fig. 2.7 (a).

The inefficiency of such overlaps can be avoided by using unidirectional rings instead of bidirectional rings. The technique called Oriented Cycle Double Covers (OCDC) was formally introduced in [23]. Figure 2.7 (b) gives a simple example to explain OCDC. In Fig. 2.7 (b), three unidirectional cycles are used instead of two bidirectional cycles used in Fig. 2.7 (a), which avoids the double coverage of span B-D in Fig. 2.7 (a). It has been shown that OCDC can achieve exactly 100% redundancy at the fiber level [23].

2.2.3 Logical Layer Survivability Techniques

All of the system layer protection schemes rely on fixed transmission and protection structures which are essentially static. In addition, after a first-failure occurs, nothing can be done to withstand a possible second failure during the period of repair. Besides, fixed system layer protection schemes do not support differentiated quality of protection.

The above consideration brings us to logical layer survivability schemes. Logical layer survivability schemes usually have the flexibility to create paths on demand between end-node pairs. They also enjoy high capacity efficiency achieved by mesh

restoration schemes which allow extensive sharing of protection capacity over non-simultaneous failure scenarios. We herein briefly introduce four commonly used solutions including p-Cycles which are closely relevant to this thesis.

Span Restoration or Protection

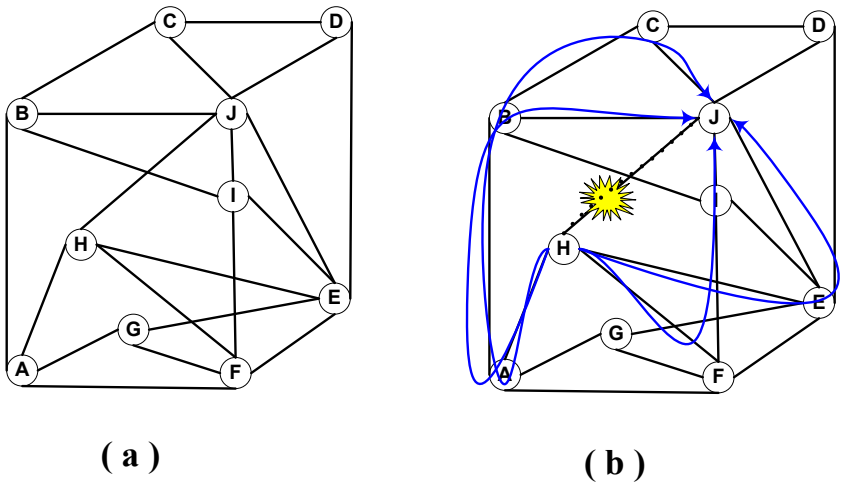

Figure 2.8: Illustration of Span Restoration (a) Network Topology (b) Restoration Routes

In span restoration, restoration paths re-route locally around the failed spans. Restoration paths are calculated and cross-connected in real-time. In the case of span protection, restoration paths follow preplans. Figure 2.8 depicts a simple example of span restoration in which Fig. 2.8 (a) shows the network topology and Fig. 2.8 (b) describes the restoration routes. As we can see in Fig. 2.8 (b), in the event of a span failure (on span H-J), all the traffic carried on the span are

re-routed locally through other routes connecting the end nodes of the failed span. It is important to note that while all the traffic on a single span is considered as a single commodity, multiple routes may be considered to effect survivability of the channels along the failed span, which is shown in Fig. 2.8 (b) using arrowed lines. In contrast, the rings (reviewed in Section 2.2.2) force the restoration of many channels to follow ring-constrained backup routes which are essentially the surviving sides of the rings. Studies have found that the capacity efficiency of a dynamic mesh network is quite high as compared to the corresponding ring network. An optimal spare capacity placement model of the path-flow type was proposed by Herzberg et al. in [24]. The Herzberg model is the foundation of many of the subsequent design models in this field. Span restoration in WDM networks is discussed in [25]. A detailed discussion is found in [1].

Path Restoration

In path restoration [26] [27] [28], restoration paths re-route between the end-nodes of the affected paths. Figure 2.9 shows an example where Fig. 2.9 (a) shows a working demand routed over a primary path described by the arrowed line and Fig. 2.9 (b) displays the possible backup paths in reaction to a span failure on span H-J. Comparing Fig. 2.8 (b) with Fig. 2.9 (b), we can find that span restoration reacts to the specific span failure by re-routing all the traffic carried by the failed span through alternative routes between the end nodes of the failed span whereas

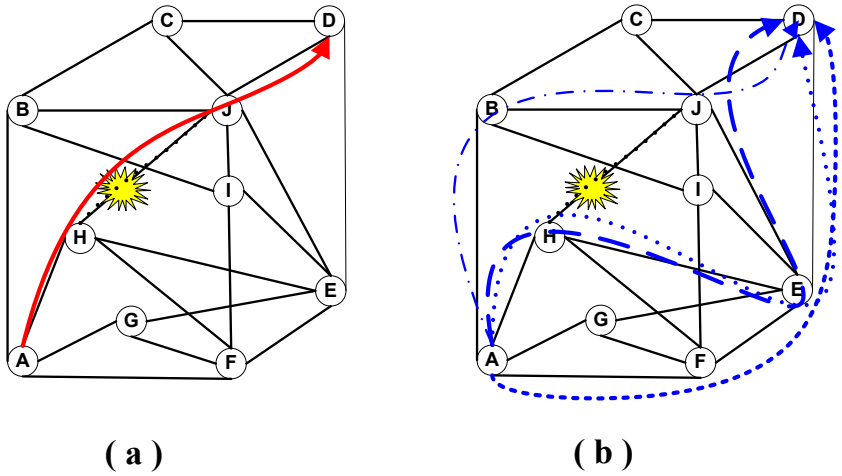

Figure 2.9: Illustration of Path Restoration (a) Working Path (b) Possible Backup Paths

path restoration reacts to the specific span failure by re-routing each single working demand (affected by the span failure) through alternative paths between the end nodes of the working demand.

Path restoration may or may not involve reusing the surviving working capacity of failed paths, which refers to "stub release". Stub release means that it is possible to release the surviving upstream and downstream portions of a failed working path and make the freed capacity available to the dynamic path restoration process. Hence, stub release makes path restoration a failure-specific scheme since the restoration response depends on the specific failure scenario. Span restoration can be viewed as a special case of path restoration with full re-use of stub released capacity. We use the example in Fig. 2.9 to explain. Among the four possible

restoration paths shown in Fig. 2.9 (b), only the path A-F-E-D (described by dotted arrowed line) shares no common span with the working path A-H-J-D. The other three all share some portion of the failed working path, which makes the calculation of the backup paths dependent on the location of the failure along the working path. The question of stub release does not arise with span restoration because the reconfiguration that occurs is around the failed span itself. However, the failure-specific stub-release routing of the backup paths in the network makes path restoration highly capacity-efficient. A more in-depth review of path restoration can be found in [1].

Shared Backup Path Protection (SBPP)

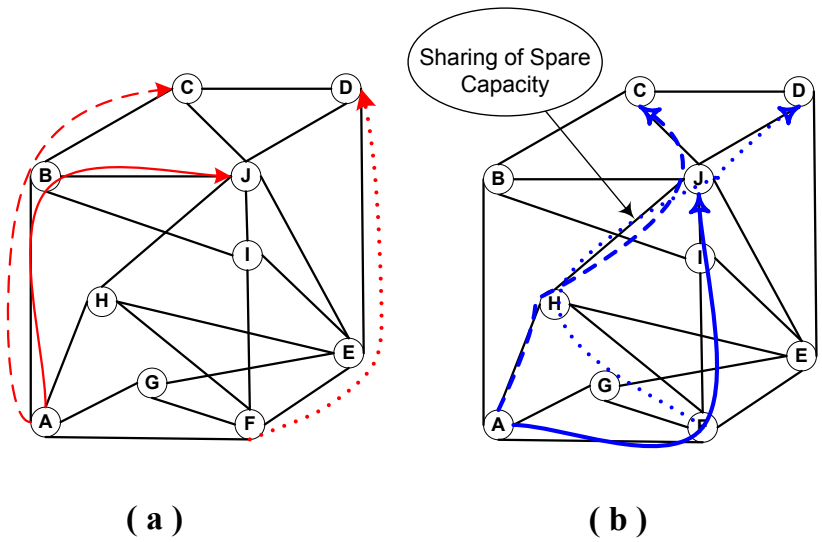

Figure 2.10: Illustration of Shared Backup Path Protection (SBPP)

Shared Backup Path Protection (SBPP) is a pre-planned path restoration

scheme standardized by the IETF [29] for use under Internet-style signaling protocols for protection of lightpaths in optical networks. In SBPP, one backup path is predefined for each working path. Although one or more backup paths are usually possible between the same end nodes of the working path, only one is chosen for the final design. To be eligible as a backup path for a working path, it has to have no span (or node if node failure is considered) in common with the path of the working path and no span (or node) in common with any other working path whose backup route has any span in common with the backup being considered. These considerations ensure that when a working path fails (under any single failure scenario) no span (or node) along its backup path is simultaneously affected. We use an example shown in Fig. 2.10 to explain. Figure 2.10 (a) shows three working demands routed over three paths A-B-C (dashed), A-B-J (solid) and F-E-D (dotted) whose backup paths are shown, respectively, in Fig. 2.10 (b) as A-H-J-C (dashed), A-F-I-J (solid) and F-H-J-D (dotted). Notice that backup paths are assembled on-the-fly when failure occurs. As the working paths A-B-C and F-E-D do not share any common span, their backup paths A-H-J-C and F-H-J-D share spare capacity on the common span H-J. In contrast, because the working paths A-B-C and A-B-J share the common span A-B, their backup paths have to be span-disjoint such as the backup paths A-H-J-C and A-F-I-J.

Further, no matter where the failure is located on the working path, restoration is via a path assembled on-demand over this one pre-determined backup path. The

approach in SBPP is simplified relative to path restoration as a single fully disjoint backup path is defined for each working path. This simplification allows failure-independent operation for each working path. Relatively high capacity efficiency is still achieved because the protection capacity is shared over backup paths whose working paths do not share common spans. Upon failure, protection paths need to be assembled in real time. Optimization models for SBPP are available in [30]. However, heuristic methods are often used such as in [31] and [32] because of the difficulty in solving SBPP's optimal design model. On the other hand, SBPP has several drawbacks. One of these is the need for each node to know the global capacity, topology and backup-sharing relationships to support dynamic provisioning with SBPP as discussed in [33] [34]. Therefore, every time a path arrives or departs, messages carrying the changes in network states need to be flooded to every single node in the network, thus leading to a non-trivial amount of control data. Besides, real-time assembly of backup path implies signaling and length dependence of restoration time.

p-Cycle

p-Cycle is a recently proposed survivability scheme [2][3][4]. In *p*-Cycle protected networks, protection capacity is formed into pre-configured rings which are similar to BLSR rings. However, working paths need not conform to ring structures but are instead routed independently and usually along the shortest routes. In other

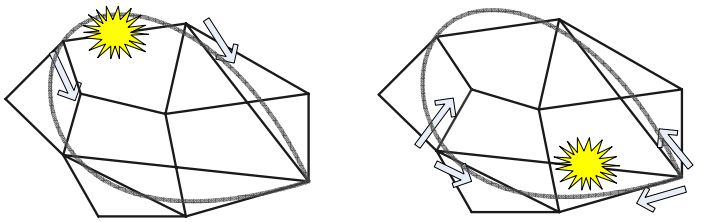

(a) On-cycle Span Failure (b) Straddling Span Failure

Figure 2.11: p-Cycle Protection Operation

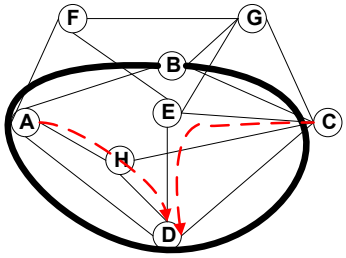

Figure 2.12: An Example of FIPP

words, p-Cycle protects both the on-cycle and straddling spans. For on-cycle failures, p-Cycle responds functionally similarly to the loop-back response in a BLSR ring (Fig. 2.11(a)). For straddling failures, p-Cycle provides two protection paths for a failed span (Fig. 2.11(b)), which effects a dramatic impact on the capacity utilization. Therefore, p-Cycle enjoys the speed of a ring topology and the efficiency of a mesh topology [2]. Although p-Cycle is originally introduced as a system layer technique, it can be easily implemented in the logical layer because of its concept of separating the routing of working flows from the configuration of

protection structures. In this case, OCX nodes can set up and tear down service paths on demand while configuring a set of p-Cycles independently.

While p-Cycle is originally proposed as a span-protection scheme, some research work has been carried out on the path-protection equivalent of p-Cycle. One such extension to a path-oriented framework is path-segment protecting p-Cycle which protects arbitrarily defined path segments rather than just spans [13]. Because of the fine-grained protection, a path-segment protecting p-Cycle has a higher capacity efficiency than a conventional span-protecting p-Cycle. However, the property of simple end-node fault detection and switch over activation is compromised and failure-specific operation is needed. A different approach has also been considered in [14] for the extension to a path-oriented scheme called Failure Independent Path-Protecting (FIPP) p-Cycle. Rather than path-segment protection, FIPP provides end-to-end path-protection with fully pre-configured backup paths and supports simple failure-independent end-node activation and control. For example, in Fig. 2.12, two working paths A-H-D and C-E-D, each carrying two units of demand, need to be protected. Then a FIPP A-B-C-D-A with one unit of spare capacity reserved on each on-cycle span is able to provide protection to these two working paths. The attractiveness of FIPP is that it remains comparable in capacity efficiency while achieving simplicity in failure-independent operation. Failure-independence herein means that whenever a failure occurs on a primary

path, its end nodes switch over to the predefined backup path without consideration of the fault location. This property is a major advantage in optical networks where fault location is slow or difficult. In addition to span failures, [35] proposed the concept of node-encircling p-Cycles (NEPCs) to combat against node failure.

Protected Working Capacity Envelope (PWCE)

PWCE was first exploited in the context of span-restorable network design [1]. Given a set of traffic demands, routing of the demands will generate the working capacity requirements on each span, based on which the allocation of spare capacity on each span can be designed to guarantee restorability from any span failure. This divides the total network capacity into a working layer and a protection layer. The application of PWCE to span-protecting p-Cycle protected network allows PWCE to possess the advantage of span-protecting p-Cycle in capacity efficiency and restoration speed [11] [12] [34]. The protection layer is structured and pre-configured using a set of span-protecting p-Cycles which divide total network capacity into a working layer and a protection layer as shown in Fig. 2.13 (c). The relationship between the two layers is that the protection layer offers 100% protection to the working layer. The protection layer remains static while the working capacity serves as a resource pool for dynamic service provisioning. We use a simple example of 7-node network shown in Fig. 2.13 to explain. Assuming each span in the network is deployed with 2 units of capacity, two span-protecting p-Cycles

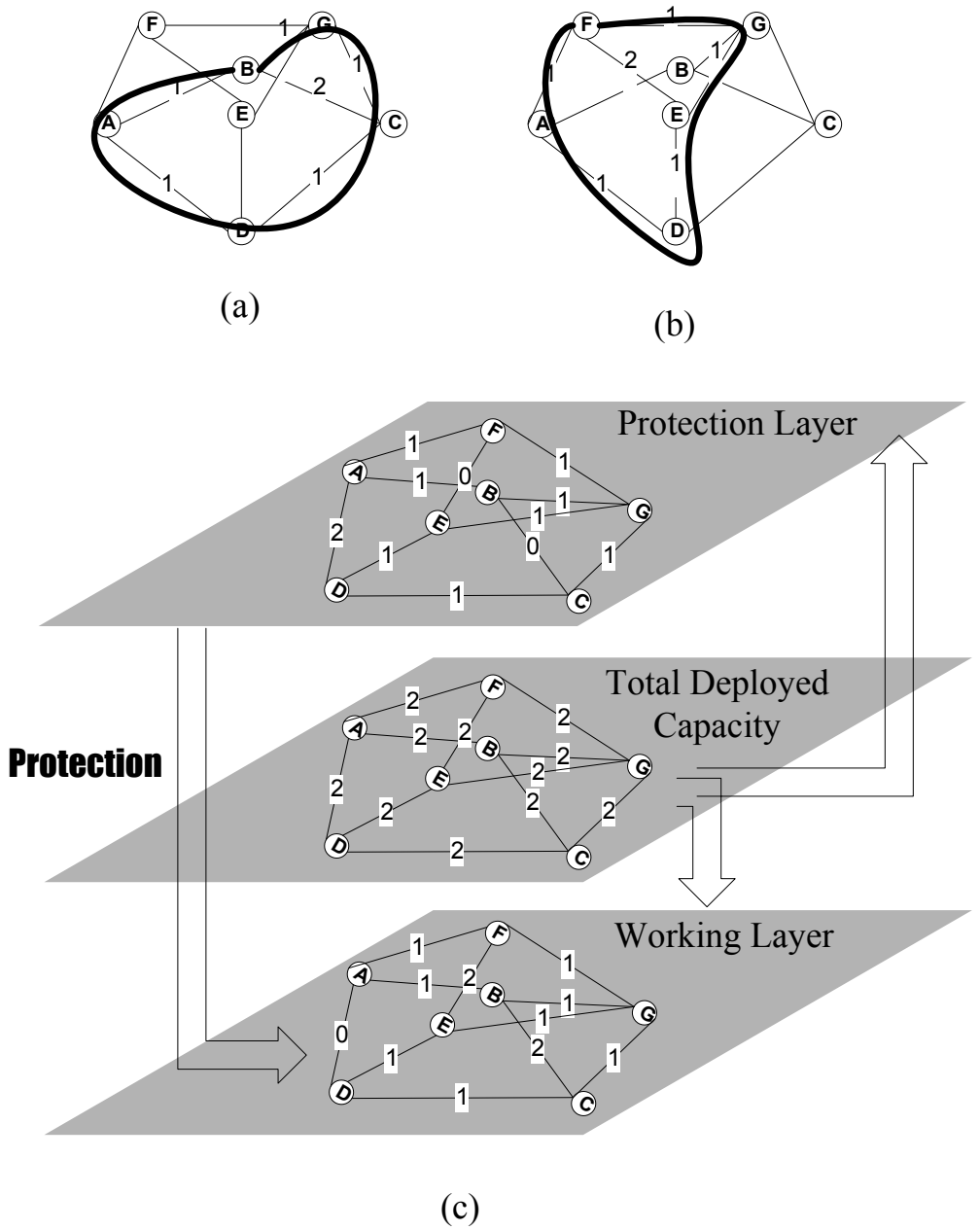

Figure 2.13: An Example of Protected Working Capacity Envelope (PWCE)

A-B-G-C-D-A (Fig. 2.13 (a)) and A-F-G-E-D-A (Fig. 2.13 (b)) are structured with one unit of spare capacity reserved on each on-cycle span. The maximum amount of working capacity that can be protected on each span by the two span-protecting p-Cycles is displayed, respectively, in Fig. 2.13 (a) and (b). Based on these two span-protecting p-Cycles, the total network capacity can be divided into a working layer (bottom in Fig. 2.13 (c)) and a protection layer (upper in Fig. 2.13 (c)).

In such network capacity division, the working layer is usually assigned with a much larger portion of total network capacity than the protection layer because the capacity division model normally targets minimizing the network spare capacity while maximizing the protected working capacity. Each survivable service provisioning only needs to establish a working path within the envelope of the protected working capacity in the working layer. Once a working path is established within the envelope, it is 100% protected by the protection layer. No explicit arrangement for protection of every individual request is needed.

Comparing p-Cycle-PWCE with SBPP, the most direct advantage of p-Cycle-PWCE over SBPP is that p-Cycle-PWCE does not have to make any online explicit arrangements for the protection of every individual request. Furthermore, as there is no need to concern about spare capacity sharing when provisioning survivable services in p-Cycle-PWCE, it is thus not necessary for the scheme to frequently update the global network state for every individual service setup (or takedown) as in SBPP, which thereby greatly simplifies the network service provisioning. It has

been shown in [36] [37] that p-Cycle-PWCE has favorable blocking performance relative to SBPP with greatly reduced signaling and network state overheads.

2.2.4 Service Layer Survivability Techniques

Service layer survivability schemes are usually based on software implementation that attempts to re-route within the working capacity visible at the service layer. A service layer re-routing response can complement a lower layer response if the latter is incomplete through logical reconfiguration of the paths or application of service prioritization to reduce delay or packet loss. While system and logical layer schemes tend to be fast-acting and either fully protect signals or not, service layer methods are generally more gradual and provide "graceful degradation" i.e. blocking, congestion and delay.

Dynamic routing in circuit switched networks and link-status adaptive routing schemes are two traditional service layer schemes. With the advent of IP-centric control, some of the logical layer schemes such as SBPP and p-Cycle are directly applied in the service layer. The main difference is that a physical circuit is replaced with a virtual path construct such as a VP or a LSP. Details of service layer survivability techniques can be found in [38].

2.2.5 Summary

In this Chapter, we have reviewed the background topics in transport networks including layering, switching technology and WDM. Then we have reviewed various survivability techniques in different layers, including physical layer, system layer, logical layer, and service layer. As this thesis focuses on survivability techniques in the logical layer, we thus have conducted a detailed review of logical layer survivability schemes including span restoration, path restoration, SBPP, p-Cycle, and PWCE.

Chapter 3

Protected Working Lightpath Envelope

3.1 Introduction

This chapter proposes Protected Working Lightpath Envelope (PWLE) as an extension of Protected Working Capacity Envelope (PWCE) to path-oriented protection. Based on lightpath-protecting p-Cycles, PWLE partitions the total network capacity into a static protection layer and a working layer protected by the former. However, two constraints arise for PWLE due to lightpath-protecting p-Cycles. Firstly, for any lightpath that is dynamically established in the working layer, its end nodes must both fall on the lightpath-protecting p-Cycle for it to protect that lightpath. Secondly, all the lightpaths protected simultaneously by a lightpath-protecting p-Cycle should be mutually link-disjoint in order to achieve full survivability against any single span failure. To account for these two constraints in the

design of PWLE, we develop an approach termed Compatible Grouping to facilitate the formulation of PWLE as an MILP model. Based on Compatible Grouping, we further propose a distributed routing algorithm for PWLE termed Compatible Group Routing (CGR) which allows each node to find suitable resources for routing immediately if available by maintaining local information. The operational issues are discussed in detail and the control overheads are investigated.

3.2 Concept of Protected Working Lightpath Envelope

As an extension of PWCE to path-oriented protection, PWLE is designed to achieve the following:

- Inherit the property of p-Cycle-based PWCE as a capacity optimization strategy at overall network level with a pre-configured protection layer protecting a working capacity layer for dynamic service provisioning

- Achieve advantages of higher capacity efficiency, better blocking performance, guaranteed optical transmission quality, and less wavelength conversions compared with p-Cycle-based PWCE

PWLE is structured based on lightpath-protecting p-Cycles. Unlike FIPP, lightpath-protecting p-Cycles are not necessarily designed for any particular demand pattern. In other words, the protected capacity is decided merely based on the topological feature of the corresponding lightpath-protecting p-Cycles. For instance, Fig.3.1 (a) shows lightpath-protecting p-Cycle A-B-C-D-A (circle) with one unit of spare capacity reserved on each on-cycle span. The maximum amount of protected capacity on each span is one unit for on-cycle spans and two units for off-cycle spans, which is independent of any demand pattern. We thus define the envelope of the working capacity as the sum of all the protected capacity which amounts to 26 for the case in Fig.3.1 (a). Instead of a fixed path-to-cycle relation, any lightpath, with end nodes on-cycle, established within such an envelope (i.e. using protected capacity) is protected. For example, the traffic demand between node pair (A,D) can be routed over protected lightpath A-H-D or A-F-E-D or both depending on the network status. Furthermore, any combination of link-disjoint lightpaths within such an envelope can be protected simultaneously by the lightpath-protecting p-Cycle against a single span failure. Link-disjointness here means sharing no common links. Such flexibility in service provisioning makes the lightpath-protecting p-Cycle a potential candidate for uncertain future demand.

Compared with the span-protecting p-Cycle, the lightpath-protecting p-Cycle has the advantage of high capacity efficiency due to its path-oriented protection

nature. Figure 3.1 (b) shows span-protecting p-Cycle A-H-C-D-A and the maximum protected capacity on each span. If the cycle A-B-C-D-A in Fig.3.1 (a) is a span-protecting p-Cycle, the protected capacity is only one unit on each on-cycle span as there is no span straddling the cycle. Intuitively, the larger the size of a lightpath-protecting p-Cycle, the larger its envelope, and the higher its capacity efficiency. However, the requirement of mutual link-disjointness among protected lightpaths makes the actual utilization of protected capacity on distinct spans interdependent, which becomes an inhibiting factor. Therefore, the size of lightpath-protecting p-Cycles is a critical parameter for PWLE. For example, in Fig. 3.1 (a), if lightpath B-G-F-E-D is established within the envelope, then the protected capacity on span A-F, C-G, C-E and E-G cannot actually be used to establish lightpaths. But if lightpath B-G-E-D instead is established within the envelope, another lightpath A-F-E-C can also be established. Thus the utilization of the protection capacity of the cycle depends on the specific routes of the protected lightpaths. This issue does not exist for the span-protecting p-Cycle in Fig. 3.1(b) since the protected capacity on distinct spans is independent of each other. The issue raised by the mutual link-disjointness resembles the trap problem in Share Backup Path Protection (SBPP) which is currently the most popular mechanism for dynamic survivable service provisioning [29]. When the trap situation occurs, protected working capacity can be wasted such as the channels on span A-F, C-E and E-G, which decreases the utilization of the protected capacity. The larger the

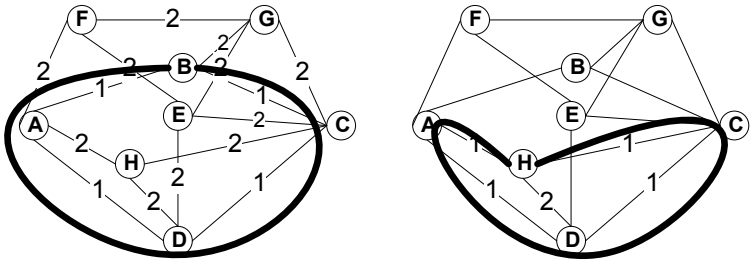

Figure 3.1: (a) An Example of Lightpath-protecting p-Cycle (b) An Example of Span-protecting p-Cycle

lightpath-protecting p-Cycle, the larger the volume of the entire envelope, but the easier trap situations will be constructed. Thus, there is a trade-off between the utilization and the volume of the protected capacity. In PWLE, we limit lightpath-protecting p-Cycles to protect lightpaths traversing up to 3 physical hops only.

With each lightpath-protecting p-Cycle protecting an envelope of working channels, PWLE partitions the total network capacity into working capacity (working layer) and protection capacity (protection layer) by using a set of lightpath-protecting p-Cycles. As a capacity optimization strategy at the overall network level, PWLE is expected to achieve higher capacity efficiency (i.e. larger working layer) than PWCE under the same capacity budget due to the properties of the underlying lightpath-protecting p-Cycles. However, unlike PWCE, lightpaths established in the working layer are subject to two constraints unique to PWLE. One is mutual link-disjointness as described above. The other is that the end nodes

of a lightpath established in the working layer should fall on the same lightpath-protecting p-Cycle embedded in the protection layer. So it is critical to find an approach to incorporate these two constraints into the design of PWLE for the purpose of optimization; this is discussed in Section 3.3. Given the two constraints, it may remain unclear about the blocking performance of PWLE with respect to PWCE despite the prospect of PWLE in capacity efficiency, which makes the comparative study on blocking performance necessary. This work is, however, currently limited to considering such study in the presence of stationary statistical demand patterns, which assume the mean traffic intensities on each node pair can be predicted, although PWLE is not limited to such demand patterns.

Assuming wavelength path (WP) working layer and wavelength path (WP) p-Cycles, wavelength converters are only needed at the intermediate nodes of multi-hopping connections in PWLE whereas wavelength converters are needed at all the on-cycle nodes for WP working paths to access WP p-Cycles in span-protecting-p-Cycle protected networks [39] [40]. In operation, due to PWLE's path-oriented nature only the end-nodes of protected lightpaths are involved in a switch over in the event of a failure, regardless of where the failure occurs. Moreover, since all backup paths are pre-connected instead of being cross connected on the fly upon failure, transmission integrity is guaranteed.

3.3 Design of PWLE

The objective of PWLE design is to maximize the volume of the working layer envelope while keeping the utilization of the working capacity high. Considering the two constraints of lightpath-protecting p-Cycles explained in Section 3.2, we introduce the concept of Compatible Grouping to organize the channels in the working layer and thus incorporate the constraints into the design of PWLE. Based on Compatible Grouping, we then develop an MILP model to design the optimal PWLE given the network capacity constraint. As mentioned in Section 3.2, PWLE is not limited to predicted stationary demand patterns and can actually be designed in the absence of traffic forecasts. However, here we assume that the prior knowledge of expected demand patterns is available, based on which we can better structure the envelope of the working layer and allocate resources where needed.

3.3.1 Compatible Grouping

We first define the following terms, based on which we will explain the concept of Compatible Grouping.

- *Attach Nodes*: For a lightpath-protecting p-Cycle, nodes, except for the on-cycle nodes, one-hop away from the on-cycle nodes are called *Attach Nodes.* For instance, in Fig. 3.2 (a), nodes E, F and G (grey nodes) are *Attach Nodes.*

- *Attach Links*: Spans linking two *Attach Node*s are called *Attach Link*s. For

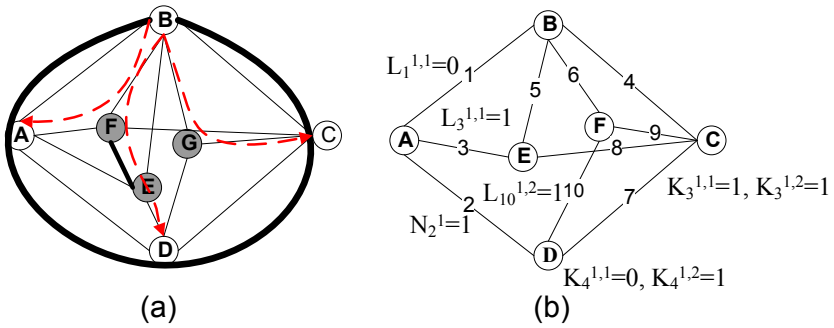

Figure 3.2: (a) Illustration of Compatible Grouping (b) Illustration of MILP Model

instance, in Fig. 3.2 (a), span E-F (thick line) is an *Attach Link*.

- *Compatible Group (CG)*: On-cycle nodes connected by the same *Attach Node* form a *Compatible Group (CG)*. Spans connecting on-cycle nodes and the associated *Attach Node* are said to belong to the associated *CG*. In addition, we say a lightpath belongs to a *CG* if both of its end nodes are contained in this *CG*. For any node, a *CG* is associated with it if the *CG* contains the node. For instance, in Fig. 3.2 (a), *CGs* are [A,B,D], [A,B,C] and [B,C,D] which are defined by *Attach Nodes* E, F and G, respectively. For *CG* [A,B,C], spans A-F, B-F and C-F are said to belong to this *CG*. In addition, lightpath B-F-A is also said to belong to *CG* [A,B,C] as both its end nodes are contained in the *CG*.

- *Joint Compatible Group (JCG)*: Two *CGs* connected by an *Attach Link* form a *Joint Compatible Group (JCG)*. The two *CGs* are called component *CGs*

of the *JCG*. The two *CGs* have a *Joint Relation*, which is not transitive. Suppose we have three *CGs* G, H and K. G is joint with H and H is joint with K, but G is not necessarily joint with K. We say a lightpath belongs to a *JCG* if both of its end nodes are contained in the *JCG*. For any node, a *JCG* is associated with it if the *JCG* contains the node. For instance, in Fig. 3.2 (a), *CG* [A,B,C] and [A,B,D] form a *JCG* through the *Attach Link* E-F. Lightpath B-F-E-D is said to belong to this *JCG*.

- *End-node disjoint*: Two lightpaths are end-node disjoint if they do not have common end nodes such as lightpaths B-F-A and B-G-C.

- *On-path node*: Nodes, except for the end nodes, traversed by a lightpath are called on-path nodes such as nodes E and F with respect to lightpath B-F-E-D.

- *Derived Graph*: For a lightpath-protecting p-Cycle, a subgraph induced by a node set comprised of its on-cycle nodes and *Attach Nodes* as well as all the spans between these nodes is called the *Derived Graph* of this cycle. The purpose of introducing *Derived Graph* is that if there exists a lightpath traversing up to 3 hops protected by a lightpath-protecting p-Cycle, it can always be found in the *Derived Graph* of the lightpath-protecting p-Cycle. Fig. 3.2 (a) is the *Derived Graph* of lightpath-protecting p-Cycle A-B-C-D-A.

In order to measure the protection capability of a lightpath-protecting p-Cycle, we define the Efficiency Ratio *(ER)* of the lightpath-protecting p-Cycle as the ratio of protected capacity in the *Derived Graph* to the spare capacity reserved on the cycle, i.e.,

$$ER = \frac{2 * \sum \textit{off-cycle spans} + \sum \textit{on-cycle spans}}{\sum \textit{on-cycle spans}} \tag{3.1}$$

In the numerator, we double the sum of off-cycle spans in the *Derived Graph* because each route with straddling relationship to the lightpath-protecting p-Cycle can bear two units of lightpaths protected per unit of spare capacity from which the p-Cycle is formed. For instance, Fig. 3.2 (a) shows a *Derived Graph* of lightpath-protecting p-Cycle A-B-C-D-A, whose *ER* is (2*10+4)/4=6.

Based on the above definitions, we now explain Compatible Grouping. Basically, Compatible Grouping is to group on-cycle nodes in a *Derived Graph* in the form of *CGs* or *JCGs* based on *Attach Nodes* and *Attach Links.* The purpose of Compatible Grouping is to explore the compatibility relation among lightpaths that can be established in the *Derived Graph*, which will be used to facilitate the development of optimization as well as the routing of PWLE. Through Compatible Grouping, we make the following claim.

Claim: If a lightpath satisfies the Routability Conditions which comprise the following three conditions, then it can be established and protected. That is, it is

compatible with all the existing lightpaths.

Condition 1 *The end nodes of the lightpath are contained in the same CG or JCG.*

Condition 2 *Within a CG, any node can be taken up by only one lightpath belonging to this CG or the JCG containing this CG*

Condition 3 *If the lightpath traverses an Attach Link in a JCG, then this Attach Link is not traversed by any other lightpath belonging to this JCG.*

Proof: To decide whether a lightpath can be established and protected, we only need to check if this lightpath is compatible with each of the existing ones. Therefore, we explore the relation between two lightpaths which can be classified into four cases. We prove the Claim from all the cases.

Case 1: Two lightpaths belong to different CGs

When two lightpaths belong to different *CGs,* they are 2-hop lightpaths with different on-path nodes. So they are link-disjoint.

Case 2: Two lightpaths belong to the same CG

Condition 2 of the Routability Conditions ensures that the two lightpaths are link-disjoint.

Case 3: Two lightpaths belong to different JCGs

When two lightpaths belong to different *JCGs,* there can be two situations:

(1) The two *JCGs* do not have a common *CG*. In this situation, the two lightpaths have different on-path nodes. So they are link-disjoint.

(2) The two *JCGs* have a common *CG*. Denote the two lightpaths as $L_1$and L_2, the common *CG* as CG_0. Let N_{ij} represent the jth end node of L_i. If the end nodes of $L_1$and L_2 do not fall in CG_0 at the same time, the situation is reduced to Case 1. So we focus on the situation that both $L_1$and L_2 are concerned with CG_0.Without losing generality, we assume N_{11} and N_{21} belong to CG_0.Then N_{11} and N_{21} are different according to *Condition* 2 of the Routability Condition. Furthermore, let N_{att0} be the *Attach Node* based on which CG_0 is defined. Then N_{att0} is the only common on-path node of $L_1$and L_2, which is one-hop away from both N_{11} and N_{21}. Therefore, $L_1$and L_2 are link-disjoint regardless of whether N_{12} and N_{22} are the same or not.

Case 4: Two lightpaths belong to the same JCG

Due to *Condition* 3 of the Routability Conditions, only one 3-hop lightpath can exist in a *JCG*. Hence, there can be only two situations:

(1) The two lightpaths are both of 2-hop long. When the two lightpaths belong to different *CGs* of the *JCG*, it is exactly Case 1. When the two lightpaths belong to the same *CG*, it is exactly Case 2.

(2) One lightpath is 2-hop and another is 3-hop. This is a special case of situation (2) of Case 3.

We use the example in Fig. 3.2 (a) to explain the Routability Conditions. Suppose lightpaths B-F-A and B-G-C are existing lightpaths, lightpath B-F-E-D can be established and protected if it satisfies all three conditions. Although it satisfies *Condition* 1 and *Condition* 3, it violates *Condition* 2 by taking up node B which has already been occupied. Therefore, lightpath B-F-E-D cannot be established. Suppose a connection request between node pair (A,B) arrives, we can identify the appropriate *CG* [A,B,D] because neither node A nor B is taken up by any lightpath belonging to this *CG*.

3.3.2 MILP Formulation

Based on Compatible Grouping, we now formulate an MILP model to optimize PWLE. PWLE builds on the virtual topology defined by the forecasted traffic demands whereas PWCE maps a given traffic matrix to the traffic load on each span based on specific routes for each demand. Since the lightpath-protecting *p*-Cycle in PWLE protects lightpaths up to 3 hops only, we need to segment the path of any node pair whose shortest path between them exceeds 3 hops. Then, we generate candidate cycles (P) with high *ER* as well as the *CGs* (G^j) associated with those cycles. We establish the protection relationship between the lightpath demands, from the virtual topology, and the candidate *CGs* so as to generate the parameter $F_d^{j,i}$ (see definition in the sequel). We note that *CGs* are the preferred form of protected capacity compared with *JCGs* or on-cycle paths. Therefore, our

objective of this MILP formulation is to maximize the protected capacity formed by *CGs* which are assigned different wavelengths independently. Once we obtain the optimization result, we need to further add in the protected on-cycle capacity and the *Attach Links* manually. We use this technique to simplify the MILP model. The outputs of the optimization are basically the selection of lightpath-protecting p-Cycles as well as the assignment of wavelengths to the selected lightpath-protecting p-Cycle and *CGs*. Additionally, we assume the lightpath-protecting cycles and demands are bidirectional. Our MILP formulation of PWLE is as follows:

Sets:

$\boldsymbol{P}$: set of topologically defined candidate lightpath-protecting cycles, indexed by j

$\boldsymbol{G}^j$: set of *CGs* belonging to the j^{th} lightpath-protecting p-Cycle, indexed by i

$\boldsymbol{D}$: set of traffic demands, indexed by d

$\boldsymbol{M}$: set of nodes of the network, indexed by m

$\boldsymbol{S}$: set of spans of the network, indexed by s

$\boldsymbol{W}$: set of wavelengths, indexed by w

Parameters:

D_d: Traffic intensity of the d^{th} demand

$Q_{d,m}$: 1 if the m^{th} node is the end node of the d^{th} demand, 0 otherwise

$L_s^{j,i}$: 1 if the sth span belongs to the i^{th} CG of the j^{th} lightpath-protecting p-Cycle, 0 otherwise

N_s^j: 1 if the s^{th} span is an on-cycle span of the j^{th} lightpath-protecting p-Cycle, 0 otherwise

$F_d^{j,i}$: Δ if the d^{th} demand can be carried by the i^{th} CG of the j^{th} lightpath-protecting p-Cycle, 0 otherwise

$K_m^{j,i}$: 1 if the m^{th} node is contained in the i^{th} CG of the j^{th} lightpath-protecting p-Cycle, 0 otherwise

T_s: The total number of deployed channels on the s^{th} span

Δ: A large positive constant (100)

Variables:

γ_w^j: 1 if the w^{th} wavelength is taken up by the j^{th} lightpath-protecting p-Cycle, 0 otherwise

$\mu_w^{j,i}$: 1 if the w^{th} wavelength is taken up by the i^{th} CG of the j^{th} lightpath-protecting p-Cycle, 0 otherwise

$\pi_d^{j,i}$: Amount of the d^{th} demands carried by the i^{th} CG of the j^{th} lightpath-protecting p-Cycle

Objective:

$$Maximize \sum_{j\in P, i\in G^j, s\in S} L_s^{j,i} \cdot \sum_{w\in W} \mu_w^{j,i} \tag{3.2}$$

Constraints:

$$\sum_{j\in P, i\in G^j} \mu_w^{j,i} \cdot L_s^{j,i} + \sum_{j\in P} \gamma_w^j \cdot N_s^j \leq 1$$

$$\forall s \in \boldsymbol{S}, w \in \boldsymbol{W} \tag{3.3}$$

$$\sum_{w\in W, j\in P, i\in G^j} \mu_w^{j,i} \cdot L_s^{j,i} + \sum_{w\in W, j\in P} \gamma_w^j \cdot N_s^j \leq T_s$$

$$\forall s \in \boldsymbol{S} \tag{3.4}$$

$$\sum_{j\in P, i\in G^j} \pi_d^{j,i} \geq D_d$$

$$\forall d \in \boldsymbol{D} \tag{3.5}$$

$$\sum_{w\in W} \gamma_w^j \leq \sum_{w\in W} \mu_w^{j,i} \leq 2 \cdot \sum_{w\in W} \gamma_w^j$$

$$\forall j \in \boldsymbol{P}, i \in \boldsymbol{G^j} \tag{3.6}$$

$$\sum_{d\in D} (\pi_d^{j,i} \cdot Q_{d,m}) \leq K_m^{j,i} \cdot \sum_{w\in W} \mu_w^{j,i}$$

$$\forall m \in \boldsymbol{M}, j \in \boldsymbol{P}, i \in \boldsymbol{G^j} \tag{3.7}$$

$$\pi_d^{j,i} \leq F_d^{j,i}$$

$$\forall d \in \boldsymbol{D}, j \in \boldsymbol{P}, i \in \boldsymbol{G^j} \tag{3.8}$$

Constraint (3.3) ensures that there is no wavelength conflict on each span. Constraint (3.4) ensures that the sum of the protected capacity and spare capacity does not exceed the total deployed capacity on each span. Constraint (3.5) guarantees that the resulting PWLE can support the forecasted traffic demands. Constraint (3.6) defines the range of number of copies of a *CG*, which is more than the number of copies of unit-capacity lightpath-protecting p-Cycles associated with it but less than twice. Constraint (3.7) is based on the second Routability Condition. Constraint (3.8) defines the integer variable based on $F_d^{j,i}$.

We use a simple example shown in Fig. 3.2 (b) to explain the model. For simplicity, we assume two wavelengths per span as the capacity budget and single forecasted traffic demand of two units between node pair (B,C) (D_1=2). Spans are numbered as in Fig. 3.2 (b) and nodes are numbered based on alphabetical order. We further assume that A-B-C-D-A is the 1^{st} among all the candidate cycles and *CG*s [A,B,C], [B,C,D] are, respectively, the 1^{st} and 2^{nd} *CG*s of A-B-C-D-A. Then parameters $L_s^{j,i}$, N_s^j and $K_m^{j,i}$ can be easily obtained, among which some are shown in Fig. 3.2 (b). As the traffic demand between node pair (B,C) can be carried by both *CG*s [A,B,C] and [B,C,D], both $F_1^{1,1}$ and $F_1^{1,2}$ equal Δ. As the optimal solution, cycle A-B-C-D-A is selected which takes up the 1^{st} wavelength. Therefore, we have γ_1^1=1 and $\mu_w^{1,i}$=1 (w=1,2; i=1,2).

3.4 Routing and Operation of PWLE

Since the protected working capacity is organized based on Compatible Grouping, a new routing algorithm is necessary. We introduce Compatible Group Routing (CGR), which is a distributed routing algorithm, here.

3.4.1 Compatible Group Routing (CGR)

We assume bidirectional rings which are composed essentially of two unidirectional rings in opposite directions. Each bidirectional lightpath-protecting p-Cycle (wavelength level) can provide protection for two bidirectional lightpaths on any straddling route. Actually, each lightpath can be independently protected by one unidirectional lightpath-protecting p-Cycle. The protection assignment can be made upon the establishment of lightpaths. We now explain how CGR operates in detail.

Based on the MILP model of PWLE, a set of lightpath-protecting p-Cycles are selected and numbered. The resulting CGs are also numbered and associated with the lightpath-protecting p-Cycles. At each node, the CGs and JCGs associated with this node as well as their protection relationships with the corresponding lightpath-protecting p-Cycles are stored. Two mapping tables, CG Table (CGT) and JCG Table ($JCGT$), are used. CGs and $JCGs$ are indexed together with regard to each lightpath-protecting p-Cycle. Indexes map to the nodes contained

in *CGs* for *CGTs* and component *CGs* in *JCGs* for *JCGTs*. For instance, suppose the network in Fig. 3.3 (a) is protected by two lightpath-protecting p-Cycles, I 0-2-3-10-6-8-0 and II 0-1-2-7-6-9-0, which are both associated with node 0. The *CGTs* and *JCGTs* at node 0 are listed in Fig. 3.3 (b)–(e) for each of these lightpath-protecting p-Cycles. The first entry in Fig. 3.3 (b) represents that the 1^{st} *CG* of I, which is [0,2,3,6,8], is associated with node 0. The first entry in Fig. 3.3 (c) represents a *JCG* comprised of the 3^{rd} and the 5^{th} *CG* of I. Since the 3^{rd} *CG* contains node 0, this *JCG* actually allows the 5^{th} *CG* also included in Fig. 3.3 (b) although node 0 is not contained in the *CG*. Otherwise, the 5^{th} *CG* must be excluded, which is the case for the entries in grey in Fig. 3.3 (d) and (e).

Based on the mapping tables, we further organize the *CGs* and *JCGs* to facilitate the development of CGR. Two tables, Inactive Table (IT) and Active Table (AT), dynamically record the local status of the evolving network. Specifically, the j^{th} column in AT at node i collects all *CGs* and *JCGs* capable of providing lightpaths between node i and node j whereas the corresponding column in IT collects the *CGs* and *JCGs* incapable of providing lightpaths between node i and node j. When a connection request arrives, the source node checks its AT and finds the suitable *CG* or *JCG* immediately if available. If the appropriate *CG* or *JCG* is identified, the source node initiates path setup using RSVP-TE [41] and specifies the route in terms of a series of nodes. Specifically, the source node sends a PATH message along the route to the destination node which sends a RESV message

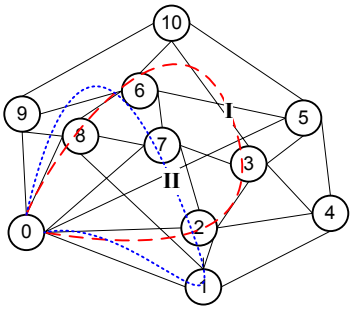

(a)

Index	Nodes in CG
1	0,2,3,6,8
2	0,6,8,10
3	0,3,6,10
4	0,2,8
5	2,3

(b)

Index	Component CGs
6	3,5
7	4,5

(c)

Index	Nodes in CG
1	0,1,6,7,9
2	0,2
3	0,6
4	0,7
5	1,2
6	2,7
7	6,9

(d)

Index	Component CGs
8	3,5
9	3,6
10	3,7
11	5,6
12	6,7

(e)

Node 0	Node 1	Node 2	Node 3	Node 4	Node 5	Node 6	Node 7	Node 8	Node 9	Node 10
(1,1)	(2,5)		(1,1)			(1,1)	(2,6)	(1,1)	(2,12)	(1,6)
(1,4)	(2,8)		(1,5)			(1,6)	(2,8)	(1,4)		
(1,6)			(1,6)			(2,9)		(1,7)		
(1,7)			(1,7)			(2,10)				
(2,2)						(2,12)				
(2,9)										
(2,10)										

(f)

Source	Des	P-Cycle	CG1	CG2

(g)

Figure 3.3: (a) Illustrative Network Protected by Two Lightpath-protecting p-Cycles: I 0-2-3-10-6-8-0 and II 0-1-2-7-6-9-0 (b) The CG Table (CGT) of I at Node 0 (c) The JCG Table ($JCGT$) of I at Node 0 (d) The CG Table (CGT) of II at Node 0 (Note: entries in grey are actually excluded) (e) The JCG Table ($JCGT$) of II at Node 0 (f) The Active Table (AT) at Node 2 (g) An Example of the Message Used in the Group Signaling in CGR

traversing the same route in the reverse direction. After a lightpath is established, the relevant *CG* or *JCG* becomes unavailable and is moved from the node's *AT* to its *IT*. Then the source node sends a message carrying the information of the established lightpath to the nodes contained in the same *CG* or *JCG* with it, which is called Group Signaling. Group Signaling is essentially an information distribution mechanism for the source node to send updating message, shown in Fig. 3.3 (g), to affected nodes. It can be implemented by defining simple extensions to OSPF-TE [42] so that the message in Fig. 3.3 (g) is included and the flooding scope is the relevant *CG* or *JCG* associated with the source node. The receiving nodes update their local information by adjusting their *AT*s and *IT*s upon receiving the Group Signaling message. Likewise, when a lightpath is released, the source node sends a PATHTEAR message and the *CG* or *JCG* concerned is moved from the source node's *IT* to its *AT*, following Group Signaling.

We use an example to explain the above process. The *AT* at node 2 is shown in Fig. 3.3 (f). The tuples in the table represent the lightpath-protecting *p*-Cycles (1^{st} term) and the corresponding *CGs* or *JCGs* (2^{nd} term). For example, the first tuple (1,1) in the first column indicates that the 1^{st} *CG* of lightpath-protecting *p*-Cycle *I* can support one protected lightpath between node 2 and node 0. Actually, since each straddling route can support two lightpaths protected by one lightpath-protecting *p*-Cycle, two *ATs* are maintained at each node. During the routing process, CGR looks up either one of them. The *IT*, which has the same structure

as the *AT*, is initially empty. As the network status evolves, tuples representing *CGs* and *JCGs* are moved between the *AT* and the *IT*. For instance, if a lightpath between node 2 and node 0 needs to be set up, node 2 searches the first column of its *ATs* for available resource. Once a tuple is found, say (1,1), a lightpath is set up in the 1^{st} *CG*, followed by the Group Signaling among nodes 0,3,6,8.

The on-cycle channels belonging to the envelope of protected capacity are also available for routing. However, in this case, decision making is a bit more complex in that a node needs to maintain information regarding the on-cycle nodes as well as their sequential ordering. Every time a node checks the resource availability of the on-cycle channels, it must search for a path along the cycle which does not overlap with any existing ones that utilize the corresponding on-cycle channels. In addition, Group Signaling here involves all the on-cycle nodes of the relevant lightpath-protecting *p*-Cycle. Since the uniqueness of *p*-Cycle-based survivability schemes is their capability to protect straddling capacity, CGR always gives priority to *CGs* and *JCGs* instead of on-cycle capacity for routing.

If a node pair (i, j) is far apart to require multi-hopping (virtual hop), an intermediate node, say k, is found so that lightpath i-k can be protected. Then node k is signaled to find another intermediate node to do likewise, if necessary, until the destination end node j is finally reached. Specifically, the source node sends a PATH message to node k indicating a connection request to between node k and j. Upon receiving a PATH message, node k searches for available *CG* or *JCG*

to establish lightpath between node k and j. If successful, node k sends a PATH message to node j or another intermediate node, if necessary. If unsuccessful, node k sends PATHERR message back to source node i. If destination node j receives a PATH message, it sends back a RESV message to the last intermediate node which also sends a RESV message to the next intermediate node and initiates Group Signaling immediately. Group Signaling is carried out in a distributed manner whenever a lightpath is set up. This procedure continues until the source node i is reached. The fact that multi-hopping is required for distant node pairs necessitates O-E-O conversions and retransmission at intermediate nodes along the path. However, retransmission might also help to improve signal quality as nonlinear effects occurring inside optical fibers accumulate over long lengths.

Since CGR is a distributed routing algorithm, signaling upon lightpath setup and teardown is inevitable. However, since *CGs* or *JCGs* are preferred protected capacity for routing, signaling involving nodes within a *CG* or *JCG* is normally over a shorter range than when involving all the nodes on a lightpath-protecting p-Cycle. Also, from a complexity point of view, CGR allows a source node to find a suitable *CG* or *JCG* immediately if one is available, which is different from a conventional shortest-path-type routing algorithm. Finally, at each node, only local information related to the node, instead of network-wide information is stored.

3.4.2 Operation Upon Failure

Every time a lightpath is set up, it is given an ID which is recorded at the source node and the destination node, which are the lightpath's custodial nodes. A mapping between the lightpath's ID and its custodial lightpath-protecting p-Cycle is also recorded at each node. Upon a single span failure, the end-nodes of the failed span insert an Alarm Inhibit Signal (AIS) onto the surviving directions of the failed paths. The AIS passes through all nodes along the failed path. Only the custodial nodes are activated to provide protection switching irrespective of the exact failure location. A single span failure can cause several lightpath failures. The protection switchings for these affected lightpaths are triggered simultaneously and independently. Since all the backup paths are pre-configured, the restoration time thus depends on the signaling and the protection switch-over. However, due to the length limit (3 physical hops) of lightpaths in PWLE, the signaling time is bounded.

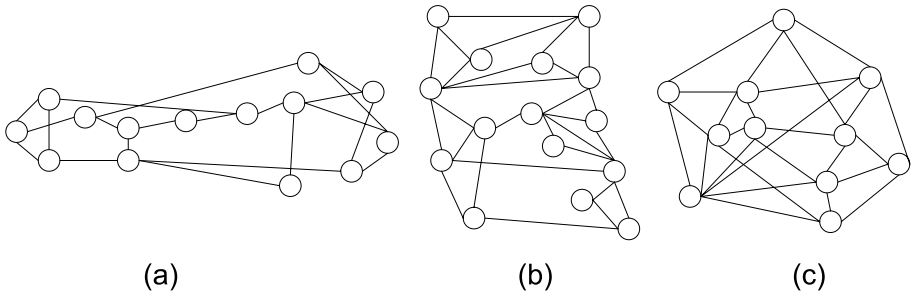

Figure 3.4: Test Networks for Optimization(a) NSFNET (b) Bellcore (c) COST239

3.5 Numerical Results and Discussions

3.5.1 Optimization Result

We use the three test networks shown in Fig. 3.4. They are NSFNET, Bellcore and COST239 whose average node degrees range from 3 to 4.7. We compare the protection capacity efficiency of PWLE with that of PWCE_WP/WC (Wavelength Path/Wavelength Cycle), a modified version of PWCE, where WP p-Cycles with WP working layer as well as converters at p-Cycle access are assumed. We choose PWCE_WP/WC instead of the original PWCE [11] in order to make a fair comparison because no wavelength conversion is allowed in both the working layer and protection layer for PWLE. Besides, locating wavelength converters at the access points of WP p-Cycles in PWCE_WP/WC offers high efficiency by striking a balance between capacity efficiency and wavelength converter consumption [39]. Since the problem formulation of PWCE_WP/WC model is not the focus of this chapter,

No. of wavelengths/fiber	10	14	20
PWLE	134(63.8%)	209(71.1%)	315(75%)
PWCE_WP/WC	109(51.9%)	176(59.9%)	254(60.5%)
PWLE vs. UpperBound	<0	6.6%	12.5%
PWLE vs. PWCE_WP/WC	22.9%	18.8%	24.0%

Table 3.1: Comparison of Volume of Working Envelope for Network NSFNET (Average Node Degree: 3)

it is shown in the Section 3.7.

For all the three test networks, we assume one fiber pair per span as the total deployed capacity. Each unit of capacity refers to two channels on the same wavelength over one fiber pair per span. We vary the number of wavelengths per span in the experiment to study its impact on the capacity efficiency. For each network, we randomly choose 3 sets of 19-demand pairs and average the results over the 3 sets. In all the cases, every demand bundle is assumed to consist of two units. All the problems are solved using ILOG \ CPLEX 9.0 on a Windows XP Professional machine with Intel(R) Pentium(R) 4CPU 2.4GHz, 1GB of RAM. Most of the tests for NSFNET and Bellcore can be solved at a MIPGAP below 3% within half an hour. For COST239, the best feasible solutions are reached at 5% MIPGAP within 5 hours for the case of 10 wavelengths per fiber and at 10% MIPGAP within 2 days for the case of 14 and 20 wavelengths per fiber.

No. of wavelengths/fiber	10	14	20
PWLE	204(72.9%)	302(77.0%)	446(79.6%)
PWCE_WP/WC	172(61.4%)	257(65.5%)	366(65.4%)
PWLE vs. UpperBound	<0	5.3%	8.7%
PWLE vs. PWCE_WP/WC	18.6%	17.5%	21.9%

Table 3.2: Comparison of Volume of Working Envelope for Network Bellcore (Average Node Degree: 3.7)

No. of wavelengths/fiber	10	14	20
PWLE	212(81.5%)	302(84.3%)	439(84.4%)
PWCE_WP/WC	196(75.4%)	287(80.2%)	410(78.8%)
PWLE vs. UpperBound	3.4%	5.2%	7.1%
PWLE vs. PWCE_WP/WC	8.2%	5.2%	7.1%

Table 3.3: Comparison of Volume of Working Envelope for Network COST239 (Average Node Degree: 4.7)

Tables 3.1, 3.2 and 3.3 list the results for the three test networks. The first two rows display the total protected capacity while the remaining two rows show the percentage improvement. The figures in brackets in the first row represent the ratio of protected capacity to the whole network capacity. From the three tables, we observe that PWLE outperforms PWCE_WP/WC due to its path-oriented protection nature. Comparing the first and second rows of the three tables, we find that the capacity efficiency of PWLE is much better than that of PWCE_WP/WC and increases with the average node degree. However, the improvement of PWLE over PWCE_WP/WC increases with the decreasing average node degree which can be found by comparing the fourth rows of the tables. This is because the impact of network density on PWCE_WP/WC is much greater than on PWLE. The Upper-Bound indicated in the third rows refers to the situation that a network deployed with uniform capacity has a Hamilton cycle so that the upper-bound capacity efficiency can be reached for conventional PWCE by reserving half of the capacity on the spans along the Hamilton cycle. Therefore, we can observe that the capacity efficiency of PWLE is normally even better than the upper bound of PWCE except for the case when the initial deployed capacity per span is small. This is because the impact imposed by the traffic load distribution on the resulting envelope of working capacity increases when the deployed capacity becomes smaller, which is more severely manifested in the case of PWCE_WP/WC as implied by the last two rows of the tables.

3.5.2 Blocking Performance

In order to investigate the advantage of PWLE in terms of blocking performance under dynamic traffic, we compare it with PWCE_WP/WC with shaping consideration which has been proven to improve blocking performance [11]. Furthermore, we choose network COST239 because the improvement of capacity efficiency of PWLE over PWCE_WP/WC is the least among the three test networks.

We test the performance with 19 and 25 source-destination node pairs. For each case, three sets of source-destination node pairs are randomly chosen. The result is averaged over the 3 sets. We assume 8 wavelengths per fiber. Under dynamic service provisioning, the network can be regarded as a discrete-event-driven system. with two types of random event, service connection arrival and service connection departure.The arriving and departing event sequences run independently on each node-pair concurrently. Arrivals follow a Poisson process. Each demand has an exponentially distributed holding time with a normalized mean of 1 unit. A total of 10^5 events are simulated. For PWCE_WP/WC with shaping consideration, the working path is found using the shortest-path algorithm based on hop-count and the first-fit algorithm for wavelength assignment. If the search is successful, then the path is established and the status of the available network resources is updated at each span with the consumed resources set as unavailable. Only when there is no free capacity left on a span is the signaling triggered by the span, and the

exhausted span is effectively removed from the graph seen by the routing algorithm for new arrivals. Upon service departure, all resources consumed by the working path channels are returned to available or unused status. For PWLE, CGR is followed for routing and signaling is triggered whenever a lightpath is setup.

From Fig. 3.5, we observe that PWLE performs better than PWCE_WP/WC in both cases of 19 (solid lines) and 25 (dashed lines) source-destination node pairs. This is due to two reasons. Firstly, PWLE supports a larger volume envelope of working capacity. Secondly, within this envelope, PWLE optimizes routing by allowing cooperation among the working paths whereas PWCE_WP/WC always finds the shortest path based on the current state of the working layer, which is greedy.

As to the percentage of the multi-hopping connections in the experiment, it rises from 3.03% to 6.1 % and from 4.8% to 7.2%, respectively, when the traffic load increases from 0.4 Erlangs to 2 Erlangs per node pair for the cases of 19 and 25 source-destination node pairs. Also, it is worth noting that the average number of physical hops of the shortest paths between node pairs is 1.6. Besides, most of the multi-hopping connections transit at nodes 3, 6, and 7. Therefore, the percentage of long connections and the number of nodes requiring wavelength conversion are both small. Such overhead is thus small.

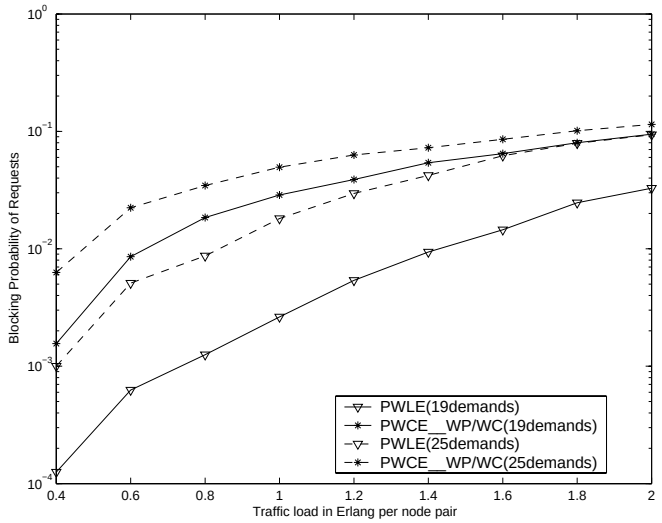

Figure 3.5: Comparison of Blocking Performance between PWLE and PWCE_WP/WC

3.5.3 Control Overheads

We conduct experiments to compare PWLE with PWCE in terms of control overheads. Although control signaling of PWLE include the resource reservation using RSVP-TE and the information distribution via Group Signaling which can be implemented with OSPF-TE with suitable extensions, the experiment here focuses on the information distribution as it differs with that of PWCE in terms of information content, signaling frequency and signaling range.

PWCE has been claimed to have operational simplicity because Link State Advertisement (LSA) message flooding is needed only when the capacity on a span is used up or becomes available again [11]. Each LSA message contains the

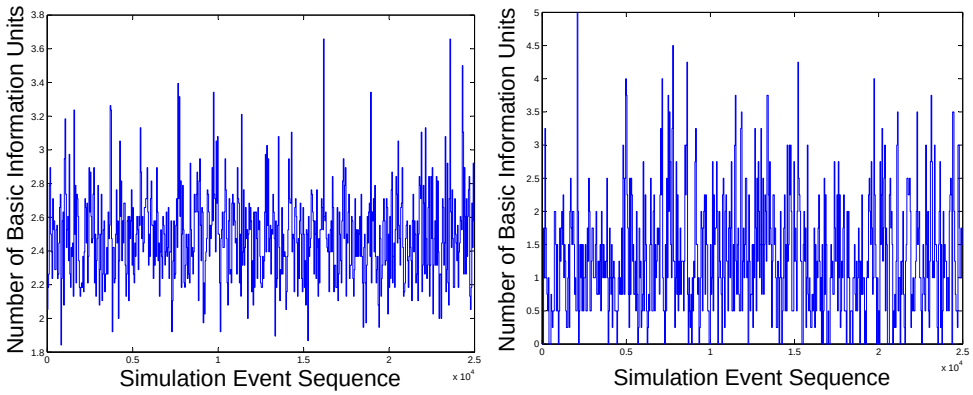

Figure 3.6: Control Overhead Comparison between PWLE (left) and PWCE (right), COST239, 19 source-destination node pairs, traffic load between each node pair: 0.8 Erlangs

ID and status of a span. We consider an LSA message as the basic unit of control overhead for PWCE.

For PWLE, a message carrying information on an established/released lightpath is sent by the source node to the nodes within the same *CG* whenever a lightpath is set up or released. Figure 3.3 (g) shows an example of the message which includes the following information: (1) Source node (2) Destination node (3) p-Cycle chosen to protect the lightpath (4) *CG1* chosen to carry the lightpath (5) *CG2* (optional) chosen to carry the lightpath. All the nodes, lightpath-protecting p-Cycles as well as the *CG*s are numbered at the initial configuration stage of the network.

The signaling range of PWLE is different from that of PWCE. The former is

the CG associated with a source node while the latter is network-wide. In order to take the signaling range into account, we weight the signaling message using the signaling range. For example, in Fig. 3.3 (a), node 0 is involved in the *CG* [0,2,3,6,8]. Suppose a lightpath is set up with node 0 as the source node. Then a message is sent by node 0 to nodes 2,3,6,8. Thus we count the number of messages sent as 4. For PWCE, if the capacity on a span is used up or becomes available, the number of messages sent is 10 for the network in Fig. 3.3 (a). We adopt the same test network and assumptions in the study of blocking performance. Fig. 3.6 shows the comparison of control overheads between PWLE and PWCE. Each point on the curve displayed in the figure is the average over every 40 events. From Fig. 3.6, we observe that the control overheads of PWLE always fluctuate around an average value while it comes to 0 from time to time in the case of PWCE. This reflects that the signaling mechanism of PWLE, which is event-based, is largely different from that of PWCE. Moreover, we find that the average number of basic information units is a bit higher in PWLE than in PWCE. However, the maximum number of basic information units is higher in PWCE than in PWLE.

We also study the impact of traffic load on control overheads in both PWLE and PWCE. We calculate the average control overhead per event using two groups of source-destination node pairs for 19 demands and 25 demands. For each group, three sets of source-destination node pairs are randomly chosen. The result is averaged over the 3 sets. As shown in Fig. 3.7, traffic load affects the control overheads

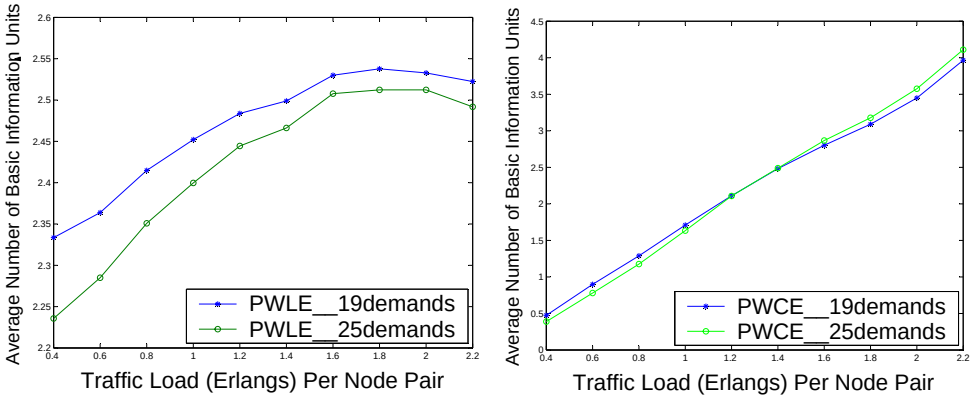

Figure 3.7: Average Control Overhead Comparison between PWLE (left) and PWCE (right), COST239, 19 and 25 source-destination node pairs, traffic load between each node pair: 0.8 Erlangs

much less in PWLE than in PWCE. In PWLE, the case of 25 demands always has lesser control overheads than the case of 19 demands because the latter has lower blocking probability than the former. For both cases, the control overheads increase until a given traffic load beyond which the control overheads begin to fall as the increasing blocking probability begins to dominate. On the other hand, the control overheads in PWCE change more significantly with increasing traffic load (from 0.5 to 4) as span status changes more frequently under high traffic loads.

Notice that all the above studies are conducted in terms of the basic information unit. However, the basic information unit of PWLE is different from that of PWCE. In order to have a direct and fair comparison between the two, we assume the size of the basic information unit of PWLE to be double that of PWCE. Using also the

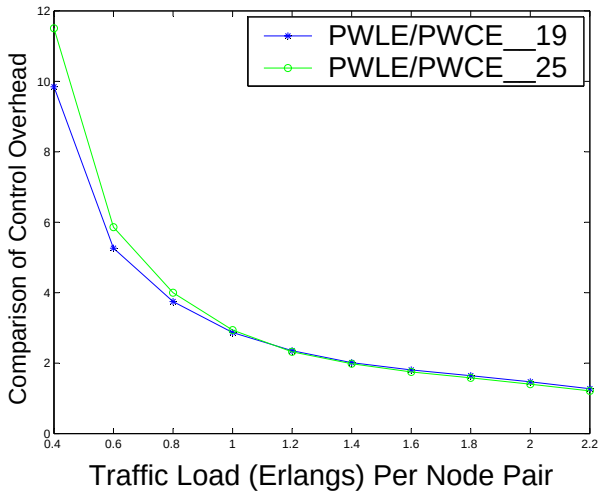

Figure 3.8: Comparison of Control Overhead between PWLE and PWCE

two groups of source-destination node pairs, we calculate the ratio of the control overheads in PWLE over that in PWCE as shown in Fig. 3.8. The ratio drops greatly with the traffic load. When the traffic load is 2 Erlangs, the ratio is around 2 while the ratio of the control overheads of SBPP over that of PWCE was reported to be around 40 [11]. Though PWLE shares the similar event-based signaling with SBPP, it has much lower control overheads due to its much smaller signaling range. Therefore, the operational complexity in terms of control overheads has not been compromised too much in PWLE while it enjoys a lot of advantages over PWCE.

3.6 Summary

In this chapter, we have proposed PWLE for dynamic provisioning of survivable services as an extension of PWCE to path-oriented protection. As it is formed based on lightpath-protecting p-Cycles, we have proposed Compatible Grouping to optimize the working layer. We have also formulated PWLE as an MILP model and solved it using CPLEX. Furthermore, we have proposed a distributed routing algorithm, Compatible Group Routing (CGR). The results we have obtained indicate that PWLE has a higher capacity efficiency, better blocking performance, less wavelength conversions, and acceptable operational complexity.

3.7 Formulation of PWCE_WP/WC Model

We formulate the PWCE_WP/WC with\without shaping consideration as an ILP model. Parameter Y_s^w is obtained by shortest-path routing all forecasted traffic demands as well as the wavelength assignment.

Sets:

$\boldsymbol{P}$: Set of topologically defined candidate span-protecting p-Cycles, indexed by j

$\boldsymbol{S}$: Set of spans of the network, indexed by s

$\boldsymbol{W}$: Set of wavelengths, indexed by w

Parameters:

Z_s^j: 1 if the s^{th} span is an on-cycle span of the j^{th} span-protecting p-Cycle, 0 otherwise

X_s^j: 2 if the s^{th} span is a straddling span of the j^{th} span-protecting p-Cycle, 1 if it is on-cycle, 0 otherwise

Y_s^w: 1 if the w^{th} wavelength is pre-assigned to forecasted traffic on the s^{th} span, 0 otherwise

T_s: The total number of deployed channels on the s^{th} span

α : A weighting factor trading off between shaping consideration and volume maximization of PWCE_WP/WC

Variables

N_s: The total number of protected channels on the s^{th} span

γ_w^j: 1 if the w^{th} wavelength is taken up by the j^{th} span-protecting p-Cycle, 0 otherwise

λ: Scaler variable

Objective:

$$Maximize \sum_{s \in S} N_s \text{ (Non-shaping)} \tag{3.9}$$

$$Maximize(\lambda + \alpha \cdot \sum_{s \in S} N_s) \text{ (Shaping)} \tag{3.10}$$

Constraints:

$$\sum_{j \in P} (Z_s^j \cdot \gamma_w^j) + Y_s^w \leq 1$$

$$\forall s \in \boldsymbol{S}, w \in \boldsymbol{W} \tag{3.11}$$

$$\sum_{j \in P, w \in W} (Z_s^j \cdot \gamma_w^j) + N_s \leq T_s$$

$$\forall s \in \boldsymbol{S} \tag{3.12}$$

$$N_s \leq \sum_{j \in P, w \in W} (\ X_s^j \ \cdot \gamma_w^j)$$

$$\forall s \in \boldsymbol{S} \tag{3.13}$$

$$N_s \geq \sum_{w \in W} Y_s^w$$

$$\forall s \in \boldsymbol{S} \text{ (Non-shaping)} \tag{3.14}$$

$$N_s \geq \lambda \cdot \sum_{w \in W} Y_s^w$$

$$\forall s \in \boldsymbol{S} \text{ (Shaping)} \tag{3.15}$$

Constraint (3.11) ensures no wavelength conflict on a span. Constraint (3.12) ensures the sum of protected capacity and spare capacity on a span does not exceed

its total capacity. Constraint (3.13) bounds the protected capacity on each span by the maximum protection capability of the chosen set of p-Cycles. Constraint (3.14) & (3.15) guarantees the resulting envelope conforms to the traffic load distribution.

Chapter 4

Lightpath-protecting p-Cycle Selection for Protected Working Lightpath Envelope

4.1 Introduction

In **Chapter 3**, we developed a new path-oriented protection scheme for dynamic traffic called Protected Working Lightpath Envelope (PWLE), which partitions the network capacity into a working layer and a protection layer using lightpath-protecting p-Cycles. To design PWLE, pre-computation of a subset of candidate cycles and cycle selection within the subset are crucial.

In existing literatures, there are briefly two approaches to designing a p-Cycle protected network: Integer Linear Programming (ILP) optimization and heuristic algorithms. The ILP is known for its intensive computational complexity which

limits its use to small or medium sized networks. Different from the ILP, heuristic algorithms iteratively select cycles based on given criteria of cycle selection. For instance, Capacitated Iterative Design Algorithm (CIDA) determines p-Cycles iteratively based on their actual efficiency [43]. Similar to CIDA in cycle selection, the ER-based unity-p-Cycles algorithm adds the consideration of unidirectional traffic and p-Cycles [44]. Besides, in [45], researchers select p-Cycles based on *Cycle Efficiency*, followed by the refinement of the selected p-Cycles. While the above three algorithms deal with span-protecting p-Cycles, the approach in [46] extends research into developing heuristic algorithms for path-protecting p-Cycles, in which a set of high-score path-protecting p-Cycles are chosen to protect pre-defined paths. On the other hand, cycle pre-computation algorithms are important to provide ILP and heuristic algorithms with an efficient and sufficient subset of p-Cycles as inputs, e.g., Straddling Link Algorithm (SLA) [47], Weighted DFS-based Cycle Search (WDCS) [48] and Dynamic p-Cycle Selection (DPS) [49]. However, they are all based on span-protecting p-Cycles.

Although PWLE is a promising scheme, the MILP solution of PWLE proposed in **Chapter 3** is computationally intensive, which gives rise to the need for heuristic algorithms. As a path-oriented protection scheme, PWLE is structured based on lightpath-protecting p-Cycles, which are designed to protect an envelope of working channels instead of pre-defined paths. Due to such uniqueness, no

existing algorithm can be applied directly for cycle selection for PWLE. Furthermore, a cycle pre-computation algorithm tailored for lightpath-protecting p-Cycles is also needed. In this chapter, we propose the AttachNode-Based Cycle Generation (ANCG) algorithm for pre-computation of candidate cycles and heuristic algorithms for lightpath-protecting p-cycle selection for PWLE.

4.2 Design of Lightpath-protecting p-Cycle Selection for PWLE

In this section, we first develop the AttachNode-Based Cycle Generation (ANCG) algorithm in order to pre-compute candidate cycles with high Efficiency Ratio *(ER)*s which have been defined for lightpath-protecting p-Cycles in **Chapter 3**. Based on the ANCG algorithm, we further introduce three heuristic algorithms for cycle selection which share the same framework but employ different strategies in cycle selection. Our objective is to volume-maximize the envelope of working layer subject to 100% restorability of the given traffic demand.

4.2.1 AttachNode-Based Cycle Generation (ANCG)

Before cycle selection, we need to generate a set of candidate cycles. Instead of enumerating all possible cycles, we propose the ANCG algorithm to find a small set

of cycles with high *ER*s. ANCG is based on the WDCS algorithm (Weighted DFS-based Cycle Search) [48] where high efficiency cycles are likely to be found early in the DFS (Depth First Search) algorithm with a controlled searching order due to the different weights assigned to edges. The edge with higher weight has a better chance to be chosen. Therefore, weight assignment function plays an essential role in the control over the order of cycles generated and thus the efficiency of the algorithm.

Further, based on the unique relation between lightpath-protecting p-Cycles and their *Attach Node*s, we notice that cycles encircling high-degree nodes usually have high *ER*s. In light of this, we choose high-degree nodes as *Attach Node*s and the nodes adjacent to them with the smallest index as the starting nodes of cycles, based on which we design the weight assignment function. Now we explain the weight assignment function. Given graph $(V,\ E)$, suppose $\mu \in V$, $\varkappa \in V$ $(\langle \mu, \varkappa \rangle \in E)$ are chosen to be an *Attach Node* and a starting node related to μ respectively. $weight\,(m, n)$ $(m, n \in V)$ is assigned in two phases.

Phase 1 When choosing among the neighboring nodes from the current node m, we prefer nodes with high node degree and adjacent to node μ. Meanwhile, we try to avoid going back to the starting node $\varkappa$. Hence, $weight\,(m, n)$ is assigned as follows.

$weight\,(m,n)$	*Condition*
$Degree[n]$	if $n \neq \varkappa,\ \langle n,\mu\rangle \notin E$
$2Degree[n]$	if $n \neq \varkappa,\ \langle n,\mu\rangle \in E,\ \langle m,\mu\rangle \notin E$
$4Degree[n]$	if $n \neq \varkappa,\ \langle n,\mu\rangle \in E,\ \langle m,\mu\rangle \in E$
Δ	if $n = \varkappa,\ \langle n,\mu\rangle \notin E$
2Δ	if $n = \varkappa,\ \langle n,\mu\rangle \in E,\ \langle m,\mu\rangle \notin E$
4Δ	if $n = \varkappa,\ \langle n,\mu\rangle \in E,\ \langle m,\mu\rangle \in E$
	Δ is a small number (0.5)

Phase 2 We adjust $weight\,(m,n)$ by taking into account two special cases:

Case 1 Node n or m coincides with the *Attach Node* μ. We set $weight\,(m,n) = 0$ as we do not allow the chosen *Attach Node* μ to fall on the cycle.

Case 2 Node m is adjacent to the *Attach Node* μ. Meanwhile, $Degree\,[n] = 2$ and the node, say k, adjacent to n is also adjacent to the *Attach Node* μ. This is exactly a situation of 2-degree chain with node n as the intermediate 2-degree vertices. We hope to include the chain into the cycle for the sake of *ER*. Similar consideration is discussed in details in [48].

Therefore, $weight\,(m,n)$ is adjusted as follows:

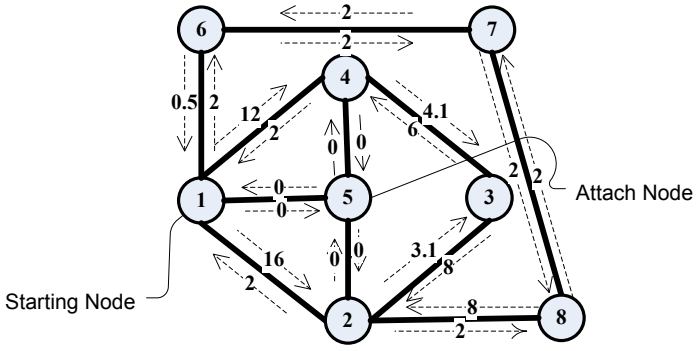

Figure 4.1: Illustration of Weight Assignment of ANCG Algorithm

$weight\,(m,n)$	*Condition*
0	if m=μ *or* n=μ
$Degree[k]+\varepsilon$	if $Degree[n]$=2 and $\exists k\ \langle m,\mu\rangle, \langle n,k\rangle, \langle k,\mu\rangle \in E$ ε is a small number (0.1)

An example in Fig.4.1 is shown to illustrate the process of weight assignment. Node 5 is chosen to be the *Attach Node* while node 1 is selected to be the starting node. Notice that 2-3-4 is a 2-degree chain where Case 2 of Phase 2 applies.

In [48], cycles with high efficiency are generated to protect each span. Therefore, WDCS is called for every node and its neighbor to generate κ cycles, which results in $2\kappa\,|E|$ cycles in total. In contrast, ANCG calls WDCS, which adopts the proposed weight assignment function, for each *Attach Node* and a selected starting node, thus generating $\kappa\,|V|$ cycles totally.

4.2.2 Heuristic Algorithms of Lightpath-protecting p-Cycle Selection (HALCS)

HALCS is a 2-phase algorithm which emphasizes 100% restorability in HALCS-Phase 1 and volume-maximization of the envelope of working layer in HALCS-Phase 2. In order to explain HALCS clearly, we first define the parameters, variables, function and metrics. Then we elaborate on the two phases of HALCS followed by the pseudocodes.

Parameters, Variables, Function, Metrics

Parameters:

D: $\{\delta_d\}$ set of traffic demands, indexed by d

N: $\{n_m\}$ set of nodes of the network, indexed by m

$N_{sd,d}$: set of end nodes of the d^{th} demand

S: $\{\tau_s\}$ set of spans of the network, indexed by s

P: $\{p_j\}$ set of topologically defined candidate lightpath-protecting cycles, indexed by j

Υ_j: $\{\gamma_{g_j}\}$ set of CGs of the j^{th} lightpath-protecting p-Cycle, indexed by g_j

$N_{on,j:}$ set of on-cycle nodes of the j^{th} lightpath-protecting p-Cycle, indexed by m_j, $N_{on,j} \subseteq N$

$S_{on,j}$: set of on-cycle spans of the j^{th} lightpath-protecting p-Cycle, indexed by s_j, $S_{on,j} \subseteq S$

S_{g_j}: set of spans belonging to the g_j^{th} CG, $S_{g_j} \subseteq S$

N_{g_j}: set of nodes contained in the g_j^{th} CG, $N_{g_j} \subseteq N$

D_{g_j}: $\left\{\delta_d | \delta_d \in D, \forall \delta_d, N_{sd,d} \subseteq N_{g_j}\right\}$ set of demands that can be carried by the g_j^{th} CG of the j^{th} lightpath-protecting p-Cycle, $D_{g_j} \subseteq D$

D_j: $\bigcup\limits_{\gamma_{g_j} \in \Upsilon_j} D_{g_j}$ set of demands that can be protected by the j^{th} lightpath-protecting p-Cycle, $D_j \subseteq D$

P_d: $\left\{p_j | p_j \in P, \forall p_j, \exists \gamma_{g_j} \in \Upsilon_j, N_{sd,d} \subseteq N_{g_j}\right\}$ set of candidate lightpath-protecting cycles capable of protecting the d^{th} demand, $P_d \subseteq P$

Variables:

D^u: set of traffic un-protected demands, index by d^u, $D^u \subseteq D$

S^r: set of spans remaining unexhausted, indexed by s^r, $S^r \subseteq S$

P^a: set of available candidate lightpath-protecting p-Cycles subject to the remaining capacity on spans

$$P^a = \{p_j | p_j \in P; S_{on,j} \subseteq S^r\}$$

$S^r_{g_j}$: set of unexhausted spans belonging to the g_j^{th} CG

$$S^r_{g_j} = S_{g_j} \cap S^r$$

$N^a_{g_j}$: set of nodes contained in the g_j^{th} CG subject to the remaining capacity on spans

$$N^a_{g_j} = F\left(S_{g_j} \cap S^r\right)$$

P_d^a: set of available candidate lightpath-protecting p-Cycles capable of protecting the d^{th} demand

$\left\{p_j | p_j \in P^a, \forall p_j, \exists \gamma_{g_j} \in \Upsilon_j, N_{sd,d} \subseteq N_{g_j}^a\right\}$

if $\delta_d \in D^u$, $\emptyset$ otherwise

$D_{g_j}^u$: set of un-protected demands that can be carried by the g_j^{th} CG of the j^{th} lightpath-protecting p-Cycle

$\left\{\delta_d | \delta_d \in D^u, \forall \delta_d, N_{sd,d} \subseteq N_{g_j}^a\right\}$

if $p_j \in P^a$, $\emptyset$ otherwise

D_j^u: set of un-protected demands that can be protected by the j^{th} candidate lightpath-protecting p-Cycle

$D_j^u = \bigcup_{\gamma_{g_j} \in \Upsilon_j} D_{g_j}^u$

Function:

F : $S_{g_j} \rightarrow N_{g_j}$: a function F from S_{g_j} to N_{g_j}

Metric:

Protection Cardinality of Demand (*PCD*)

Defined for demands as the amount of available candidate lightpath-protecting p-Cycles capable of protecting them.

$$\mho = \{\varpi_d |\ \varpi_d = \#P_d^a\} \tag{4.1}$$

Actual Efficiency Ratio (*AER*)

Defined for available lightpath-protecting p-Cycles as their ERs yet calculated based on the remaining network capacity.

$$\Psi = \left\{ \left(2 \times \left|\overline{S}_j^r\right| + \#S_{on,j}\right) \ / \ \#S_{on,j} \mid p_j \in P^a \right\} \tag{4.2}$$
$$\overline{S}_j^r = \left\{ \#S_{g_j}^r, \gamma_{g_j} \in \Upsilon_j \right\}$$

Traffic Pattern Relevance for Cycle (*TPRC*)

Defined for available lightpath-protecting p-Cycle as the ratio of amount of demands protectable to the maximum amount of node pairs among its on-cycle nodes. $TPRC$ helps to evaluate the relevance between a lightpath-protecting p-Cycle and the un-protected traffic demands.

$$\mathbb{R} = \left\{ \Phi_j \mid \Phi_j = \#D_j^u \ / \ \binom{\#N_{on,j:}}{2}, \ p_j \in P^a \right\} \tag{4.3}$$

Traffic Pattern Relevance for CG (*TPRG*)

Defined similarly with $TPRC$ to evaluate the relevance between a CG and the un-protected traffic demands:

$$\mathcal{L} = \left\{ \xi_j | \ \xi_j = \left\{ \#D_{g_j}^u \ / \ \binom{\#N_{g_j}^a}{2} | \ \gamma_{g_j} \in \Upsilon_j \right\} \right\} \tag{4.4}$$

Traffic Pattern Related AER (*TAER*)

Defined for a lightpath-protecting p-Cycle as the ratio of weighted sum of its straddling capacity, with $TPRG$ as weight factors, to the amount of its on-cycle

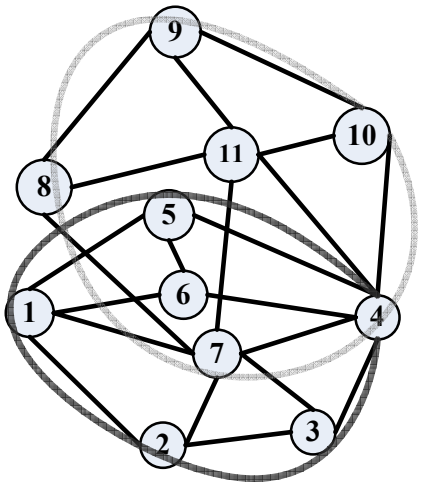

Figure 4.2: Illustration of the Calculation of Metrics.

spans. *TAER* of a lightpath-protecting *p*-Cycle measures both the capacity efficiency and the relevance with the traffic demand.

$$\mathbb{C} = \left\{ \Omega_j \mid \Omega_j = \overline{S}_j^r \cdot \xi_j \ / \ \#S_{on,j},\ p_j \in P^a \right\} \tag{4.5}$$

where $\#X$ denotes the cardinal number of set X, $|X|$ the 1-norm of X ($|X|=\Sigma x_i$, $x_i \in X$). In addition, $X \cdot Y$ represents the dot product of X and Y. For unavailable lightpath-protecting *p*-Cycle, we assign 0 to their *AER*, *TPRC*, and *TAER*

We use an example to illustrate the calculation of *AER*, *TPRC*, and *TAER*. In Fig. 4.2, there are two candidate lightpath-protecting *p*-Cycles: A(1-2-3-4-5-1) and B(4-10-9-8-7-4). For A, the *Attach Node*s are node 6 and 7 while the *Compatible Groups (CG)* are [1,4,5] and [1,2,3,4]. Similarly, for B, the *Attach Node* is node 11 and *CG* is [4,7,8,9,10]. Further, we have 5 un-protected traffic demands between

node pairs: (1,4), (2,4), (4,9), (7,9), (8,10). Suppose no span is exhausted at first.

$AER(A)$=(2×7+5)/5=3.8, $AER(B)$=(2×5+5)/5=3

$TPRC(A)$=2/$\binom{5}{2}$=0.2, $TPRC(B)$=3/$\binom{5}{2}$=0.3

$TAER(A)$=(3×(1/$\binom{3}{2}$)+4×(1/$\binom{4}{2}$))/5=1/3

$TAER(B)$=(5×(3/$\binom{5}{2}$))/5=0.3

Suppose B is chosen to protect demand (7,9), (8,10) and span 4-7 is exhausted. Then the three metrics need to be calculated again. Notice that the three metrics of B are set to 0 since B becomes unavailable caused by exhausted span 4-7.

$AER(A)$=(2×6+5)/5=3.4, $AER(B)$=0

$TPRC(A)$=2/$\binom{5}{2}$=0.2, $TPRC(B)$=0

$TAER(A)$=(3×(1/$\binom{3}{2}$)+3×(1/$\binom{3}{2}$))/5=0.4

$TAER(B)$=0

HALCS-Phase 1

The objective of phase 1 is to ensure 100% restorability of the given traffic demands. Recall that PWLE is not limited to predicated demand patterns and can actually be designed in the absence of traffic forecasts, in which case phase 1 will be skipped.

From the un-protected demands, we firstly choose the one that can be protected by the least amount of available candidate lightpath-protecting p-Cycles. In other words, we choose the un-protected demand with the minimum *PCD*. Secondly, among those candidate lightpath-protecting p-Cycles capable of protecting this demand, we choose the one with the best qualification. The evaluation of the

qualification depends on the metric (*AER* or *TPRC* or *TAER*) to be chosen, thus generating three variants of the algorithm, namely, HALCS_AER, HALCS_TPRC, HALCS_TAER. After choosing a best qualified cycle, we search among the remaining un-protected traffic demands for any one protectable by this cycle. Finally, we update the network status, which triggers the update of all variables and metric. In this way, we iteratively choose lightpath-protecting p-Cycles until no un-protected traffic demand remains.

HALCS-Phase 2

The objective of phase 2 is to volume-maximize the envelope of working layer. Therefore, capacity efficiency of lightpath-protecting p-Cycles becomes the main consideration in phase 2. We thereby iteratively choose the one with the highest *AER* among the available candidate lightpath-protecting p-Cycles until there is no available candidate cycle.

Pseudocodes of HALCS

The pseudocodes shown in Algorithms (1) & (2) are generic frameworks for HALCS_AER, HALCS_TPRC, HALCS_TAER. The function *MaxCycleQualification* highlighted in Algorithm (1) needs to be specified based on the different metric adopted. Algorithm (3) defines the *MaxCycleQualification* specified for HALCS_TAER. In a similar way, we can also define the *MaxCycleQualification* for HALCS_AER and

Algorithm 1 HALCS-Phase 1

Require: $D\{\delta_d\}, P\{p_j\}$

Ensure: P_{Select}

$P_{Select} \leftarrow \emptyset$,

$\left(P^a, D^u_{g_j}, P^a_d,\ S^r_{g_j}, N^a_{g_j}\right) \leftarrow \left(P, D_{g_j}, P_d, S_{g_j}, N_{g_j}\right)$

Phase 1: Satisfy Traffic Demands

while $D^u \neq \emptyset$ **do**

Sort $\mho$ in ascending PCD value

Select the demand with minimum PCD

$d \leftarrow Min(\mho)$

$D^u \leftarrow D^u \backslash \delta_d$

$\boxed{j \leftarrow MaxCycleQualification(P^a_d)}$

$D^u_j \leftarrow D^u_j \cap D^u$

$P_{Select} \leftarrow P_{Select} \cup p_j$

Sort D^u_j in ascending PCD value

for $k = 1$ to $\left|D^u_j\right|$ **do**

if δ_k can also be protected by p_j **then**

$D^u \leftarrow D^u \backslash \delta_k$

$D^u_j \leftarrow D^u_j \cap D^u$

end if

end for

Update S^r

Update $\left(P^a, D^u_{g_j}, P^a_d,\ S^r_{g_j}, N^a_{g_j}\right)$

Update $(\mho, \Psi, \mathbb{R}, \mathcal{L}, \mathbb{C})$ based on Eq.4.1∼Eq.4.5

end while

Algorithm 2 HALCS-Phase 2

Phase 2: Volume-Maximize the envelope of working layer

while $P^a \neq \emptyset$ **do**

Sort Ψ in descending AER value

Select cycle $p_j \in P^a$ with maximum AER

$j \leftarrow Max\,(\Psi)$

Update $S^r, \left(P^a, D^u_{g_j}, P^a_d,\ S^r_{g_j}, N^a_{g_j}\right)$ and Ψ

end while

Algorithm 3 *MaxCycleQualification*

Require: $P^a_d, \mathbb{C}$

Ensure: j

$\mathbb{C}|_d \longleftarrow \{\Omega_j \mid \Omega_j,\ p_j \in P^a_d\}$

Sort $\mathbb{C}|_d$ in descending $TAER$ value

Select the cycle with maximum $TAER$

$j \leftarrow Max\,(\mathbb{C}|_d)$

HALCS_TPRC.

4.3 Numerical Results and Discussions

We use three test networks whose topologies can be found in Fig. 3.4. They are NSFNET, Bellcore and COST239, whose average node degrees range from 3 to 4.7. For all the three test networks, we assume one fiber-pair per span as the total deployed capacity. Each unit of capacity refers to two channels on the same wavelength over one fiber pair per span. For each network, we randomly choose 3 sets of 19-demand pairs and average the results over the three. In all the cases, every demand bundle is assumed two units. The computation platform is Intel Pentium IV 2.4-GHz PC running Windows XP with 1-GB memory and 40-GB hard disk.

4.3.1 Pre-computation of Candidate Cycles

In ANCG, each node is given a chance to be selected as an *Attach Node*. However, different *Attach Node*s are assigned with different κ based on their node degrees. The differentiation of κ is made due to the consideration that an *Attach Node* with higher node degree usually has a better chance to generate cycles of high *ER*. In our experiment, we choose the average node degree as a threshold to differentiate κ. The results are displayed in Table 4.1. The bottom row shows the ratio of the

	NSFNET	Bellcore	COST239
Average Node Degree	3	3.7	4.7
κ(>Avg. Node Degree)	10	25	35
κ($\leq$Avg. Node Degree)	5	20	25
Number of Cycles	65	328	343
Improvement	46.76%	42.05%	27.86%

Table 4.1: Precomputed Candidate Cycles by ANCG

amount of cycles generated by ANCG to the amount of those used by the optimal design in **Chapter 3**. From the results, we can see that ANCG can greatly reduce the amount of candidate cycles. As these candidate cycles serve as the inputs to the optimization model or heuristic algorithms, this improvement would be very useful to reduce the computational time of the optimization model or heuristic algorithms.

4.3.2 Performance Comparison with the Optimal

Tables 4.2, 4.3 and 4.4 list the resultant total protected capacity of the three heuristic algorithms and the differences from the optimal design. The figures in brackets represent the ratio of protected capacity to the whole network capacity. We observe from the tables that the Diff% is within 8% for HALCS_TAER and

Wavelengths/fiber		10	14	20
PWLE_OPT	Vol.	134(63.8%)	209(71.1%)	315(75%)
HALCS_AER	Vol.	120(57.14%)	190(64.62%)	285(67.85%)
	Diff%	6.66	6.48	7.15
HALCS_TPRC	Vol.	123(58.57%)	189(64.29%)	282(67.14%)
	Diff%	5.23	6.81	7.86
HALCS_TAER	Vol.	125(59.5%)	194(65.98%)	289(68.8%)
	Diff%	4.3	5.12	6.2

Table 4.2: Comparison of Volume of Working Envelope between HALCS Algorithms and MILP for Network NSFNET

within 10% for HALCS_AER and HALCS_TPRC, which suggests the effectiveness of the heuristic algorithms in selecting lightpath-protecting p-Cycles with good quality. It also implies the good quality of the candidate cycles pre-computed by the ANCG algorithm. As we increase the deployed capacity on each span, we notice that the Diff % generally increases. This is because the subset of candidate cycles used by the optimal design also includes small cycles with lower ER while the subset generated by ANCG algorithm usually contains only cycles with high ERs which are usually relatively large cycles. As the deployed capacity increases, small cycles can help to further extend the envelope of working layer while high-ER cycles may not be available due to the insufficient incremental network capacity. Additionally,

Wavelengths/fiber		10	14	20
PWLE_OPT	Vol.	204(72.9%)	302(77.0%)	446(79.6%)
HALCS_AER	Vol.	186(66.4%)	279(71.17%)	413(73.75%)
	Diff%	6.5	5.83	5.85
HALCS_TPRC	Vol.	197(70.36%)	282(71.93%)	404(72.14%)
	Diff%	2.54	5.07	7.46
HALCS_TAER	Vol.	199(71.07%)	284(72.44%)	415(74.11%)
	Diff%	1.83	4.56	5.49

Table 4.3: Comparison of Volume of Working Envelope between HALCS Algorithms and MILP for Network BellCore

in the case of HALCS_AER, the Diff% decreases first and then increases, which implies that it is sensitive to the impact imposed by the traffic demand. This is because HALCS_AER uses AER to choose cycles in HALCS-Phase 1 and thus always chooses the cycle with high capacity efficiency rather than high relevance to the remaining un-protected traffic. Thus the cycles chosen in HALCS_AER might not be best customized for the given traffic demands. When the deployed capacity decreases, the protection requirement imposed by traffic demands can prohibit HALCS_AER from generating higher volume of protected capacity. For all the test networks, the computation time of the three heuristic algorithms is within 2 seconds in the case of 10 and 14 wavelengths per fiber and within 4 seconds in the

Wavelengths/fiber		10	14	20
PWLE_OPT	Vol.	212(81.5%)	302(84.3%)	439(84.4%)
HALCS_AER	Vol.	188(72.3%)	275(75.55%)	391(75.19%)
	Diff%	9.2	8.75	9.21
HALCS_TPRC	Vol.	191(73.46%)	271(74.45%)	388(74.6%)
	Diff%	8.04	9.85	9.8
HALCS_TAER	Vol.	198(76.15%)	282(77.47%)	398(76.53%)
	Diff%	5.35	6.83	7.87

Table 4.4: Comparison of Volume of Working Envelope between HALCS Algorithms and MILP for Network COST239

case of 20.

4.3.3 Performance Comparison among HALCSs

In order to compare the performance among HALCS_AER, HALCS_TPRC and HALCS_TAER, we investigate their performances with the deployed capacity ranging from 10 to 20. In Fig. 4.3, the figures along the Y axis represent the ratio of the protected capacity to the whole network capacity. From Fig. 4.3, we discover that HALCS_TAER performs the best among the three. This is because in the *MaxCycleQualification*, HALCS_TAER chooses the best qualified cycle with the consideration of both capacity efficiency and traffic relevance while

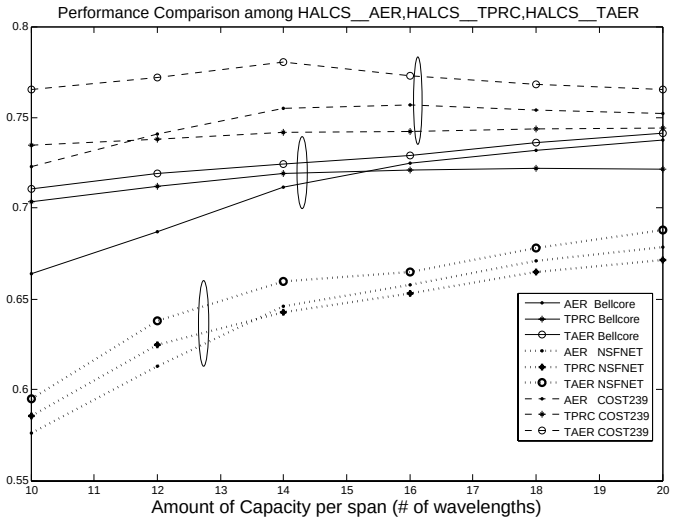

Figure 4.3: Performance Comparison among HALCSs

HALCS_TPRC and HALCS_AER consider either of the two factors. Furthermore, by comparing the performance between HALCS_TPRC and HALCS_AER, we find that HALCS_TPRC always outperforms HALCS_AER at first and then gets exceeded when the deployed capacity increases. This is due to the different metrics they use in *MaxCycleQualification*. In HALCS-Phase 1, HALCS_TPRC always chooses the cycle most relevant to the remaining un-protected traffic, which enables it to exit HALCS-Phase 1 and enter HALCS-Phase 2 faster than HALCS_AER. In other words, HALCS_TPRC usually requires less lightpath-protecting p-Cycles than HALCS_AER for the purpose of satisfying traffic demands, thus having more remaining network capacity for volume-maximization in HALCS-Phase 2. This is manifested when the deployed capacity is low because the amount of available candidate cycles decreases quickly during cycle selection. However, the impact

imposed by traffic demand decreases as the deployed capacity increases, which facilitates HALCS_AER to outperform HALCS_TPRC due to its emphasis on the capacity efficiency of cycles.

4.4 Summary

In this chapter, we have proposed a cycle pre-computation algorithm (ANCG) to generate candidate lightpath-protecting p-Cycles with high ERs. In order to select a set of lightpath-protecting p-Cycles from the candidate cycles effectively for PWLE, we have then developed a heuristic algorithm with three variants (HALCS_AER, HALCS_TPRC, HALCS_TAER). Numerical results show that ANCG generates a small subset of candidate cycles of good quality with high ERs. Besides, the results obtained by the heuristic algorithms are close to those of optimal solutions obtained in **Chapter 3** but with much reduced computational time. Further, the comparative study among the heuristic algorithms shows that HALCS_TAER performs the best among the three variants.

Chapter 5

Connectivity Aware Protected Working Lightpath Envelope

5.1 Introduction

In this chapter, we study the role the network connectivity plays in PWLE and integrate the factor of network connectivity into the design of PWLE. As discussed in **Chapter 3**, lightpath-protecting p-Cycle is designed to protect a group of channels available for routing rather than a set of pre-defined end-to-end paths. However, the utilization of these protected channels is constrained by the requirement of mutual link-disjointness imposed on the lightpaths protected by lightpath-protecting p-Cycles for the purpose of full survivability against any single failure. Therefore,

the topological features, such as network connectivity, need to be taken into account to properly reflect the protection capability of lightpath-protecting p-Cycles. In light of this, we propose a concept termed *Effective Envelope*, developed based on the Maximum Concurrent Flow Problem (MCFP) [50] [51], to evaluate the protected capacity of lightpath-protecting p-Cycles from a combined perspective of volume and connectivity. Based on *Effective Envelope*, we develop Connectivity Aware Protected Working Lightpath Envelope (CAPWLE) which is optimized by an MILP model with the objective to enhance the connectivity of the working layer while maintaining the high capacity efficiency.

5.2 Motivation and Concept of CAPWLE

As a critical role in PWLE, lightpath-protecting p-Cycles are designed to protect, instead of a set of pre-defined lightpaths, a group of channels that can be flexibly utilized to establish lightpaths between on-cycle nodes. A lightpath-protecting p-Cycle is capable of protecting multiple lightpaths simultaneously subject to the constraint of mutual link-disjointness so as to achieve full survivability against any single span failure. For example, Fig. 5.1 (a) displays a lightpath-protecting p-Cycle where dashed lines represent on-cycle spans and solid lines off-cycle spans (the same for Fig. 5.1 (b) and (c)). The possible scenarios of coexisting protected

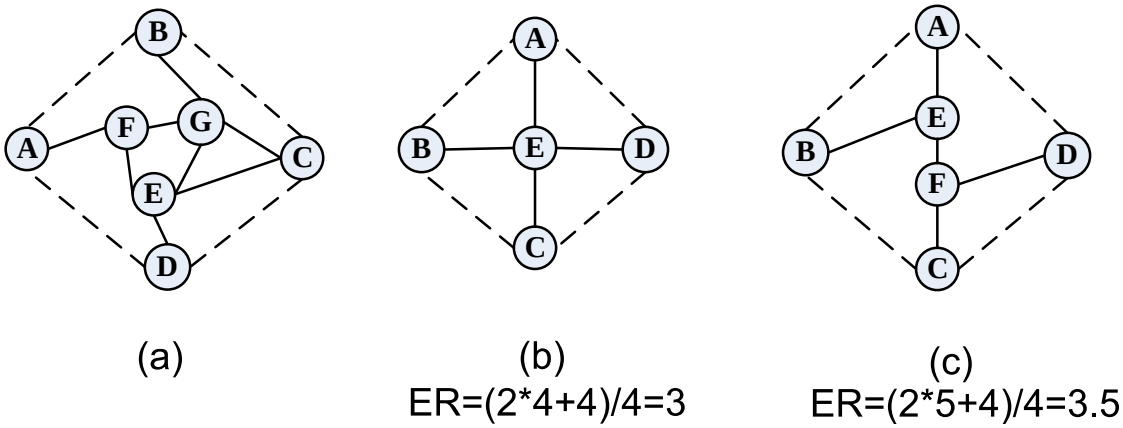

Figure 5.1: (a) Illustration of Lightpath-protecting p-Cycle (b) & (c) Illustration of the Imperfection of *ER*

straddling lightpaths can be A-F-G-C and B-G-E-D, A-F-E-D and B-G-C, or A-F-G-B and D-E-C and so forth. For each straddling path, such as A-F-G-C, the lightpath-protecting p-Cycle can provide two backup paths such as A-B-C and A-D-C. Therefore, the protected capacity defined for the lightpath-protecting p-Cycle is the sum of two units on each of the off-cycle spans and one unit on each of the on-cycle spans where one unit of capacity is herein denoted as one wavelength on each span.

Due to path-oriented protection mechanism, lightpath-protecting p-Cycles have high intrinsic capacity efficiency in terms of high *ER*. Intuitively, the larger the size of a lightpath-protecting p-Cycle, the higher its *ER*. However, the requirement of mutual link-disjointness imposed on the protected lightpaths makes the protected capacity on distinct spans interdependent, which becomes an inhibiting factor. For

instance, in Fig. 5.1 (a), if lightpath B-G-F-E-D is established and protected, then no other straddling lightpath can be further established and protected. To deal with the trade-off between utilization and capacity efficiency, i.e., *ER*, we limited the size of lightpath-protecting p-Cycles to protecting lightpaths traversing up to 3 physical hops in the model in **Chapter 3**.

Although we explicitly limited the size of lightpath-protecting *p*-Cycles to take into account the trade-off between utilization and capacity efficiency, we have not paid enough attention to this factor for lightpath-protecting *p*-Cycles within the size limit. Recall from **Chapter 3**, for each lightpath-protecting *p*-Cycle, *ER* is calculated based on its *Derived Graph* via the following formula.

$$ER = \frac{2 * \sum \textit{Off-cycle Spans} + \sum \textit{On-cycle Spans}}{\sum \textit{On-cycle Spans}} \tag{5.1}$$

$$= \frac{\textit{Off-cycle Protected Capacity}}{\textit{Spare Capacity}} + 1 \tag{5.2}$$

ER, as a core metric in PWLE, is a volume-based metric (i.e., the ratio of the volume of protected capacity to the volume of spare capacity). It does not reflect the topological feature of the *Derived Graph* which plays an essential role in the utilization of the protected capacity. Fig. 5.1 (b) and (c) depict the scenario where *ER* may not evaluate lightpath-protecting *p*-Cycles with different *Derived Graph*s properly. Using Eq. (5.1), we can obtain the *ER*s for the two as 3 and

3.5, respectively, which makes (c) outweigh (b). Nevertheless, in (b), two link-disjoint lightpaths, A-E-C and B-E-D can be established simultaneously between node pairs (A,C) and (B,D) whereas it is impossible for (c) because link E-F forms a bottleneck. The unfairness of *ER* lies in its failure to capture the impact of connectivity of the *Derived Graph* on the actual utilization of the protected capacity. PWLE, thereby, may also implicitly overlook the importance of the connectivity of the resulting working layer. In light of this, we introduce Connectivity Aware Protected Working Lightpath Envelope (CAPWLE) to factor the connectivity in.

Sharing the same framework with PWLE, CAPWLE also partitions the network capacity into a working layer and a protection layer based on lightpath-protecting p-Cycles yet with a different objective which combines volume-maximization and connectivity enhancement of the working layer. To fulfill the target, we will evaluate the protection capability of lightpath-protecting p-Cycles from a new perspective by means of *Effective Envelope* which embeds topological information into the conventional volume-based evaluation. *Effective Envelope* will be introduced and developed based on the Maximum Concurrent Flow Problem (MCFP) [50] in the next section.

5.3 Design of CAPWLE

In **Chapter 3**, we "volume-maximize" the envelope of working layer, as the objective of PWLE, so as to achieve high capacity efficiency. By integrating the connectivity-awareness into the volume-maximization, we set the objective of maximizing the *Network Effective Envelope*in the design of CAPWLE. The *Network Effective Envelope* is defined as the aggregate of the *Effective Envelope* of all the selected lightpath-protecting p-Cycles. In this section, we will first introduce the concept of *Effective Envelope* and the method of the calculation, based on which we will then explain the optimization of CAPWLE.

5.3.1 Effective Envelope

Definition of Effective Envelope

Firstly, we focus on a single lightpath-protecting p-Cycle as it is the building block. Eq. (5.2) reveals that it is the off-cycle protected capacity that dominates the *ER*. Thus we cast our attention on the off-cycle protected capacity which can also be basically viewed as the sum of the protected capacity of *Compatible Groups (CG)*s. In order to reflect the connectivity of the *Derived Graph* where the protected capacity is distributed, we discount the volume of the protected capacity of each *CG* at a rate calculated based on the topology. By summation of the discounted protected capacity of each *CG*, we can get the effective volume of the protected

capacity of a single lightpath-protecting p-Cycle, which is defined as the *Effective Envelope* of the lightpath-protecting p-Cycle. Further, from the network-wide point of view, since the working envelope is comprised of the protected capacity of all the lightpath-protecting p-Cycles, the *Network Effective Envelope* is thereby defined as the aggregate of the *Effective Envelope* of all.

By substituting the off-cycle protected capacity (i.e., numerator) with the *Effective Envelope* in Eq. (5.2), we can integrate connectivity-awareness into *ER* to generate a connectivity-adjusted metric as shown in Eq. (5.3).

$$\textit{Connectivity-based ER} = \frac{\textit{Effective Envelope}}{\textit{Spare Capacity}} + 1 \tag{5.3}$$

This metric can be applied to the HALCS algorithms developed in **Chapter 4** to improve the algorithm of lightpath-protecting p-Cycle selection.

Obviously, the discount rate to be calculated to capture the topological feature of the *Derived Graph* is the key to the *Effective Envelope*. As we hope the protected capacity of a lightpath-protecting p-Cycle can be shared by its on-cycle nodes as flexibly as possible, we propose an approach to calculate the discount rate based on the Maximum Concurrent Flow Problem (MCFP) [50] [51]. Before detailing the calculation, we briefly introduce the basics of MCFP.

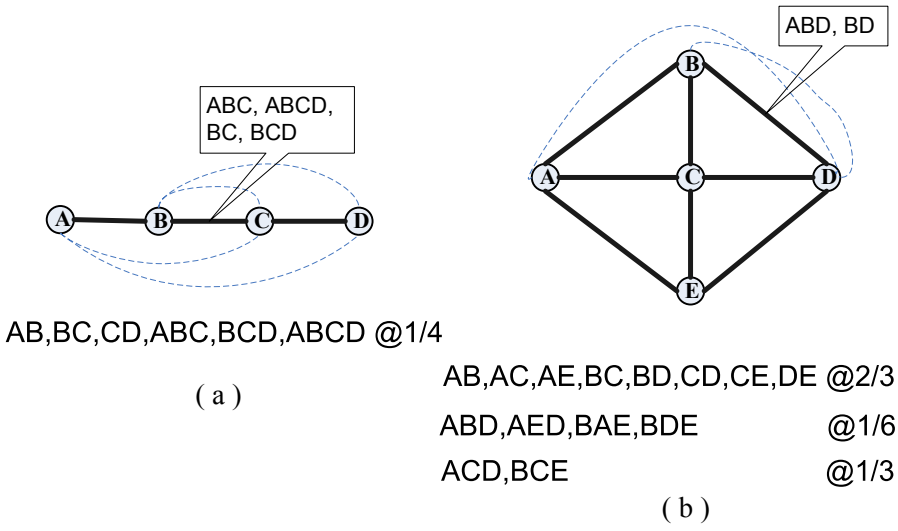

Figure 5.2: Concurrent Flow and Concurrent Connectivity [15].

Maximum Concurrent Flow Problem (MCFP)

Suppose there exists a flow of traffic between all pairs of nodes that must be hosted concurrently. The Maximum Concurrent Flow Problem (MCFP) can be defined as follows:

MCFP: For a graph G, a fractional flow is assigned to each path so that the sum of the flows on all paths between each node pair is the same value (termed the "throughput") where the sum of flows on all paths containing any given edge is at most unity. The objective of MCFP is to obtain the maximum throughput of concurrent flow in the graph (termed the "concurrent connectivity $\kappa(G)$").

Figure 5.2 shows two simple examples to illustrate MCFP. For instance, in Fig. 5.2 (a), a 4-node network comprised of node A, B, C and D connected by edges A-B, B-C and C-D. Assuming unity capacity on each edge, concurrent flows among nodes A, B, C and D yield concurrent connectivity (i.e., maximum throughput) of 1/4. The paths traversing edge B-C are A-B-C (i.e.,the path connecting node A and C through node B), A-B-C-D, B-C and B-C-D. So the total traffic on edge B-C equals 1 whereas the total traffic on edges A-B and C-D are both 3/4. Edge B-C is the bottleneck in this example. In Fig. 5.2 (b), traffic between a pair of nodes can be distributed among several paths connecting the pair of nodes. For example, the traffic between nodes A and D is carried by paths A-B-D, A-E-D and A-C-D, whose flows are 1/6, 1/6 and 1/3, respectively. Such distribution of traffic is displayed in Fig. 5.2 (b), from which the concurrent connectivity can be calculated as 2/3.

MCFP can be formulated as a linear program in either edge-path form or the node-arc form which is solvable in polynomially bounded time but practically ineffective [50]. Since the MCFP-based calculation of the discount rate is to be applied to all the candidate lightpath-protecting p-Cycles to be used as the input to the optimization of CAPWLE, we will not adopt the linear programming approach for MCFP. Instead, we will simplify the calculation by breaking down the targeted off-cycle protected capacity into independent CGs where the concurrent connectivity can be obtained based on the cut upper bound of MCFP. The cut upper bound

can be depicted as follows [51].

Cut Upper Bound:

For any graph G=(V, E), let $\left(A, \overline{A}\right)$ denote the set of all edges of E having one end vertex in $A \subset V$, and the other end vertex in $\overline{A} = V - A$, the concurrent connectivity $\kappa(G)$ satisfies

$$\kappa(G) \leq \frac{\left|\left(A, \overline{A}\right)\right|}{|A|\left|\overline{A}\right|} \text{ for any cut } \left(A, \overline{A}\right) \text{ of } G$$

Calculation of Discount Rate

Now we explain in detail the procedures of the calculation which is focused on the off-cycle protected capacity of a single lightpath-protecting p-Cycle.

Firstly, we notice the independence among the separate *CG*s (or *Joint Compatible Groups (JCG)* which are composed of *CG*s whose *Attach Nodes* are adjacent). Hence, we isolate each *CG* (or *JCG*) for calculation. Fig. 5.3 describes the procedure of isolation. In Fig. 5.3, we display two simply but typical scenarios where black nodes are on-cycle nodes and white nodes off-cycle. In addition, as on-cycle protected capacity is not considered, the on-cycle spans are neglected and absent in the figure. In Fig. 5.3 (a), the off-cycle protected capacity is separated into two independent *CG*s whereas in (b) it is separated into a *CG* (lower) and a *JCG* (upper) comprised by a K-node *CG* (i.e., a *CG* consisting of K on-cycle nodes) and a M-node *CG*.

Next, we focus on a single *CG* (or *JCG*). For a single *CG* (or *JCG*), the

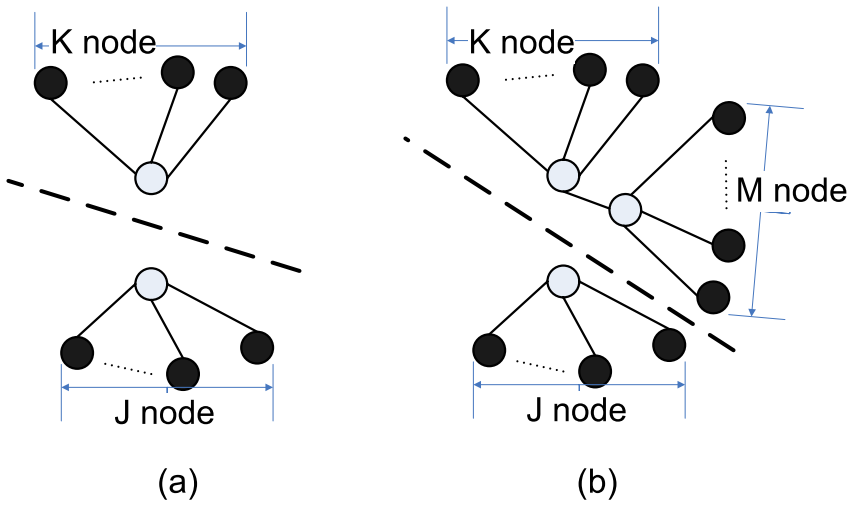

Figure 5.3: Divide Off-cycle Protected Capacity into CGs (or JCGs)

subsequent procedures mainly involve the calculation of the concurrent connectivity and the residual capacity on each edge (i.e., unity capacity less the multiplication of the concurrent connectivity and the amount of paths passing through the edge). Then we seek for the maximum residual capacity to be used to obtain the discount rate, expressed in Eq. (5.5), for the particular CG (or JCG).

$$Residual\ Capacity = 1 - \min_{l \in E} \{\beta_l * \kappa(G)\} \tag{5.4}$$

$$Discount\ Rate = 1 - Residual\ Capacity \tag{5.5}$$

Where G in Eq. (5.4) represents the topology of a single CG (or JCG) such as the isolated portion in Fig. 5.3. β_l denotes the number of paths passing edge l where $l \in E$. The incentive behind Eq. (5.4) and (5.5) is that we discount the protected capacity, in order to reflect the connectivity, based on the most

underutilized link according to the calculation of concurrent connectivity. Instead of such an aggressive discounting approach, we can, alternatively, adopt a moderate approach by using the average residual capacity instead of the maximum. In this chapter, we follow Eq. (5.4).

From Eq. (5.4), we can observe that the concurrent connectivity $\kappa(G)$ is the key factor. In order to calculate $\kappa(G)$, we will investigate three basic topologies, from which other possible topologies can be derived.

Basic Topology I:

As shown in Fig. 5.4 (a), basic topology I is a single K-node *CG*. Assume the size of edge cut 2 is T (T<K). Since we only consider concurrent flow among on-cycle nodes (black nodes), we can obtain the concurrent connectivity according to the Cut Upper Bound as follows.

$$\kappa(\mathrm{I}) \leq \frac{T}{(K-T)*T} = \frac{1}{(K-T)}$$

Since,

$$\frac{1}{(K-1)} \leq \frac{1}{(K-T)}$$

Therefore, the sparsest cut occurs when T equals 1 such as the edge cut 1 in Fig. 5.4 (a). On the other hand, we can verify the existence of a concurrent flow of $1/(K-1)$ among on-cycle nodes through observation. Hence $\kappa(\mathrm{I}) = 1/(K-1)$.

Basic Topology II:

Basic topology II is the simplest form of *JCG* consisting of two *CG*s depicted

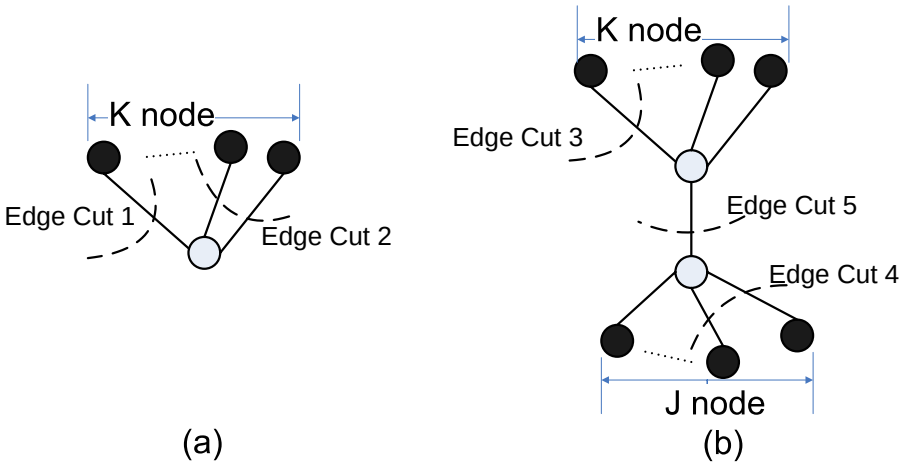

Figure 5.4: Basic Topology (a)Topology I (b)Topology II

in Fig. 5.4 (b). Similarly, we look for the sparsest cut. Basically, there are two types of edge cuts. The first type is similar to the one studied in basic topology I such as edge cut 3 and 4. Based on the prior analysis, edge cut 3 is the sparsest among the first type. Assuming a K-node CG and a J-node CG compose the JCG, we can obtain

$$\kappa(\text{II}) \leq \frac{1}{(K+J-1)} \tag{5.6}$$

The second type is edge cut 5. Again, according to Cut Upper Bound, we can have

$$\kappa(\text{II}) \leq \frac{1}{K*J} \tag{5.7}$$

Now we need to compare the two bounds in Eq. (5.6) and Eq. (5.7). Since we have

$$K*J-(K+J-1) = (K-1)(J-1) \geq 0$$

Therefore, the sparsest cut is edge cut 5. Also, we can verify the existence of a concurrent flow of $1/(K * J)$ among all the on-cycle nodes (K+J nodes totally). Hence, κ(II)= $1/(K * J)$.

Note that the on-cycle nodes in the two composing *CG*s might overlap, in which case some minor modifications need to be made. However, our purpose is to capture the dominant feature of the topology rather than calculate precisely. So we ignore these modifications for the sake of simplicity.

Basic Topology III:

From the bottom upwards, we now confront topologies consisting of over two *CG*s. The simplest among them is the basic topology III shown in Fig. 5.5 (a). Instead of exploring various edge cuts directly, we decompose the basic topology III into two basic topology II depicted in Fig. 5.5 (b) and (c). If we assume (b) and (c) are decoupled, we can obtain the concurrent connectivity as $1/(K * J)$ and $1/(K * M)$ determined by edge cuts 1 and 2, respectively, based on the analysis of basic topology II. Nonetheless, (b) and (c) are coupled and the total protected capacity in the K-node *CG* of (a) can be split into the corresponding K-node *CGs* of (b) and (c). The concurrent connectivity of (a), thereby, is bounded by the lower of $1/(K * J)$ and $1/(K * M)$ and also subject to the upper bound constraint raised by edge cut 3 which is $1/(K + J + M - 1)$. Hence, κ(III)=$\min\{1/(K * J), 1/(K * M), 1/(K + J + M - 1)\}$

Now we consider again the example in Fig. 5.1 (b) and (c) in Section 5.2 to

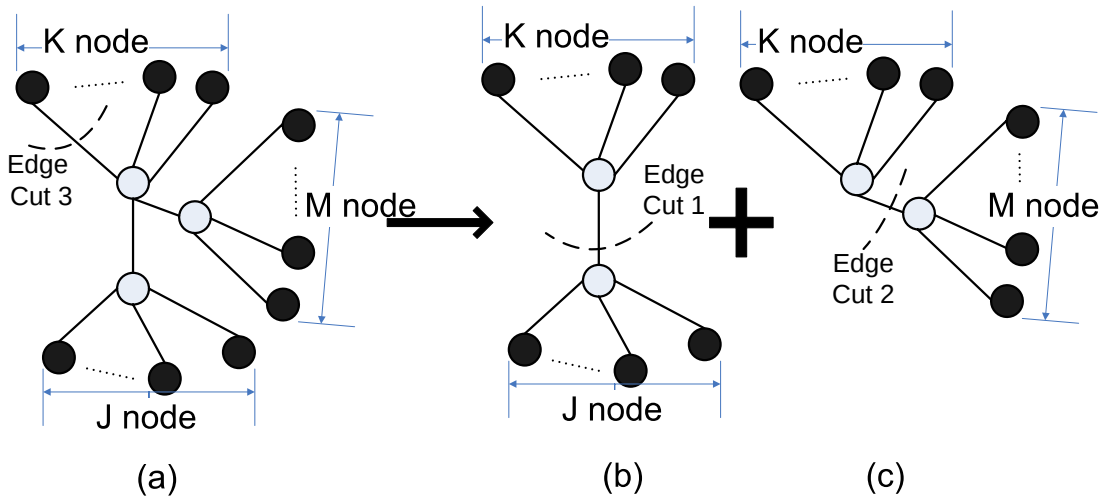

Figure 5.5: (a) Basic Topology III (b) Decomposition Component A (c) Decomposition Component B

see how we can improve the evaluation of the protected capacity by means of the *Effective Envelope*. With the on-cycle spans (dashed lines) neglected, (b) is basic topology I whereas (c) is basic topology II. Based on the previous analysis, the concurrent connectivity of (c) is 1/4. By comparing the residual capacity over all the off-cycle spans in (c), we can get the maximum value of 1/4 on span B-E, which determines the discount rate as 3/4 according to Eq. (5.5). Therefore, the *Effective Envelope* is 2*5*3/4=7.5. Likewise, we can obtain the *Effective Envelope* of (b) as 8. Substituting into Eq. (5.3), we can get the *Connectivity-based ER*s for (b) and (c) as 3 and 2.875, respectively, which, contrary to the result in Section 5.2, make (b) outweigh (c). Thus we can see that by virtue of *Effective Envelope*, *Connectivity-based ER* can evaluate the protection capability of lightpath-protecting p-Cycles in

a fairer way in the sense that it reflects the connectivity in addition to the volume of the protected capacity.

5.3.2 Optimization of CAPWLE

In **Chapter 3**, we formulate the optimization of PWLE as an MILP model to determine an optimal set of lightpath-protecting p-Cycles so as to define a volume-maximized protected working layer. Through the example discussed above, we have seen the advantage of the *Effective Envelope* in evaluating the protection capability of lightpath-protecting p-Cycles from a combined perspective of volume and connectivity of the protected capacity. Therefore, we will optimize CAPWLE by integrating the *Effective Envelope* into the MILP model of PWLE with an objective of the enhancement in connectivity in addition to the volume-maximization. Since the optimization of CAPWLE is developed based on that of PWLE in **Chapter 3**, we will emphasize the changes to the latter by listing only the important parameters and constraints. The CAPWLE model can be defined as follows:

Parameters:

$\kappa^{j,i}$: Discount rate of the i^{th} CG of the j^{th} lightpath-protecting p-Cycle

α: Compromising factor (0.03)

Ψ: Volume of the working layer maximized by the PWLE model

D_d: Traffic intensity of the d^{th} demand

$Q_{d,m}$: It is 1 if the m^{th} node is the end node of the d^{th} demand, 0 otherwise

$L_s^{j,i}$: It is 1 if the s^{th} span belongs to the i^{th} CG of the j^{th} lightpath-protecting p-Cycle, 0 otherwise

$K_m^{j,i}$: It is 1 if the m^{th} node is contained in the i^{th} CG of the j^{th} lightpath-protecting p-Cycle, 0 otherwise

Variables:

γ_w^j: It is 1 if the w^{th} wavelength is taken up by the j^{th} lightpath-protecting p-Cycle

$\mu_w^{j,i}$: It is 1 if the w^{th} wavelength is taken up by the i^{th} CG of the j^{th} lightpath-protecting p-Cycle

$\pi_d^{j,i}$: Amount of the d^{th} demand carried by the i^{th} CG of the j^{th} lightpath-protecting p-Cycle

Objective:

$$Maximize \sum_{j,i,s} \kappa^{j,i} \cdot L_s^{j,i} \cdot \sum_w \mu_w^{j,i} \tag{5.8}$$

Constraints:

$$\sum_{j,i,s} L_s^{j,i} \cdot \sum_w \mu_w^{j,i} \geq (1-\alpha) \cdot \Psi \tag{5.9}$$

$$\sum_{j,i} \pi_d^{j,i} \geq D_d \quad \forall d \tag{5.10}$$

$$\sum_w \gamma_w^j \leq \sum_w \mu_w^{j,i} \leq 2 \cdot \sum_w \gamma_w^j \quad \forall j,i \tag{5.11}$$

$$\sum_d (\pi_d^{j,i} \cdot Q_{d,m}) \leq K_m^{j,i} \cdot \sum_w \mu_w^{j,i} \quad \forall m,j,i \tag{5.12}$$

Prior to optimization, a set of candidate lightpath-protecting p-Cycles along with their CGs ($L_s^{j,i}$, $K_m^{j,i}$) and corresponding discount rates ($\kappa^{j,i}$) are calculated as the inputs to the optimization. In addition, the maximum volume of the protected capacity (Ψ) is also calculated beforehand through the PWLE model. The rationale of the optimization is to enhance the connectivity of the protected capacity through maximizing the *Network Effective Envelope*, the aggregate of the *Effective Envelope* of all the selected cycles, in Objective (5.8) without compromising the volume of the protected capacity over a factor of α shown in Constraint (5.9). As a joint optimization of cycle selection and demand routing, the model utilizes CGs as intermediates to link the demands and the cycles without pre-defining the routes of demands. Specifically, Constraint (5.10) guarantees the protection coverage of the forecasted demands, Constraint (5.11) limits the allowable capacity of CGs based on cycles and Constraint (5.12) reveals the internal constraint of a CG on the simultaneous accommodation of multiple demands.

5.4 Numerical Results and Discussions

5.4.1 Optimization Result

We choose as test networks COST239 and NSFNET whose topologies can be found in Fig. 3.4. Assuming one fiber-pair per span as the total deployed capacity, we define one unit of capacity as two channels on the same wavelength over one fiber pair per span. For each network, we randomly choose 3 sets of 19-demand pairs, with each demand bundle assumed to be two units, and average the results over the three. All the problems are solved using ILOG \ CPLEX 9.0 on a Windows XP Professional machine with Intel(R) Pentium(R) 4CPU 2.4GHz, 1GB of RAM. In the case of NSFNET, the solutions can be obtained with a MIPGAP below 7% within half an hour while the best feasible solutions are reached at 10% MIPGAP within 1.5 days for COST239. Table 5.1 exhibits the optimization results. The figures refer to the total protected capacity while the percentages in brackets represent the ratio of the protected capacity to the total network capacity. Due to the *Effective-Envelope*-based objective in Eq. (5.8), the selected lightpath-protecting p-Cycles possess high *Connectivity-based ER* (Eq. (5.3)) instead of ER (Eq. (5.1)), which is the major reason of the possible contraction in the total protected capacity. However, the extent of such contraction is well controlled within 3% through the compromising factor α in the optimization of CAPWLE. Despite the compromise in the volume of protected capacity, CAPWLE incorporates connectivity-awareness

Network	Wavelengths/fiber	10	14	20
COST239	PWLE	212(81.5%)	302(84.3%)	439(84.4%)
	CAPWLE	205(78.84%)	296(81.31%)	426(81.92%)
NSFNET	PWLE	134(63.8%)	209(71.1%)	315(75%)
	CAPWLE	128(61%)	202(68.71%)	306(72.86%)

Table 5.1: Working Envelope of PWLE and CAPWLE

to enhance the actual utilization of the protected capacity, which will be examined through the blocking performance under dynamic traffic next.

5.4.2 Blocking Performance: Dynamic Stationary Traffic

Dynamic stationary traffic refers to random arrival and departure of requests at fixed Erlang loads (i.e., statistically stationary). For comparison with PWLE, we choose COST239 with 8 wavelengths per fiber which was tested in **Chapter 3**. Following the similar setting in **Chapter 3**, we randomly choose 3 sets of source-destination node pairs, over which the results are averaged. Arrivals follow a Poisson process. Totally 10^5 events are simulated. From Fig. 5.6, we see that CAPWLE (triangle-upward) outperforms PWLE (circle) and the spread widens with the traffic load, which indicates the advantage of CAPWLE over PWLE in hosting heavy traffic. Though the improvement of CAPWLE over PWLE is less than that of PWLE over PWCE (upmost), the former is obtained without extra

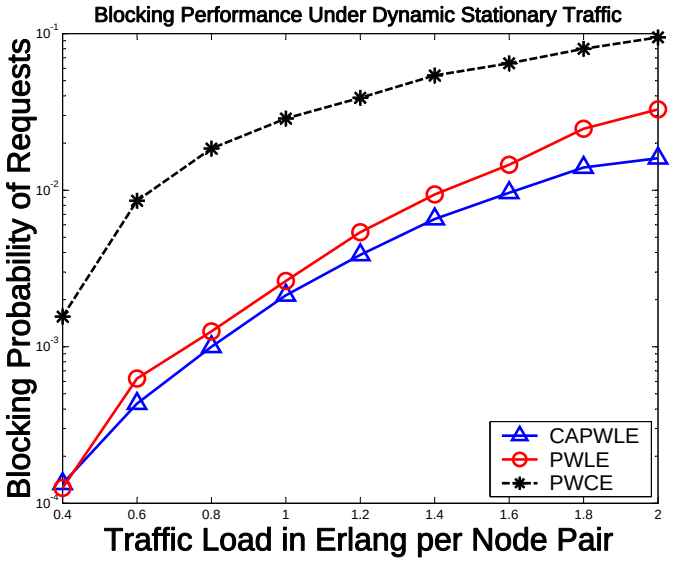

Figure 5.6: Improvement in Blocking Performance

cost while the latter incurs the cost of signaling overhead and implementation complexity due to the difference in the mechanisms of PWLE and PWCE.

5.4.3 Blocking Performance: Dynamic Evolving Traffic

Since the incentive for CAPWLE is to improve the actual utilization of protected capacity, we extend our experiments to investigate the blocking performance under dynamic evolving traffic (i.e., non-stationary). We adopt the method of traffic pattern generation introduced by [52], in which a reconfiguration model for PWCE under evolving traffic pattern was proposed. However, our purpose of involving evolving traffic is to study the endurance of CAPWLE under traffic patterns deviated from what it is initially designed for. Now we briefly explain the process of

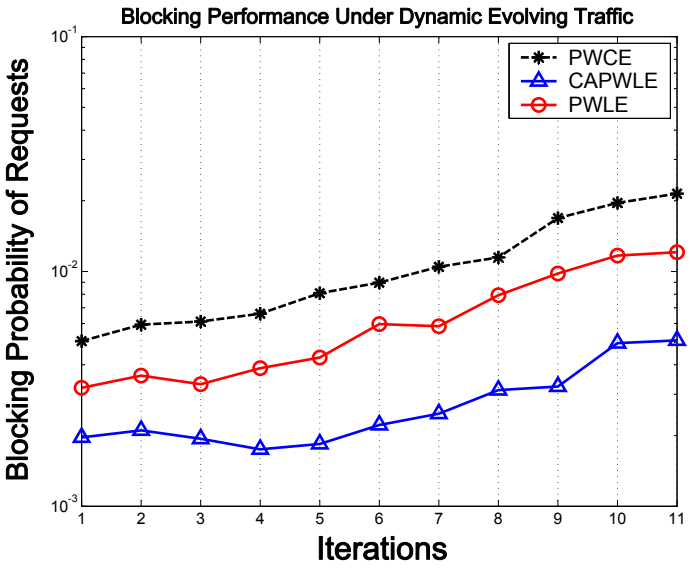

Figure 5.7: Blocking Performance Under Evolving Traffic

traffic pattern generation. Given an initial pattern, we make random step increase or decrease in load to each node pair with step change proportional to the initial traffic intensity at the beginning of each iteration. All newly generated loads are scaled based on the initial total loads. We follow the same network configurations in Section 5.4.2 except the initial traffic patterns. We choose 19 source-destination node pairs with 1.2 Erlangs per node pair for CAPWLE and PWLE. However, we notice that the blocking probability of PWCE with 1.2 Erlangs per node pair is around 7 times that of PWLE from Fig. 5.6, thus we use 0.6 Erlangs per node pair as initial traffic pattern for PWCE in order to observe the blocking performance in a same range. The reason to include PWCE for comparison is to verify the advantage of PWLE in combating evolving traffic pattern so as to validate the

meaningfulness of further exploring CAPWLE. 10 iterations are carried out with totally 10^6 events simulated in each iteration.

As displayed in Fig. 5.7, after 10 iterations, the blocking probability of PWCE (upmost) rises 4.25 times while it rises 3.78 times for PWLE (circle) and 2.59 times for CAPWLE (triangle-upward). CAPWLE excelling PWLE indicates the connectivity-awareness in CAPWLE does augment the utilization of protected capacity in the working layer even under evolving traffic. On the other hand, the reason of PWLE, as well as CAPWLE, outperforming PWCE is two-fold. Firstly, thanks to the path-oriented mechanism, high capacity efficiency of PWLE (CAPWLE) facilitates large-volume working layer. Secondly, the actual routing of demands is governed by *CG*s which take the role as intermediates between demands and lightpath-protecting p-Cycles. This has been reflected in both the optimization of PWLE (CAPWLE) or the routing and operation of PWLE illustrated in **Chapter 3**. With *CG*s structuring the working layer, each demand can be routed with the consideration of future connections between other node pairs. In contrast, in PWCE, demands are routed via shortest-path algorithms which only ensure local optimality on a connection basis and can allow the working layer to evolve incrementally into a poor global configuration under random demands.

5.5 Summary

In this chapter, we have developed CAPWLE which partitions the network capacity into a static protection layer and a working layer optimized from a combined perspective of volume and connectivity. The connectivity-awareness is integrated into CAPWLE through the *Effective Envelope* which is a MCFP-based approach aimed at evaluating lightpath-protecting p-Cycles in a fair way in a sense that the impact of network connectivity can also be considered. The results obtained indicate that CAPWLE enhances the actual utilization of the working layer under both dynamic stationary and non-stationary traffic patterns.

Chapter 6

Efficient Configuration of p-Cycles Under Time-variant Traffic

6.1 Introduction

Chapters 3-5 have focused on dynamic traffic which can be characterized by, if available, a single traffic matrix. However, traffic entering a network is intrinsically variable in time. Even on a daily basis, there can be structural differences between day and evening traffic. The time-variant traffic can undergo predicted periodic changes on a daily or weekly basis [53]. In this chapter, we use, instead of a single traffic matrix, a set of traffic matrices sampled at characteristic time instants to represent predicted periodic time-variant traffic. In the presence of such time-variant traffic, we consider the design of p-Cycles to provide survivable services to

the entire set of traffic matrices.

In existing literatures regarding the optimal configuration of span-protecting p-Cycles, the objective is to achieve 100% single-failure restorability while minimizing total spare capacity usage. This problem can be solved jointly with the routing of the demands [54], or by a two-step approach where the demands are routed first and then the span-protecting p-Cycles are formed [3] [55]. The configurations designed based on these methods are limited to a specific static traffic matrix. To tackle the traffic pattern variation, a more advanced scheme called Adaptive PWCE (APWCE) was developed in [52]. Derived from PWCE, APWCE is equipped with a control system in which measurements of utilization on each span are taken to drive an optimization problem to reconfigure the PWCE recursively in order to track the evolving traffic load distribution. However, an on-line feedback system tracking the network status and an on-line reconfiguration algorithm need to be in place.

In this chapter, with a priori knowledge of the set of traffic matrices, we propose an off-line static configuration, called *Joint Static Configuration Approach (JSCA)*, to accommodate the traffic demand set with minimum spare capacity by taking advantage of the non-coincidence of the traffic demands belonging to different traffic matrices. By taking into account the entire traffic demand set, we formulate JSCA as an MILP model which essentially exploits the sharing of working capacity

among traffic matrices in order to minimize the spare capacity usage. For comparison, we also provide two simple approaches, namely, *Independent Reconfiguration Approach (IRA)* and *Maximal Static Configuration Approach (MSCA)*. IRA is basically a periodical reconfiguration approach which is very capacity-efficient. MSCA is a static configuration which is obtained based on the maximum amount of traffic between each node pair over the traffic demand set. For the sake of resolution time, we also propose a 2-phase sub-optimal solution of JSCA by decomposing the original problem into a succession of two sub-problems. Moreover, we also study the applications of JSCA in PWCE.

Starting with span-protecting p-Cycles, our study then extends to path-protected networks. Specifically, we apply the idea of JSCA to lightpath-protecting p-Cycles to generate *Joint Static Configuration Approach for Path Protection (JSCAP)*. Based on JSCAP, we further investigate its applications in PWLE. In the next section, we will introduce JSCA.

6.2 Joint Static Configuration Approach

6.2.1 Concept of JSCA

Given a single traffic matrix, operators typically try to minimize the spare capacity reserved for span-protecting p-Cycles to provide full survivability for the estimated traffic. However, traffic entering a network changes in time and spatial distribution

over different time scales, e.g. weekly over different days, daily over different hours, etc. A better description of the traffic requirements can be done by a set of traffic matrices. Different traffic matrices represent traffic requirements predicted on the basis of past measurements for different characteristic time instants. In this chapter, we focus on daily variation over different hours.

Given a network topology and resources, we aim to decide span-protecting p-Cycle configuration solutions to accommodate a traffic demand set $\boldsymbol{D}=\{D^1, D^2...D^T\}$ representative of different characteristic instants t=1,2...T in a day. There are two straightforward approaches as described below which have their own advantages and drawbacks. We use them as comparison references for the scheme developed by us.

- *Independent Reconfiguration Approach (IRA)*: For each traffic matrix D^t in the traffic demand set $\boldsymbol{D}$, we independently optimize the network configuration by minimizing the spare capacity reserved for span-protecting p-Cycles. The IRA is very efficient in terms of allocated resources (spare capacity). However, the network is provided with different solutions at different characteristic instants, which makes dynamic reconfigurations capability necessary. We note that reconfigurations incur overhead and the throughput is reduced during reconfigurations.

- *Maximal Static Configuration Approach (MSCA)*: Instead of dynamic reconfiguration, this approach provides a static configuration to accommodate the whole traffic demand set. The optimization is performed based on a traffic matrix D^{max} in which each element is obtained by taking the maximum value of the traffic between the corresponding node pair over the whole traffic demand set $\boldsymbol{D}$. The MSCA eliminates the need for reconfiguration but at the cost of the increase in the allocation of resources in terms of spare capacity with respect to the IRA.

IRA and MSCA stand for two extreme approaches which focus only on either operational simplicity or capacity efficiency. However, it would be desirable to take both considerations into account so as to combine the benefits of both IRA and MSCA. With such concerns in mind, we propose an approach, called *Joint Static Configuration Approach (JSCA)*, to generate a single static configuration to accommodate the whole traffic demand set $\boldsymbol{D}$ with a little increment in reserved spare capacity with respect to IRA. The key idea is to exploit the sharing of bandwidth required at different characteristic instants. Below we use a simple example to illustrate this idea.

Consider a 4-node network and a traffic demand set with two element traffic matrices representing two characteristic instants (t=1, 2) as shown in Fig. 6.1. Assuming bidirectional connections and span-protecting p-Cycles, one p-Cycle 1-3-4-1 and one p-Cycle 1-2-3-4-1 of one unit need to be configured, respectively,

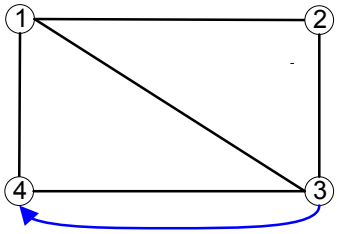

Node	1	2	3	4
1				
2				
3				1
4			1	

(a) Traffic Matrix D^1
p-Cycle: 1-3-4-1

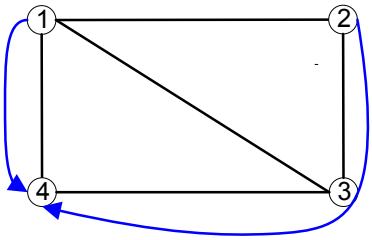

Node	1	2	3	4
1				1
2				1
3				
4	1	1		

(b) Traffic Matrix D^2
p-Cycle: 1-2-3-4-1

Node	1	2	3	4
1				1
2				1
3				1
4	1	1	1	

(b) Traffic Matrix D^{max}
p-Cycle: 1-2-3-4-1 & 1-3-4-1

Figure 6.1: Sharing of Resources Between Traffic Matrices at Different Characteristic Instants (a) Traffic Matrix D^1 (b) Traffic Matrix D^2 (c) Traffic Matrix D^{max}

for traffic matrix D^1 and D^2 if IRA is adopted. We take the average of the two configurations. Then 3.5 ((3+4)/2=3.5) units of spare capacity is required in the case of IRA. If MSCA is employed, we need to derive D^{max} by taking the maximum amount of traffic between each node pair over the two characteristic instants as shown in Fig. 6.1 (c). Based on D^{max}, both span-protecting *p*-Cycles 1-3-4 and 1-2-3-4 are needed to form a static configuration with totally 7 units of spare capacity reserved.

Now we explain the solution obtained by JSCA. Noticing that connection 3-4 in Fig. 6.1 (a) and connection 2-4 in Fig. 6.1 (b) exist in different time period, we discover that they can actually share the bandwidth on link 3-4. Therefore, if the sharing between different characteristic instants is taken into account, we can use only a p-Cycle 1-2-3-4 of one unit, which requires 4 units of spare capacity, to protect all the traffic. Compared with the results obtained under IRA and MSCA above, JSCA can provide a single static configuration (p-Cycle 1-2-3-4) but with a marginal increment in spare capacity (4-3.5=0.5 unit). This illustrates the key idea we will use to develop the optimization model in Section 6.3.

6.2.2 Value of JSCA

JSCA can provide network operators with an operationally simple and efficient way for capacity planning at the overall network level. The purpose of developing JSCA is twofold.

- JSCA enables a single static configuration which is based on span-protecting p-Cycles to provide survivable services to the given traffic demand set $\boldsymbol{D}$ from the perspective of minimizing spare capacity usage. In other words, reconfigurations are avoided while the increment in spare capacity with regard to the amount required under IRA is minimized.

- The above potential of JSCA can give us an insight into the minimum requirement of spare capacity for a given traffic demand set $\boldsymbol{D}$. If we take a different point of view, a question can be asked that "If there is a constraint on spare capacity, how much more capacities can be protected with JSCA than that protected without JSCA? "The answer to the question in effect reveals the potential of JSCA in the design of PWCE. In fact, when the constraint of spare capacity budget is imposed in the design of PWCE, the capacity-efficient feature of JSCA gives it an edge in enhancing the optimization from two aspects. Firstly, given traffic demand set $\boldsymbol{D}$, the optimization model of PWCE design becomes unsolvable when schemes other than JSCA are employed and the minimum spare capacity required under such schemes exceed the spare capacity budget. As JSCA is designed to be capacity-efficient, the employment of JSCA in PWCE can allow the otherwise unsolvable optimization model to generate optimal solutions. Secondly, when the optimization model of PWCE is already solvable under schemes other than JSCA, the employment of JSCA in PWCE can make the optimization less constrained by the spare capacity budget and thus expand the feasible region, leading to better solution with higher volume of working capacity envelope.

6.3 Optimization Model

As stated in Section 6.2.2, JSCA is advantageous in 1) providing a capacity-efficient p-Cycle-based static configuration and 2) enhancing the optimization model of PWCE given the constraint of spare capacity budget. Therefore, we first optimize the static configuration for JSCA based on an MILP formulation with the objective to minimize the spare capacity usage. Then we extend the optimization model to the JSCA-based PWCE design under spare capacity budgets. The MILP formulation takes the whole traffic demand set $\boldsymbol{D}$ as the input. The selection of routes to distribute the traffic load for all the traffic matrices are considered jointly in order for the sharing of working capacity to be fully exploited.

6.3.1 Terminology and Notation

First, we introduce the terminology and notation used in the model.

Parameters:

$\boldsymbol{PS}$: Set of topologically defined span-protecting p-cycles, indexed by j

$\boldsymbol{S}$: Set of network spans, indexed by s

T_s : Total capacity on span s

B_s : Spare capacity budget on span s

B : Network-wide spare capacity budget

$\boldsymbol{D}$: $\{D^t\}$, set of traffic matrices at characteristic instants t=1,2...T

D^t_{mn}: Traffic intensity between node pair (m,n) at time instant t

W^t : Total working capacity required for D^t based on the shortest-path routing algorithm

γ : Limit of inflation of working capacity

R_{mn} : Set of available routes between node pair (m,n), indexed by r_{mn}

H^{rmn}_s : 1 if the s^{th} span is on the the r^{th}_{mn} route

K^j_s : 1 if the s^{th} span is the j^{th} span-protecting p-cycle's on-cycle span, 2 for straddling span, 0 otherwise

G^j_s : 1 if the s^{th} span is the j^{th} span-protecting p-cycle's on-cycle span, 0 otherwise

α : Weighting factor to indicate the dominance between the working capacity and the spare capacity in the objective function

Variables:

$\Gamma^{rmn}_{D^tmn}$: 1 if D^t_{mn} is assigned with the r^{th}_{mn} route

θ_s : Amount of protected capacity on the s^{th} span

Φ^j : Number of the j^{th} span-protecting p-cycle reserved

R_s : Traffic load on the s^{th} span (to be used in Section 6.4)

The whole set of traffic matrices ($\boldsymbol{D}$) will be taken explicitly as the input to the optimization. For each node pair, there is a set of routes (R_{ij}) pre-computed for selection. It is worth nothing that routes longer than the corresponding shortest

length might be chosen in the optimization for the sake of bandwidth sharing. Hence, the total working capacity required for each traffic matrix D^t can be greater than the amount calculated based on the shortest-path routing algorithm, in which case we say that the working capacity is inflated. As we hope the inflation of working capacity remains under a threshold, we introduce a control parameter γ to limit the inflation.

6.3.2 MILP Formulation

Now we provide the MILP formulation of JSCA which aims to minimize the spare capacity usage.

Objective:

$$Minimize \sum_{j \in PS, s \in S} \Phi^j \cdot G_s^j + \alpha \sum_{s \in S} \theta_s \tag{6.1}$$

Constraints:

$$\sum_{m,n \in M} D_{mn}^t \cdot \sum_{rmn \in R_{mn}} \Gamma_{D^t mn}^{rmn} \cdot H_s^{rmn} + \sum_{j \in PS} \Phi^j \cdot G_s^j \leq T_s$$

$$\forall s \in \boldsymbol{S}, \forall t \tag{6.2}$$

$$\sum_{m,n \in M} D_{mn}^t \cdot \sum_{rmn \in R_{mn}} \Gamma_{D^t mn}^{rmn} \cdot H_s^{rmn} \leq \theta_s$$

$$\forall s \in \boldsymbol{S}, \forall t \tag{6.3}$$

$$\theta_s \leq \sum_{j \in PS} K_s^j \cdot \Phi^j$$

$$\forall s \in \boldsymbol{S} \tag{6.4}$$

$$\sum_{s \in S} \sum_{m,n \in M} D_{mn}^t \cdot \sum_{rmn \in R_{mn}} \Gamma_{D^t mn}^{rmn} \cdot H_s^{rmn} \leq \gamma \cdot W^t$$

$$\forall t \tag{6.5}$$

Objective (6.1) is a generic form which can either merely minimize spare capacity usage ($\alpha = 0$) or consider the working capacity as well ($0 \leq \alpha \leq 1$). In this chapter, we focus on minimizing total spare capacity. Constraint (6.2) is a capacity constraint which guarantees that the sum of the maximum traffic load and the spare capacity reserved is bounded by the total capacity on each span. In fact, this constraint is equivalent to the following constraint:

$$\underset{t}{Max}\{\sum_{i,j} D_{ij}^t \cdot \sum_{rij} \Gamma_{D^t ij,rij} \cdot H_{rij,s}\} + \sum_p \Phi_p \cdot G_{p,s} \leq C_s \quad \forall s$$

However, we use Constraint (6.2) (along with the introduction of variable θ_s) to preserve the linearity of the formulation. Constraint (6.3) defines the variable θ_s as the upper bound of the traffic load on span s. On each span, the upper bound of the traffic load is constrained by the amount of span-protecting p-Cycles protecting the span as described in Constraint (6.4). Finally, Constraint (6.5) deals with the inflation of working capacity discussed in Section 6.3.1. For every traffic matrix D^t, we pre-compute the required total working capacity (W^t) using the shortest-path routing algorithm. By means of Constraint (6.5), we can guarantee that the

total working capacity of the optimization output might only be inflated at most by a factor of γ. On the other hand, limiting the inflation of the working capacity can affect the selection of routes and thus may inhibit the sharing of bandwidth. Therefore, the optimization result might be compromised, which will be further studied in Section 6.6.3.

6.3.3 Extension to JSCA-based PWCE

Based on the above MILP model of JSCA, we can build the optimization model of JSCA-based PWCE which aims at maximizing the volume of the working capacity envelope given the spare capacity budgets under traffic demand set $\boldsymbol{D}$. The volume-maximization objective is given as follows:

$$Maximize \sum_{s \in S} \theta_s \tag{6.6}$$

As to constraints, we retain Constraint (6.2), Constraint (6.3), Constraint (6.4) and add the constraint of spare capacity budgets shown as below:

$$\sum_{j \in PS} \Phi^j \cdot G_s^j \leq B_s$$

$$\forall s \in \boldsymbol{S} \tag{6.7}$$

$$\sum_{s \in S} \sum_{j \in PS} \Phi^j \cdot G_s^j \leq B \tag{6.8}$$

Constraint (6.7) stands for span-based spare capacity budget whereas Constraint (6.8) stands for network-wide spare capacity budget. Parameters B_s and B

are provided as the inputs to the optimization.

Notice that MSCA can also be applied to PWCE to form the MSCA-based PWCE. Such application is straightforward as the only modification is to use traffic matrix D^{max} as the input to the optimization of PWCE.

6.4 Sub-optimal Solution

6.4.1 Sub-optimal Solution to JSCA

As the MILP formulation of JSCA considers jointly the routing of the entire traffic demand set and the selection of span-protecting p-Cycles, the computation complexity is high for large or medium-size networks. Therefore, for the sake of efficiency, we propose a sub-optimal solution by decomposing the optimization of JSCA into a succession of two sub-problems. In the first phase, we focus on the routing of the whole traffic demand set in order to minimize the sum of the maximum traffic load on each span (Objective (6.9)). The optimization of the sub-problem can be modeled as an MILP formulation with objective shown as follows:

$$Minimize \sum_{s} R_s \tag{6.9}$$

In addition to Constraint (6.5), we have the following constraints:

$$\sum_{m,n \in M} D^t_{mn} \cdot \sum_{rmn \in R_{mn}} \Gamma^{rmn}_{D^t mn} \cdot H^{rmn}_s \leq R_s$$

$$\forall s \in \boldsymbol{S}, \forall t \tag{6.10}$$

$$R_s \leq T_s \quad \forall s \tag{6.11}$$

Notice that we still include Constraint (6.5) in this model to control the inflation of working capacity required for each single traffic matrix. However, this constraint plays a minor role in this model since the objective function promotes the minimization of working capacity required for the whole traffic demand set.

In the second phase, we optimize the selection of span-protecting p-Cycles based on the distribution of traffic load on spans (R_s) obtained in the first phase. The problem of minimizing the spare capacity usage can then be reduced to a conventional span-protecting p-Cycles selection which has been extensively studied and can be found in [1]. Specifically, to obtain the formulation in the second phase, we modify the MILP model in Section 6.3.2 by substituting Constraint (6.2) and Constraint (6.3) with the following constraints:

$$R_s + \sum_{j \in PS} \Phi^j \cdot G^j_s \leq T_s$$

$$\forall s \in \boldsymbol{S} \tag{6.12}$$

$$R_s \leq \theta_s \quad \forall s \in \boldsymbol{S} \tag{6.13}$$

This 2-phase sub-optimal solution is efficient in terms of resolution time. The performance difference between the sub-optimal and the optimal solutions will be studied in Section 6.6.4.

6.4.2 Sub-optimal Solution to JSCA-based PWCE

The idea of decomposing a complex optimization into a succession of two sub-problems to improve computational efficiency is also applicable to JSCA-based PWCE. The first sub-problem is the same as that of the sub-optimal solution to JSCA, in which the distribution of traffic load on spans (R_s) is obtained. With (R_s) in place, the second sub-problem is in effect a conventional optimization model of PWCE with span-based traffic load and spare capacity budgets. The MILP model can be built with Objective (6.6), Constraint (6.7) (or Constraint (6.8)), Constraint (6.4), Constraint (6.12) and Constraint (6.10).

6.5 Extension to Path-protected Networks

We have so far addressed the optimization of JSCA and JSCA-based PWCE as well as the sub-optimal solutions to both. Though JSCA is introduced with regard to span-protecting p-Cycles, it is not restrained to span-protected networks. Rather, the essence of JSCA being both capacity-efficient and operationally simple by exploring the temporal sharing of bandwidth required at different characteristic

time instants is also applicable to path-protected networks. To differentiate from JSCA, we term the extension of JSCA to path-protected networks as *Joint Static Configuration Approach for Path Protection (JSCAP)*. Similarly, the two reference schemes, IRA and MSCA, can also directly apply to path-protected networks with the underlying protection structures being replaced with lightpath-protecting p-Cycles. To avoid confusion, these extensions are termed as *Independent Reconfiguration Approach for Path Protection (IRAP)* and *Maximal Static Configuration Approach for Path Protection (MSCAP)*, respectively.

Recall that as an extension of PWCE to path-oriented protection, PWLE is proposed in **Chapter 3** where the lightpath-protecting p-Cycle is proposed as the underlying protection structure. Under time-variant traffic, the same philosophy of exploring sharing of resources in the time dimension, which is the essence of JSCAP, can also be practiced in two aspects.

- To achieve a static configuration of lightpath-protecting p-Cycles with minimal spare capacity given traffic demand set $\boldsymbol{D}$
- To improve the optimization of PWLE given traffic demand set $\boldsymbol{D}$ and spare capacity budgets on the basis of spans or the overall network

Just as we address the optimization of JSCA and JSCA-based PWCE to exploit the value of JSCA, we will conduct the optimization of JSCAP and JSCAP-based PWLE for the two purposes listed above, respectively.

6.5.1 Optimization of JSCAP

Unlike span-protecting p-Cycles, lightpath-protecting p-Cycles are designed to protect an envelope of working capacity which can be grouped into *Compatible Groups (CG)* defined based on the topological features of the lightpath-protecting p-Cycles (introduced and described in **Chapter 3**). In other words, while span-protecting p-Cycles protect spans, it is *CG*s that are protected by lightpath-protecting p-Cycles. In the case of span-protecting p-Cycles, given a forecast traffic, the routing of traffic demands is usually required to generate the traffic load distribution over all spans, which serves as the input to the optimization model. By contrast, there is no need for pre-determined paths of traffic demands prior to the optimization in the case of lightpath-protecting p-Cycles. Rather, traffic demands are treated as the direct inputs to the optimization model in which traffic demands are required to be carried by *CG*s protected by the selected lightpath-protecting p-Cycles.

Owing to such differences between span-protecting p-Cycles and lightpath-protecting p-Cycles, the optimization of JSCA and that of JSCAP also differ. Under time-variant traffic, while JSCA exploits the sharing of working capacity required at different characteristic time instants on the basis of spans, JSCAP aims at such sharing of working capacity on the basis of *CG*s. The terminology and the model are given as follows.

Sets:

PL: Set of topologically defined candidate lightpath-protecting cycles, indexed by j

$\boldsymbol{G}^j$: Set of CGs belonging to the j^{th} lightpath-protecting p-Cycle, indexed by i

D: $\{D^t\}$, set of traffic matrices at characteristic instants t=1,2...T

D^t_{mn}: Traffic intensity between node pair (m,n) at time instant t

S: Set of spans of the network, indexed by s

W: Set of wavelengths, indexed by w

B_s : Spare capacity budget on span s

B : Network-wide spare capacity budget

Parameters:

$Q^{k,t}_{m,n}$: 1 if the k^{th} node is the end node of the demand D^t_{mn}, 0 otherwise

$L^{j,i}_s$: 1 if the s^{th} span belongs to the i^{th} CG of the j^{th} lightpath-protecting p-Cycle, 0 otherwise

N^j_s: 1 if the s^{th} span is an on-cycle span of the j^{th} lightpath-protecting p-Cycle, 0 otherwise

$K^{j,i}_k$: 1 if the k^{th} node is contained in the i^{th} CG of the j^{th} lightpath-protecting p-Cycle, 0 otherwise

T_s: The total number of deployed channels on the s^{th} span

Variables:

γ_w^j: 1 if the w^{th} wavelength is taken up by the j^{th} lightpath-protecting p-Cycle, 0 otherwise

$\mu_w^{j,i}$: 1 if the w^{th} wavelength is taken up by the i^{th} CG of the j^{th} lightpath-protecting p-Cycle, 0 otherwise

$\pi_{m,n}^{j,i,t}$: Amount of the demands D_{mn}^t carried by the i^{th} CG of the j^{th} lightpath-protecting p-Cycle

Objective:

$$Minimize \sum_{j \in PL, s \in S} N_s^j \cdot \sum_{w \in W} \gamma_w^j \tag{6.14}$$

Constraints:

$$\sum_{j \in PL, i \in G^j} \mu_w^{j,i} \cdot L_s^{j,i} + \sum_{j \in PL} \gamma_w^j \cdot N_s^j \leq 1$$

$$\forall s \in \boldsymbol{S}, w \in \boldsymbol{W} \tag{6.15}$$

$$\sum_{w \in W, j \in PL, i \in G^j} \mu_w^{j,i} \cdot L_s^{j,i} + \sum_{w \in W, j \in PL} \gamma_w^j \cdot N_s^j \leq T_s$$

$$\forall s \in \boldsymbol{S} \tag{6.16}$$

$$\sum_{w \in W} \gamma_w^j \leq \sum_{w \in W} \mu_w^{j,i} \leq 2 \cdot \sum_{w \in W} \gamma_w^j$$

$$\forall j \in \boldsymbol{PL}, i \in \boldsymbol{G}^j \tag{6.17}$$

$$\underset{t}{Max}\left\{\sum_{m,n\in M}(\pi_{m,n}^{j,i,t}\cdot Q_{m,n}^{k,t})\right\}\leq K_k^{j,i}\ \cdot\sum_{w\in W}\mu_w^{j,i}$$

$$\forall k\in \boldsymbol{M}, j\in \boldsymbol{PL}, i\in \boldsymbol{G}^j \tag{6.18}$$

$$\sum_{j\in PL, i\in G^j}\pi_{m,n}^{j,i,t}\geq D_{mn}^t$$

$$\forall d\in \boldsymbol{D}, \forall t \tag{6.19}$$

Constraint (6.15) ensures that there is no wavelength conflict on each span. Constraint (6.16) ensures that the sum of the protected capacity and spare capacity does not exceed the total deployed capacity on each span. Constraint (6.17) defines the range of number of copies of a *CG*, which is more than the number of copies of unit-capacity lightpath-protecting p-Cycles associated with it but less than twice. Constraint (6.18) and Constraint (6.19) guarantee that all traffic demands at any time instants can be carried by the *CG*s protected by the selected lightpath-protecting p-Cycles.

6.5.2 Extension to JSCAP-based PWLE

Just as the optimization model of JSCA-based PWCE is constructed based on the optimization model of JSCA, the optimization model of JSCAP-based PWLE can also be derived from the optimization model of JSCAP with the spare-capacity-minimization objective replaced with the volume-maximization objective shown as

follows.

$$Maximize \sum_{j\in PL, i\in G^j, s\in S} L_s^{j,i} \cdot \sum_{w\in W} \mu_w^{j,i} \tag{6.20}$$

In addition to the constraints in the optimization model of JSCAP, we include the constraints imposed by the spare capacity budgets given as follows.

$$\sum_{w\in W, j\in PL} \gamma_w^j \cdot N_s^j \leq B_s$$

$$\forall s \in \boldsymbol{S} \tag{6.21}$$

$$\sum_{s\in S, w\in W, j\in PL} \gamma_w^j \cdot N_s^j \leq B \tag{6.22}$$

Constraint (6.21) stands for span-based spare capacity budget whereas Constraint (6.22) stands for network-wide spare capacity budget.

Just as MSCA can be applied to PWCE by using the traffic matrix D^{max} as the input to the optimization of PWCE, MSCAP can also be applied to PWLE in a similar fashion, which is termed as MSCAP-based PWLE.

6.6 Numerical Results and Discussions

We carry out performance studies for both span-protected networks and path-protected networks. For span-protected networks, the performance study is conducted from four aspects. First, we compare the resource usage of JSCA with those of IRA and MSCA. Then the trade-off between the inflation of working capacity and the optimization results is investigated. Third, the relative difference

in resource usage between sub-optimal and optimal solutions is studied. Finally, the improvement of JSCA-based PWCE in the volume of working envelope is investigated and compared with those of MSCA-based PWCE and the sub-optimal solution to JSCA-based PWCE. Notice that Constraint (6.5) is not included in the model in the first phase of the sub-optimal solution to JSCA-based PWCE (Section 6.4.2). For path-protected networks, the resource usage of JSCAP is compared with those of IRAP and MSCAP. Also, the performance of JSCAP-based PWLE in enhancing the volume of working envelope is studied and compared with that of MSCAP-based PWLE.

The test networks we choose are NSFNET, Bellcore and COST239 as shown in Fig. 3.4. Assuming one fiber-pair per span and 16 wavelengths per fiber as total deployed capacity, we define one unit of capacity as two channels on the same wavelength over one fiber pair per span. All the problems are solved using ILOG \ CPLEX 9.0 on a Windows XP Professional machine with Intel(R) Pentium(R) 4CPU 2.4GHz, 1GB of RAM. Before we proceed to present the numerical results, we need to explain the method of traffic pattern generation.

6.6.1 Traffic Pattern Generation

The principle of the traffic pattern generation method used in this chapter is to model the spatial pattern changes on a short-term time-scale but without significant overall volume change. It is sensible to make such assumptions on the overall

volume change. If the total demand volume drops significantly, then all blocking may reduce essentially to zero. And if the total demand volume grows significantly, this inevitably requires additional physical capacity placements. Although we cannot guarantee that traffic pattern changes in real networks follow exactly the way we describe here, the method to be introduced is expected to generate a sequence of traffic patterns that effectively reflect the characteristic of time-variant traffic.

Assuming that there exists correlation between successive traffic matrices, we use the following method to generate the traffic demand set. Starting with an initial traffic pattern, we make random step increase or decrease in load to each node pair with the step change proportional to the traffic intensity defined by the preceding traffic matrix. Specifically, given the preceding traffic matrix D^{t-1}, we make random step changes proportional to βD_{ij}^{t-1} (β is a scaling parameter) to generate D_{ij}^{t}. If a negative step results in negative load, we set D_{ij}^{t} to zero. To guarantee that there are spatial variations of traffic patterns, we make random step changes of δ (δ is a small number) to the node pairs with traffic load of zero in the preceding traffic matrix. Finally, we limit the total traffic volume of each traffic matrix D^t within a range $\left[\mu \sum_{i,j} D_{ij}^{t-1} , \nu \sum_{i,j} D_{ij}^{t-1} \right]$ by scaling all newly generated load based on the upper or lower bounds. μ and ν are two scaling parameters defining the upper and lower bounds.

6.6.2 Optimization of JSCA

We assume that the traffic dynamics within a day are captured by a traffic demand set which contains 5 traffic matrices representative of 5 characteristic instants. The initial traffic matrices are originated with randomly chosen sets of 25-demand pairs. Each demand bundle is assumed to consist of 2 units. By virtue of the traffic pattern generation approach above, we generate 5 traffic demand sets for each test network in Fig. 3.4 with the parameters set as follows: β=0.5, μ=0.8, ν=1.2. For each traffic demand set, the best feasible solutions of JSCA are reached within 32 hours for COST239 and 7 hours for NSFNET and Bellcore with a 5% MIPGAP.

For comparison, we also generate optimal results for IRA and MSCA for all cases. Since IRA requires periodic reconfiguration which means each traffic demand set is actually matched with a set of configurations, we take the average of the spare capacity usage of the configurations as the optimal results. Figure 6.2 shows resource usage in terms of spare capacity obtained under different approaches. Each experiment number corresponds to a traffic demand set. The numbers above the bars represent the percentage increase in resource usage of JSCA with respect to IRA. From the results of COST239 and Bellcore, we can observe that JSCA uses approximately 21% on average (28% for NSFNET) additional resources to provide optimal static configurations for traffic demand sets which require MSCA to use around 90% additional resources. Comparing results

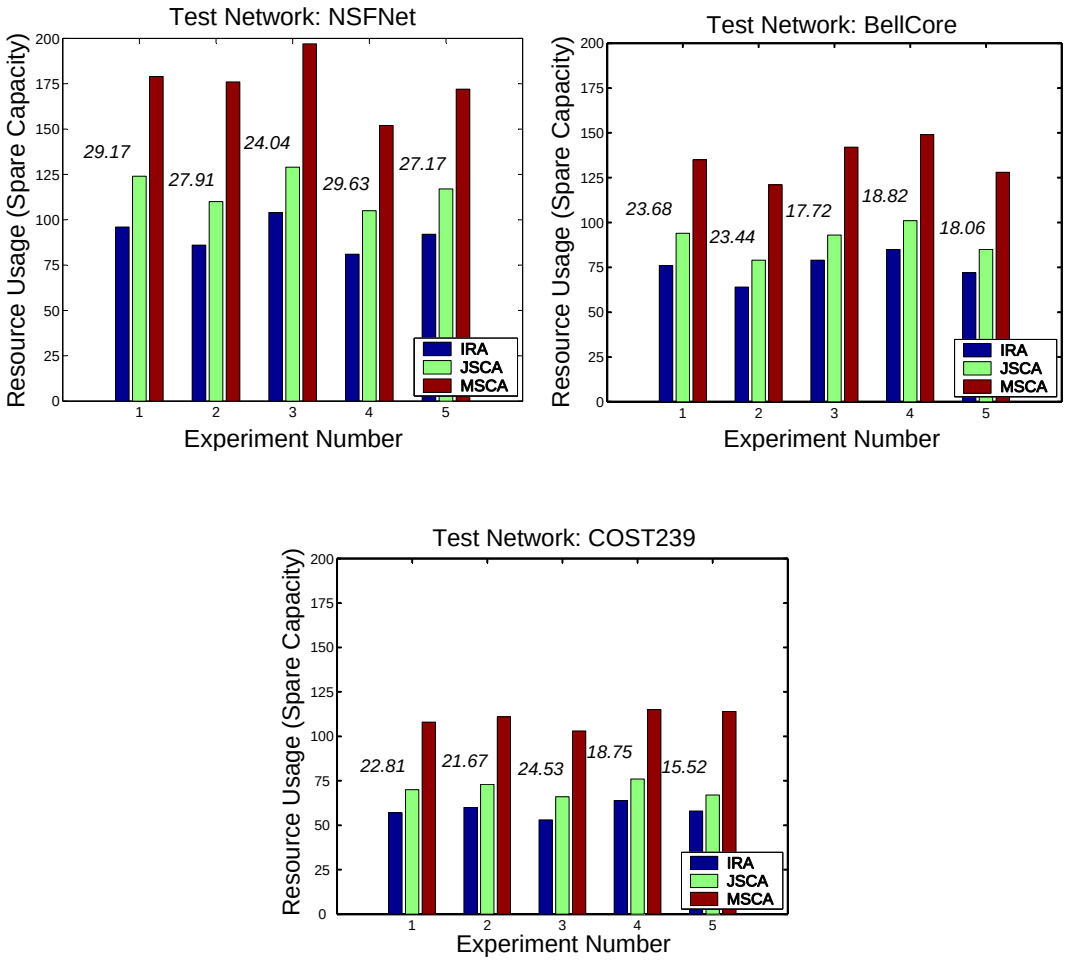

Figure 6.2: Comparison of Resource Usage under Different Approaches (IRA, JSCA, MSCA)

between different test networks, we see that not only the overall resource usage but also the increment relative to IRA fall with the average node degree (NSFNET: 3 Bellcore: 3.7 COST239: 4.7). This is because the sparser the network, the more the spare capacity is required for protection and the less the sharing of bandwidth can be exploited by JSCA.

6.6.3 Impact of Limiting Inflation Of Working Capacity

In Section 6.3.2, we have discussed that the inflation of working capacity can occur in the optimization of JSCA, for which we have introduced the parameter γ along with Constraint (6.5) into the MILP model. To obtain an insight into this issue, we investigate the impact of limiting inflation on the optimization results as shown in Fig. 6.3. The figures along the Y axis indicate the optimization results obtained under the condition of limited inflation at a particular degree (X axis: γ) and are normalized to the pure optimization results which are obtained without such a constraint. As we can observe in Fig. 6.3, the increase in resource usage of the conditioned optimization results with respect to the pure optimization results rises when γ decreases as Constraint (6.5) becomes tighter and begins to dominate. Furthermore, it can also be noted that limiting inflation affects the results of NSFNET most, followed by Bellcore and COST239. The reason is that the optimization of JSCA for sparse networks tends to select longer routes for single traffic matrices for the sake of sharing so as to minimize spare capacity usage. In

other words, the inflation of working capacity for single traffic matrix in a traffic demand set can be greater for sparse networks than for dense networks. Therefore, limiting inflation can exert greater impact on sparse networks.

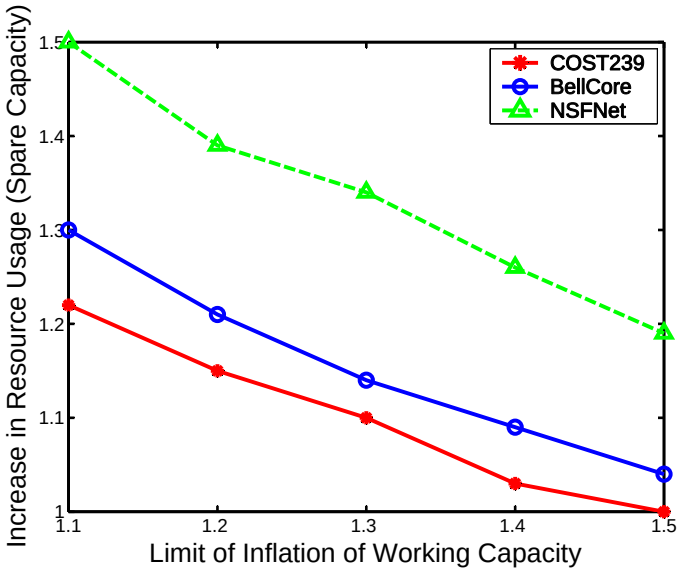

Figure 6.3: The Impact of Limiting Inflation of Working Capacity

6.6.4 Sub-optimal Solution to JSCA

For the sake of efficiency in terms of resolution time, we have proposed the sub-optimal solution in Section 6.4 in which the optimization model of JSCA is decomposed into two sub-problems. To examine the effectiveness of the sub-optimal solutions, we test the approach on COST239, Bellcore and NSFNET using the same traffic demand sets (notated as Traffic Pattern 1) as used in the optimization of JSCA. In addition, we also originate another group of traffic demand sets

(notated as Traffic Pattern 2) by adjusting the parameters in the process of traffic pattern generation (β=0.8, μ=0.6, ν=1.4) in order to study the impact of traffic volatility on the effectiveness of sub-optimal solutions. The best feasible solutions can be obtained at a 3% MIPGAP within 30mins for all the cases.

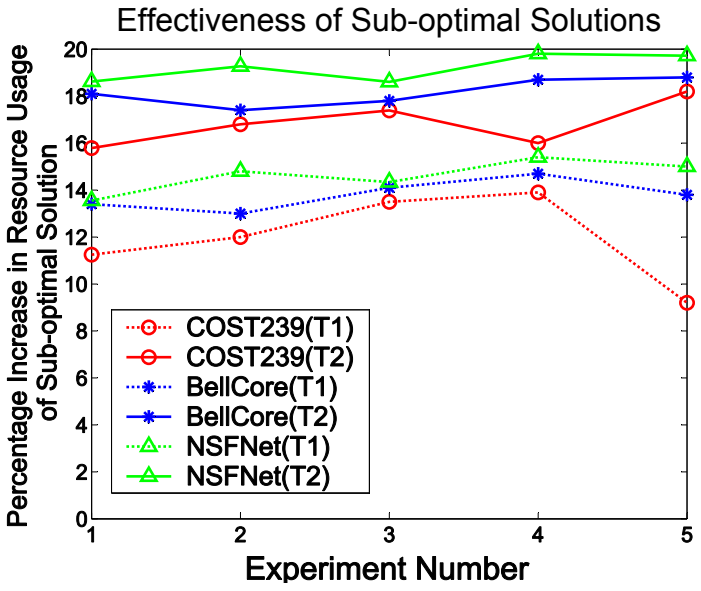

Figure 6.4: The Effectiveness of Sub-optimal Solutions in Resource Utilization

In Fig. 6.4, the results are described as the percentage increase in resource usage of the sub-optimal solutions with respect to the optimization results. As we can see, the sub-optimal solutions trade resource usage with resolution time. For test networks COST239, Bellcore and NSFNET, the average differences between the sub-optimal and optimal solutions are approximately 12%, 13.5% and 14.5% more resource usage for Traffic Pattern 1 and 17%, 18% and 19% for Traffic Pattern 2, respectively. The enlarged gap for Traffic Pattern 2 relative to Traffic

Pattern 1 implies that increasing traffic volatility can degrade the effectiveness of sub-optimal solutions. This can be explained as follows. Under volatile traffic condition, successive traffic matrices in the traffic demand set can differ greatly from each other. As the process of optimization tends to exploit the sharing of working capacity required by traffic matrices, longer routes are likely to be chosen, which can lead to higher inflation of working capacity. On the other hand, the first phase of the sub-optimal solution aims at minimizing total working capacity, which may exaggerate the deviation of the sub-optimal solution from the optimal when the high inflation of working capacity occurs in the optimal solution. Further, the percentage increase in resource usage of the sub-optimal solutions increases as the average network node degree decreases, which implies that the effectiveness of sub-optimal solutions declines as the network becomes sparser. This is because network sparsity contributes to the high inflation of working capacity in a similar way the traffic volatility does, thus leading to the pronounced gap between sub-optimal and optimal solutions.

6.6.5 Optimization of JSCA-based PWCE

Now we study the performance of JSCA-based PWCE in terms of the improvement in the volume of working capacity envelope in comparison with the sub-optimal solution to JSCA-based PWCE and MSCA-based PWCE given different spare

capacity budgets. From the study on the optimization of JSCA and the corresponding sub-optimal solution, we can see that different levels of minimum spare capacity usage are required under JSCA, the corresponding sub-optimal solution and MSCA given the same traffic matrix set $\boldsymbol{D}$, with the lowest level being for JSCA followed by the corresponding sub-optimal solution and MSCA. For simplicity, we denote these three levels of minimum spare capacity usage as Level I, Level II, Level III (from lowest to highest). The performances of JSCA-based PWCE, the corresponding sub-optimal solution and MSCA-based PWCE depend on the level of the spare capacity budget to be imposed as the constraint with regard to the three levels. If the level of the spare capacity budget is below Level I, it is obvious that there exists no solution to all the three schemes. If the level of the spare capacity budget lies between Level I and Level II, only JSCA-based PWCE is solvable and can generate the optimal solution. When the level of the spare capacity budget ranges between Level II and Level III, only JSCA-based PWCE and the corresponding sub-optimal solution are feasible. All three schemes are feasible when the level of the spare capacity budget is beyond Level III. Figure 6.5 illustrates the relation between the level of the spare capacity budget and the feasibility of the three schemes.

As we aim to investigate the performance of JSCA-based PWCE compared with those of the corresponding sub-optimal solution and MSCA-based PWCE, we choose Level II and Level III as the level of the spare capacity budget. Notice

Spare Capacity Budget / Feasibility	<Level I	Level I ~ Level II	Level II - Level III	>Level III
JSCA-based PWCE		√	√	√
JSCA-based PWCE__Sub			√	√
MSCA-based PWCE				√

Figure 6.5: Relation Between the Level of the Spare Capacity Budget and the Feasibility of Schemes (JSCA-based PWCE, Sub-optimal Solution to JSCA-based PWCE, MSCA-based PWCE)

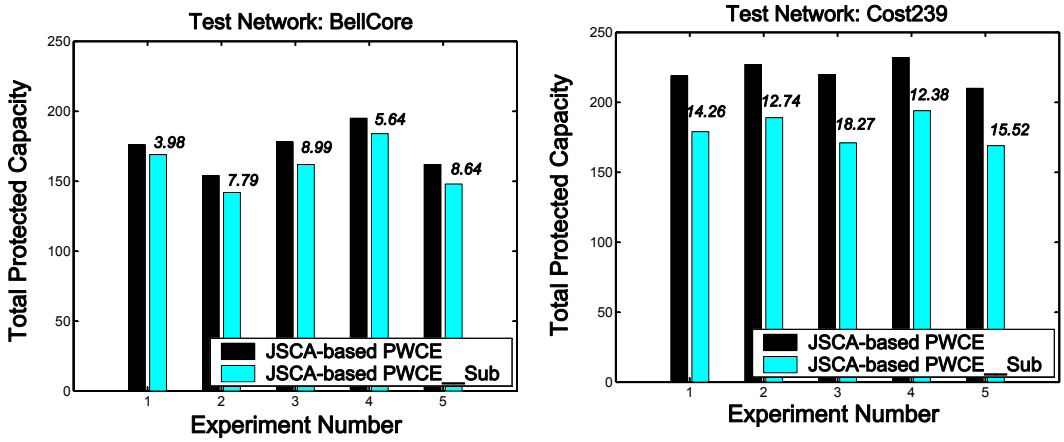

Figure 6.6: Comparison of the Volume of Working Capacity Envelope under Different Approaches (JSCA-based PWCE, the Sub-optimal Solution to JSCA-based PWCE) given the spare capacity budget (Level II)

that while all the levels of spare capacity budgets discussed here can be span-based (i.e., in the form of the distribution of spare capacity budget on all spans), we focus on network-wide spare capacity budgets in this chapter. The performance study is carried out on networks COST239 and Bellcore with the same traffic demand sets used in Section 6.6.2. For each traffic demand set, we first use the spare capacity usage required by the sub-optimal solution to JSCA (Level II) obtained in Section 6.6.4 as the level of the spare capacity budget. Based on such level of the spare capacity budget, the volume of working capacity envelope is maximized under JSCA-based PWCE and the corresponding sub-optimal solution, which is shown in Fig. 6.6. The numbers above the bars stand for the percentage increase of the volume of working capacity envelope of JSCA-based PWCE over the corresponding sub-optimal solution. As we can see, JSCA-based PWCE improves the maximum volume of working capacity envelope by 14.6% and 7% on average for networks COST239 and Bellcore, respectively. We observe that the improvement of JSCA-based PWCE is higher in network COST239 than in network Bellcore. This is because span-protecting p-Cycles usually have higher capacity efficiency in dense networks than in sparse networks, which thus makes the impact of the spare capacity budget on the volume of working capacity envelope greater in dense networks.

Next, we use the spare capacity usage required by MSCA-based PWCE (Level III) obtained in Section 6.6.2 as the level of the spare capacity budget. As seen

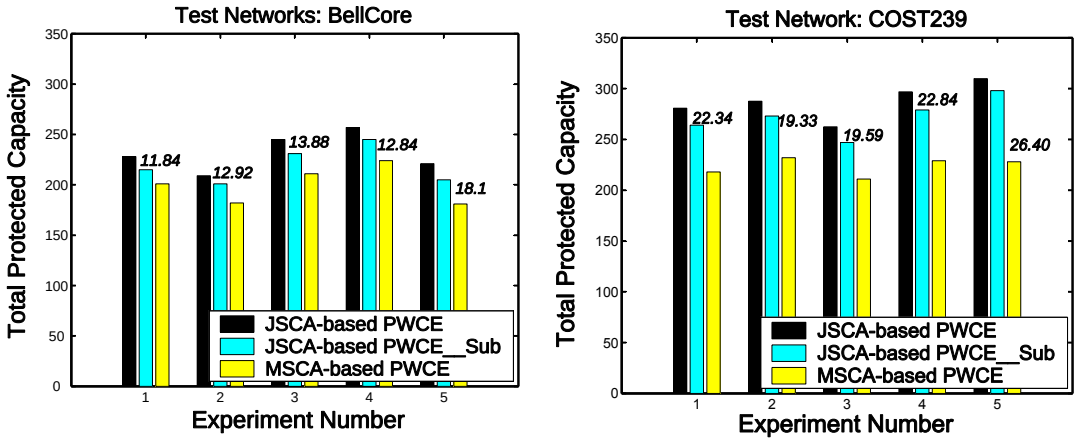

Figure 6.7: Comparison of the Volume of Working Capacity Envelope under Different Approaches (JSCA-based PWCE, the Sub-optimal Solution to JSCA-based PWCE, MSCA-based PWCE) given the spare capacity budget (Level III)

in Fig. 6.5, all three schemes can generate solutions given such a constraint on the spare capacity budget. The maximum volume of working capacity envelope of the three schemes are displayed in Fig. 6.7 in which the numbers on the bars stand for the percentage increase of the volume of working capacity envelope of JSCA-based PWCE over MSCA-based PWCE. As shown in Fig. 6.7, JSCA-based PWCE improves the maximum volume of working capacity envelope by 22% and 14% on average with regard to MSCA-based PWCE for networks COST239 and Bellcore, respectively. Given such level of the spare capacity budget (Level III), we see in Fig. 6.7 that the improvement of JSCA-based PWCE over the corresponding sub-optimal solution is smaller than the improvement of the corresponding

sub-optimal solution over MSCA-based PWCE, which is pronounced when the network becomes denser. This indicates that the sub-optimal solution to JSCA-based PWCE performs comparably to JSCA-based PWCE and thus can be a good alternative to JSCA-based PWCE given its advantage in computational efficiency over JCSA-based PWCE.

6.6.6 Extension to Path-oriented Protection

We have so far investigated the performance of JSCA and JSCA-based PWCE which are both designed for span-oriented protection. Now we carry out studies on JSCAP and JSCAP-based PWLE as an extension to path-oriented protection with assumptions similar to those used in Section 6.6.2 and Section 6.6.5.

Optimization of JSCAP

The optimization of JSCAP is conducted on the COST239, Bellcore and NSFNET networks. For each network, 5 traffic demand sets are generated in a similar way as in Sec. 5.7.2 with the traffic parameters set as follows: β=0.5, μ=0.8, ν=1.2. For each traffic demand set, the best feasible solutions of JSCA are reached within 122 hours for COST239 and 41 hours for NSFNET and Bellcore with a 5% MIPGAP. For comparison, we also generate optimal results for IRAP and MSCAP in a similar way we do for IRA and MSCA.

Figure 6.8 displays resource usage in terms of spare capacity obtained under

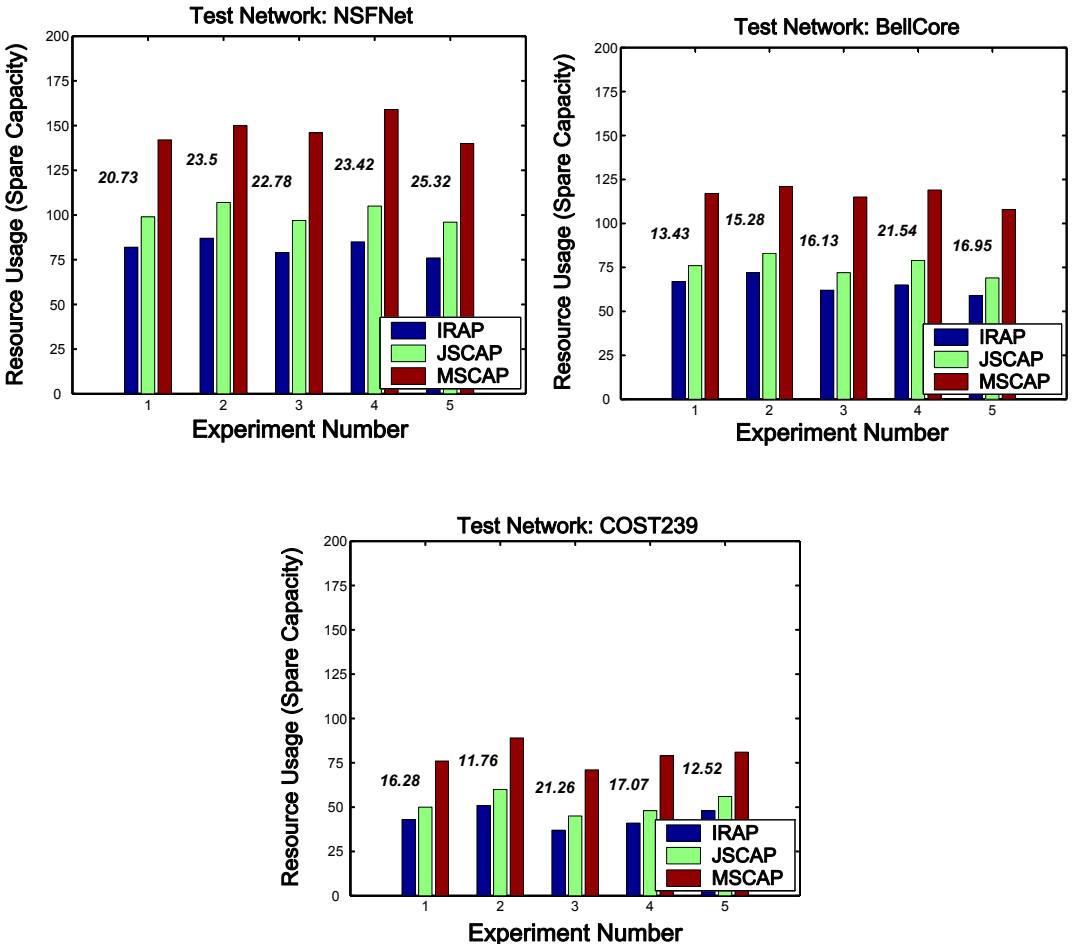

Figure 6.8: Comparison of Resource Usage under Different Approaches (IRAP, JSCAP, MSCAP)

different approaches. The numbers above the bars represent the percentage increase in resource usage of JSCAP with respect to IRAP. From the results of network COST239, Bellcore and NSFNET shown in Fig. 6.8, JSCAP uses, on average, approximately 16%, 17% and 23% additional resources, respectively, to provide optimal static configurations for traffic demand sets which require MSCAP to use around 81% additional resources. Compared with the results in Section 6.6.2, we find that JSCAP uses less additional resources with respect to IRAP than JSCA does with respect to IRA. This finding can be explained by the higher capacity efficiency of lightpath-protecting p-Cycles used by JSCAP in comparison with span-protecting p-Cycles used by JSCA. Moreover, we observe the trend, which is also observed in Section 6.6.2, that not only the overall resource usage but also the increment with respect to IRAP fall as the average node degree increases, which can be explained by the same reason in Section 6.6.2.

Optimization of JSCAP-based PWLE

Next we study the performance of JSCAP-based PWLE in terms of the improvement in the volume of working capacity envelope in comparison with the MSCAP-based PWLE given the level of the spare capacity budget equal to minimum spare capacity usage under MSCAP (which is conceptually equivalent to Level III). The study is carried out on COST239 and Bellcore networks with the same traffic demand sets used in the optimization of JSCAP above. For each traffic demand set,

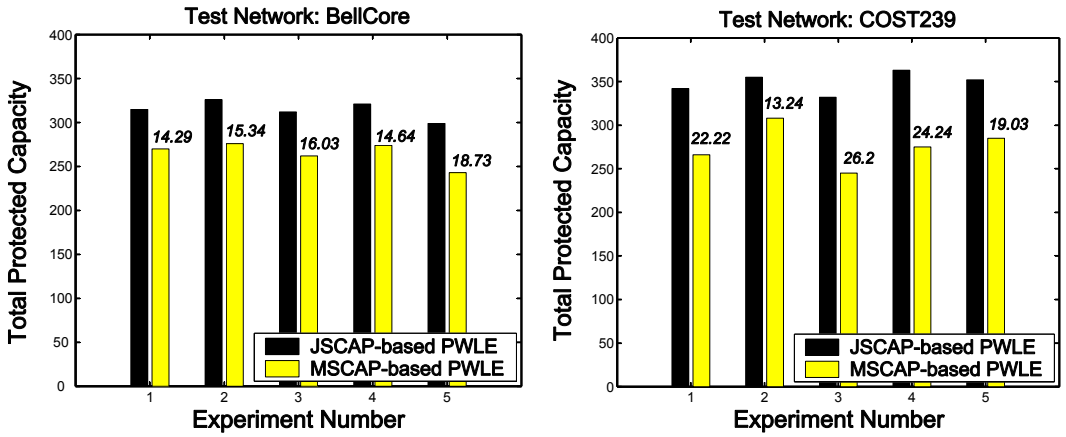

Figure 6.9: Comparison of the Volume of Working Capacity Envelope under Different Approaches (JSCAP-based PWLE, MSCAP-based PWLE) given the spare capacity budget (Level III)

the volume of working capacity envelope is maximized under both JSCAP-based PWLE and MSCAP-based PWLE. Figure 6.9 displays the maximized results where the numbers above the bars stand for the percentage increase of the volume of working capacity envelope of JSCAP-based PWLE over MSCA-based PWLE. As we can see, JSCAP-based PWLE improves the maximum volume of working capacity envelope by 20.3% and 15.8% on average for COST239 and Bellcore networks, respectively.

6.7 Summary

In this chapter, we have proposed an efficient off-line static configuration of span-protecting p-Cycles, JSCA, to provide survivable services under time-variant traffic characterized by a traffic demand set. Then we have formulated JSCA as an MILP model with the objective to minimize the spare capacity required. The issues associated with the inflation of working capacity in the optimization have been discussed. Based on JSCA, we have studied its applications in PWCE and thus proposed JSCA-based PWCE. To tackle the issue of computational complexity, we have also developed sub-optimal solutions to JSCA and JSCA-based PWCE to trade the effectiveness of optimization results with resolution time. Moreover, we have extended the studies to path-protected networks by applying the idea of JSCA to lightpath-protecting p-Cycles and PWLE.

The results obtained indicate that JSCA can avoid periodic reconfiguration with much less spare capacity than MSCA, and just a minor increment compared with IRA. The applications of JSCA in PWCE can improve the solution by generating higher volume of working capacity envelope. The same performance improvements have also been observed in the extension to path-protected networks.

Chapter 7

Conclusions and Further Research

7.1 Conclusions

In this thesis, a new scheme, PWLE, for dynamic provisioning of survivable services has been proposed. As PWLE is formed based on lightpath-protecting p-Cycles, a method called Compatible Grouping has been developed to facilitate the optimization of the working layer. The optimization of PWLE has been formulated as an MILP model and solved with CPLEX. In the aspects of routing and operation of PWLE, a distributed routing algorithm, Compatible Group Routing (CGR), has been developed and the operations upon failure have also been discussed. The results obtained show that PWLE has a higher capacity efficiency, better blocking performance, less wavelength conversions and acceptable operational complexity.

In order to improve the efficiency of the cycle selection process of PWLE, a

cycle pre-computation algorithm (ANCG) and heuristic algorithms (HALCS_AER, HALCS_TPRC, HALCS_TAER) have been developed. Numerical results show that ANCG can efficiently generate a small-size set of candidate cycles with high *ER*s and the heuristic algorithms can generate solutions close to those of optimal solutions yet with much reduced computational time.

To further improve PWLE, CAPWLE has been proposed by taking into accout network connectivity so that the capacity division of the working layer and the protection layer can be optimized from a combined perspective of volume and connectivity. To integrate connectivity-awareness into CAPWLE, *Effective Envelope* has been developed based on MCFP. The results obtained under both dynamic stationary and non-stationary traffic patterns indicate that the actual utilization of the working layer is enhanced in CAPWLE relative to PWLE.

Finally, the configuration of p-Cycle-based survivability schemes under time-variant traffic characterized by a traffic demand set has been studied. Starting with span-protecting p-Cycles, an efficient off-line static configuration of span-protecting p-Cycles, JSCA, has been proposed and optimized with the objective of minimizing the spare capacity required. Then the applications of JSCA in PWCE have also been discussed and has thus produced JSCA-based PWCE. To deal with the high computational complexity of optimization models, the sub-optimal solutions to JSCA and JSCA-based PWCE have been further developed. Furthermore, the studies have been extended to path-protected networks by applying the idea of

JSCA to lightpath-protecting p-Cycles and PWLE. The results obtained show that JSCA can avoid periodical reconfiguration with with just a minor increment in spare capacity required. The applications of JSCA in PWCE can enlarge the working capacity envelope and thus improve the solutions. Same performance improvements have also been observed in the extended studies on path-protected networks.

7.2 Contributions of this Thesis

1. Conception and development of PWLE

   A new scheme called PWLE has been proposed as an extension of PWCE to path protection to achieve higher capacity efficiency, better blocking performance and less wavelength conversions compared with conventional schemes under dynamic traffic. The optimization of PWLE has been carried out. In addition, due to the uniqueness of PWLE, a distributed routing algorithm has also been developed.

2. Design of cycle selection algorithms for PWLE

   A cycle pre-computation algorithm (ANCG) tailored for lightpath-protecting p-Cycles has been developed to generate high quality cycles which can be useful for either the optimization of PWLE or the heuristic algorithms of

PWLE. Further, heuristic algorithms have also been developed for cycle selection which have achieved near-optimal solutions with much reduced computational complexity.

3. Conception and development of CAPWLE

   A new concept called *Effective Envelope* and a new metric called *Connectivity-based ER* have been introduced to factor in network connectivity in the design of CAPWLE. Then the calculation of *Effective Envelope* has been derived based on a study on concurrent flow in graph theory. Finally, CAPWLE has been optimized based on *Effective Envelope*.

4. Effective configuration of p-Cycle-based survivability schemes under time-variant traffic

   A new scheme called JSCA has been developed for the effective configuration of span-protecting p-Cycles under time-variant traffic. It is capable of providing a static configuration with minimal spare capacity usage. The application of JSCA in PWCE has been carried out to enhance the capacity efficiency of PWCE. Then, sub-optimal solutions to JSCA and JSCA-based PWCE have been designed to enhance the practicability of these schemes. Finally, the extension of JSCA and JSCA-based PWCE to path-protected networks has been made.

7.3 Further Research

1. This thesis concentrates mainly on survivability techniques against single span failures. However, fully restorable networks against single span failures are not completely immune from failures and thus do not guarantee that service outages will not happen. Multiple failures, which are less frequent, can still affect services. Nowadays, there is abundant interest in understanding the impact of dual-failure scenario on survivability schemes. As a metric to characterize the network's reliability, availability is the probability that a system is found operative at an arbitrary given time [56] [57]. For a survivable networking scheme against all single failures, dual failures come up next to dominate availability. It would be interesting to determine the availability of service paths and the network as a whole in PWLE so as to analyze how PWLE withstands dual-span failures given the investment in single-failure survivability. Based on the findings in the analysis, it would be useful to develop approaches to enhance PWLE's dual-failure restorability.

2. This thesis focuses on single level of survivability which is full protection against single span failures. However, in a competitive business with a diverse set of users and applications, it is generally desirable to be able to provide multiple differentiated levels of survivability service offerings for individual demands in some efficient way. As an extension of the general concept of Quality of Service (QoS), Quality of Protection (QoP) was first researched in [58] in which a four tier QoP

class set was proposed for Asynchronous Transport Mode (ATM) networks. Gerstel and Sasaki adapted and extended this for ring-oriented broadband transport networks in [59]. The optimal capacity design models for span restorable mesh networks with a mix of QoP types was treated in [60]. It would be interesting to carry out a study on the development of a PWLE multi-QoP capacity design model and the integration of a dual-failure survivability service class into an overall multi-QoP framework.

3. This thesis considers dynamic traffic which can be characterized, if available, by a single forecasted demand matrix or a demand matrix set. However, as the uncertainty increases, there are more levels of demand uncertainties and traffic patterns to be considered. A general framework proposed in [61] classifies the notion of uncertainty into four different levels. Level I is the simplest case of all, where deterministic demand forecast is considered for the capacity planning problem. Level II captures uncertainty by a limited set of scenarios. In a capacity planning problem, these scenarios might correspond to a distinct set of demand forecasts. Level III identifies a range of potential future demand scenarios. But there are no natural discrete scenarios. By increasing the uncertainty to Level IV, it is impossible to identify a range or the domain of potential outcomes. Notice that Level III might seem to be better described with the continuum of future demand scenarios, but in practice most planners would assume Level II uncertainty and work with a smaller number of characteristically different scenarios as in [62] which proposed capacity

planning optimization models for explicitly capturing uncertainty and network survivability. Level IV uncertainty often prohibits us from planning vigorously. One of the possible approaches is stochastic programming (SP) [63] which provides a more sophisticated framework to incorporate uncertainty into the planning process and allows a planner to deal with a situation where some of the input parameters are characterized by probability distributions or a set of scenarios. The use of SP to deal with uncertainty is well recognized in the areas of electric utility, finance and logistic industries. However, the application of SP to the capacity design of transport network with uncertainty and survivability schemes has been minimal. It could be interesting to develop advanced PWLE models to incorporate various traffic demand uncertainties.

7.4 Publications

This thesis is based on the publications listed as follows.

1. R.He, K.C.Chua and G.Mohan "Protected Working Lightpath Envelope: a New Paradigm for Dynamic Survivable Routing," in *Proceeding of the 14th International Conference on Computer Communication and Networks (ICCCN 2007)*, August 2007.

2. R.He, K.C.Chua and G.Mohan, "Lightpath-protecting p-Cycle Selection for Protected Working Lightpath Envelope," in *Proceedings of GLOBECOM*

2008, December 2008.

3. R.He, K.C.Chua and G.Mohan, "Connectivity Aware Protected Working Lightpath Envelope," in *Proceeding of the 16th International Conference on Computer Communication and Networks (ICCCN 2009)*, August 2009. (Nominated for Best Paper)

Bibliography

[1] W.D.Grover, *Mesh-Based Survivable Networks: Options and Strategies for Optical, MPLS,SONET, and ATM Networking*. Prentice Hall PTR, 2004.

[2] W.D.Grover and D.Stamatelakis, "Cycle-oriented distributed preconfiguration: Ring-like speed with mesh-like capacity for self-planning network restoration," in *Proceedings of IEEE International Conference on Communications (ICC 1998)*, pp. 537–543, June 1998.

[3] W.D.Grover and D.Stamatelakis, "Bridging the ring-mesh dichotomy with p-cycles," in *Proc. IEEE / VDE DRCN 2000*, pp. 92–104, April 2000.

[4] D.Stamatelakis and W.D.Grover, "Theoretical underpinnings for the efficiency

of restorable networks using preconfigured cycles (p-cycles)," *IEEE Transactions on Communications*, vol. 48, no. 8.

[5] R.Ramaswami and K.N.Sivarajan, *Optical Networks: A Practical Perspective, Second Edition*. Morgan Kaufmann Publishers, 2002.

[6] M.To and P.Neusy, "Unavailability analysis of long-haul networks," *IEEE Journal on Selected Areas in Communications*, vol. 12, pp. 100–109, January 1994.

[7] A.J.Vernon and J.D.Portier, "Protection of optical channels in all-optical networks," in *Proceedings of the 18th Annual National Fiber Optic Engineers Conference (NFOEC 2002)*, pp. 1695–1706, September 2002.

[8] T. A. for Telecommunications Industry Solutions (ATIS) Committee T1A1, *ATIS Telecom Glossary 2000*. Online: http://www.atis.org/tg2k, 2001.

[9] D.Crawford, *Fiber Optic Cable Dig-ups - Causes and Cures*. Network Reliability and Interoperability Council website. Online: http://www.nric.org/pubs/nric1/sections/abody.pdf, 1992.

[10] W.D.Grover, "The protected working capacity envelope concept: An alternative paradigm for automated service provisioning," *IEEE Communication Magazine*, pp. 62–69, Januray 2004.

[11] G.X.Shen and W.D.Grover, "Design and performance of protected working capacity envelopes based on p-cycles for dynamic provisioning of survivable services," *Journal of Optical Networking*, vol. 4, June 2005.

[12] W.S.He, J.Fang, and A.K.Somani, "A p-cycle based survivable design for dynamic traffic in wdm networks," in *Proceedings of Globecom 2005*, pp. 1896–1873, 2005.

[13] G.X.Shen and W.D.Grover, "Extending the p-cycle concept to path-segment protection for span and node failure recovery," *IEEE Journal on Selected Areas in Communications*, vol. 21, pp. 1306–1319, October 2003.

[14] A.Kodian and W.D.Grover, "Failure-independent path-protecting p-cycles: Efficient and simple fully preconnected optical-path protection," *Journal of Lightwave technology*, vol. 23, October 2005.

[15] D.Lastine and A.K.Somani, "Supplementing non-simple p-cycles with preconfigured lines," in *Proceeding of IEEE International Conference on Communication (ICC 2008)*, pp. 5443–5447, 2008.

[16] S.V.Kartalopoulos, *Introduction to DWDM Technology: Data in a Rainbow*. SPIE and IEEE Press Publishers, 2000.

[17] R.L.Freeman, *Fiber-Optic Systems for Telecommunications*. Wiley-Interscience, 2002.

[18] G.P.Agrawal, *Fiber-Optic Communication Systems*. John Wiley Sons, 2002.

[19] W. G. on Network Performance, *A Technical Report on Network Survivability Performance. Report No.24*. November 1993.

[20] ANSI, *A Technical Report on Network Survivability Performance. Report No.24*. Tech. Rep. ANSI T1.105.01.

[21] Bellcore, *SONET Bidirectional Line-Switched Ring (BLSR) Equipment Generic Criteria, Issue 4*. Tech. Rep. GR-1400-Core, Issue 1, Revision 1.

[22] Telecordia, *SONET Bidirectional Line-Switched Ring (BLSR) Equipment Generic Criteria, Issue 4*. Tech. Rep. GR-1230-CORE, Issue 4.

[23] G.Ellinas, A.G.Hailemariam, and T.E.Stern, "Protection cycles in mesh wdm networks," *IEEE Journal on Selected Areas in Communications*, pp. 1924–1937, October 2000.

[24] M.Herzberg, S.J.Bye, and A.Utano, "The hop-limit approach for spare- capacity assignment in survivable networks," *IEEE/ACM Transactions on Networking*, vol. 3, pp. 775–784, December 1995.

[25] S.V.Kartalopoulos, *Introduction to DWDM Technology*. IEEE Press and SPIE Press.

[26] R.R.Iraschko, M.MacGregor, and W.D.Grover, "Optimal capacity placement for path restoration in stm or atm mesh survivable networks," *IEEE/ACM Transaction on Networking*, vol. 6, pp. 325–336, June 1998.

[27] R.R.Iraschko, W.D.Grover, and M.H.MacGregor, "A distributed real time path restoration protocol with performance close to centralized multi-commodity maxflow," in *Proceedings of the 1st International Workshop on the Design of Reliable Communication Networks (DRCN 1998)*, May 1998.

[28] Y.Xiong and L.G.Mason, "Restoration strategies and spare capacity requirements in self-healing atm networks," *IEEE/ACM Transactions on Networking*, vol. 7, pp. 98–110, February 1999.

[29] S.Kini, M.Kodialam, T.V.Laksham, and C.Villamizar, *Shared Backup Label Switched Path Restoration*. Internet Draft draft-kini-restoration-shared-backup-01.txt, May 2001.

[30] J.Doucette, M.Clouqueur, and W.D.Grover, "On the availability and capacity requirements of shared backup path-protected mesh networks," *Optical Networks Magazine*, Nov./Dec. 2000.

[31] C. et al., "Near-optimal approaches for shared-path protection in wdm mesh networks," in *Proceeding of IEEE International Conference on Communication (ICC 2003)*, p. 1320C1324, May 2003.

[32] Y.Xiong, D.Xu, and C.Qiao, "Achieving fast and bandwidth efficient shared-path protection," *Journal of Lightwave technology*, vol. 21, no. 2.

[33] G.X.Shen and W.D.Grover, "Performance of protected working capacity envelopes based on *p*-cycles: Fast, simple, and scalable dynamic service provisioning of survivable services," in *Proceedings of Asia-Pacific Optical and Wireless Communications Conference (APOC 2004)*, vol. 5626, November 2004.

[34] G.X.Shen and W.D.Grover, *Design of Protected Working Capacity Envelopes Based on p-Cycles: An Alternative Framework for Survivable Automated Lightpath Provisioning*. Springer.

[35] J.Doucette and W.D.Grover, "Node-inclusive span survivability in an optical mesh transport network," in *Proceedings of the 19th Annual National Fiber Optics Engineering Conference (NFOEC 2003)*, p. 634C643, 2003.

[36] Z.Zhang, W.Zhong, and S.K.Bose, "*p*-cycle-based protected working capacity envelope design for dynamically survivable wdm networks," in *Proceedings of the 3rd International Conference on Optical Communications and Networks (ICOCN 2004)*, November 2004.

[37] Z.Zhang, W.Zhong, and S.K.Bose, "Dynamically survivable wdm network design with p-cycle-based pwce," *IEEE Communications Letters*, vol. 9, pp. 756–758, August 2005.

[38] G.Ash, J.S.Chen, A.Frey, and B.Huang, "Real-time network routing in a dynamic class-of-service network," in *Proceedings of the 13th International Teletraffic Congress*, p. 187C194, 1991.

[39] D.A.Schupke, M.Scheffel, and W.D.Grover, "Configuration of p-cycles in wdm networks with partial wavelength conversion," *Photonic Network Communications*, vol. 6, no. 3, pp. 293–252, 2003.

[40] D.A.Schupke, M.Scheffel, and W.D.Grover, "An efficient strategy for wavelength conversion in wdm p-cycle networks," in *Proceedings of the 4th International Workshop on the Design of Reliable Communication Networks (DRCN 2003)*, pp. 221–227, 2003.

[41] L.Berger, *Generalized Multi-Protocol Label Switching (GMPLS) Signaling Resource ReserVation Protocol-Traffic Engineering (RSVP-TE) Extensions.* http://www.faqs.org/rfcs/rfc3473.html, January 2003.

[42] K.Kompella and Y.Rekhter, *Routing Extensions in Support of Generalized Multi-Protocol Label Switching (GMPLS).* http://www.faqs.org/rfcs/rfc4202.html, October 2005.

[43] J.Doucette, W. D.He, and O.Yang, "Algorithmic approaches for efficient enumeration of candidate p-cycles and capacitated p-cycle network design," in *Proceedings of the 4th International Workshop on the Design of Reliable Communication Networks (DRCN 2003)*, pp. 212–220, 2003.

[44] H.Zhang, O.Yang, J.Wu, J.M.Savoie, T.Shan, and G.Wang, "A cycle-based rerouting scheme for wavelength-routed wdm networks," in *Proceeding of the 2004 International Conference on Parallel Processing Workshops (ICPPW 04)*, pp. 427–433, 2004.

[45] K.Lo, D.Habibi, Q.V.Phung, A.Rassau, and H.N.Nguyen, "Efficient p-cycle design by heuristic p-cycle selection and refinement for survivable wdm mesh networks," in *Proceeding of GLOBECOM 2006*, 2006.

[46] F.Zhang and W.D.Zhong, "A novel path-protecting p-cycle heuristic algorithm," in *Proceeding of International Conference on Transparent Optical Networks (ICTON 2006)*, pp. 203–206, June 2006.

[47] H.Zhang and O.Yang, "Finding protection cycles in dwdm networks," in *Proceeding of IEEE International Conference on Communication (ICC 2002)*, pp. 2756–2760, April 2002.

[48] C.Liu and L.Ruan, "Finding good candidate cycles for efficient p-cycle network design," in *Proceeding of the 13th International Conference on Computer*

Communication and Networks (ICCCN 2004), pp. 321–326, 2004.

[49] K.Lo, D.Habibi, Q.V.Phung, and H.N.Nguyen, "Dynamic p-cycles selection in optical wdm mesh networks," in *Proceeding of IEEE Malaysia International Conference on Communications and IEEE International Conference on Networks (MICC-ICON 2005)*, 2005.

[50] F.Shahrokhi and D.W.Matula, "The maximum concurrent flow problem," *Journal of the ACM*, vol. 37, no. 2, pp. 318–334, 1990.

[51] D.W.Matula, "Concurrent flow and concurrent connectivity on graphs," *Graph Theory with Applications to Algorithms and Computer Science*, pp. 543–559, 1985.

[52] G.X.Shen and W.D.Grover, "Automatic lightpath service provisioning with a adaptive protected working capacity envelope based on p-cycles," in *Proceedings of the 5th International Workshop on the Design of Reliable Communication Networks (DRCN 2005)*, pp. 375–383, October 2005.

[53] B.Fortz and M.Thorup, "Optimizing ispf/is-is weights in a changing world," *IEEE Journal on Selected Areas in Communications*, vol. 20, no. 4, pp. 756–777, 2002.

[54] W.D.Grover and J.E.Doucette, "Advances in optical network design with *p*-cycles: Joint optimization and pre-selection of candidate *p*-cycles," in *Proceedings of IEEE-LEOS Summer Topical Meeting*, July 2002.

[55] D.A.Schupke, G.G.Gruber, and A.Autenrieth, "Optimal configuration of *p*-cycles in wdm networks," in *Proceedings of IEEE International Conference on Communication (ICC 2002)*, vol. 5, pp. 2761–2765, April 2002.

[56] J.Doucette, M.Clouqueur, and W.D.Grover, "On the availability and capacity requirements of shared backup path-protected mesh networks," *Optical Networks Magazine*, Nov./Dec.

[57] M.A.H.Clouqueur, *Availability of Service in Mesh-restorable Transport Networks*. Ph.D. dissertation, University of Alberta, 2004.

[58] P.Veitch, I.Hawker, and G. Smith, "Administration of restorable virtual path mesh networks," *IEEE Communication Magazine*, vol. 34, pp. 96–101, December 1996.

[59] O.Gerstel and G.Sasaki, "Quality of protection (qop): A quantitative unifying paradigm to protection service grades," *Optical Networking and Communications 2001*, vol. 4599, pp. 12–23, August 2001.

[60] W.D.Grover and M.Clouqueur, "Span-restorable mesh network design to support multiple quality of protection (qop) service-classes," in *Proceedings of*

the 1st International Conference on Optical Communications and Networks (ICOCN 2002), pp. 321–323, 2002.

[61] H.Courtney, J.Kirkland, and P. Viguerie, "Strategy under uncertainty," *Harvard Business Review*, vol. 75, pp. 67–79, November 1997.

[62] J.Kennington, E.Olinick, K.Lewis, A.Ortynski, and G.Spiride, "Robust solutions for the dwdm routing and provisioning problem: Models and algorithms," *Optical Networks Magazine*, vol. 4, pp. 74–84, March 2003.

[63] P.Kall and S.Wallace, *Stochastic Programming*. John Wiley Sons, 1994.